UNIVERSITAT POLITÈCNICA DE VALÈNCIA

Universitat Politècnica de València

Instituto Universitario de Investigación de Ingeniería Energética

Research about refrigerant charge in domestic heat pumps

PhD Thesis

Luis Sánchez-Moreno Giner

Supervisors

Dr. José Gonzálvez Maciá

Dr. Francisco Barceló Ruescas

June 2023

Acknowledgments

En primer lugar, me gustaría agradecer a mis directores de tesis, por brindarme la oportunidad de poder realizar el presente trabajo en el IUIIE y por guiarme durante este proceso para poder hacer un trabajo de calidad.

De igual manera, también quiero agradecer a todo el área térmica del IUIIE por generar un ambiente inmejorable. Gracias a vosotros ir a trabajar no suponía tanto esfuerzo como si no estuvierais, y además, siempre estabais ahí en caso de que se necesitara un poco de ayuda. Mil gracias y seguid así. Dentro de este grupo me gustaría hacer especial mención a Alex y Rafa por su apoyo incondicional y por su ayuda inmediata en reuniones improvisadas en vuestro despacho, ya fuera de cuestiones de trabajo en sí o no. También agradecer a Jose Miguel, sin el cual todo esto no habría sido posible y, lamentablemente, no podrá ver la culminación de este trabajo, descanse en paz.

I would also like to mention the Fraunhofer Institut ISE to allow me to do an international stay and get experimental data. I would especially like to thank Lena for the organization and the follow-up, Hannes for caring for me during those six months, and Timo for being the colleague and friend I needed.

Gracias también a la Universitat Politècnica de València por brindarme la financiación y los medios a través del programas "Ayudas para movilidad de estudiantes de Doctorado de la Universitat Politècnica de València" y "Programa de Ayudas de investigación y Desarrollo" (PAID-01-17)

Por otro lado, gracias de corazón a mi familia y amigos, por darme apoyo y entender que hubiera momentos que desapareciera del panorama.

Mención especial a mis padres y hermanos, quienes aun estando a veces lejos, su apoyo siempre se ha sentido muy cerca. Miguel, espero que esto marque el comienzo de un buen cambio.

Por último y por ello más importante, muchas gracias Pilar por aguantarme 24/7, en los periodos más relajados y los más estresantes. Por hacerte cargo de todo para que yo sea capaz de avanzar en esto y por hacer el primer check de todo para poder cubrir mis inseguridades. Este trabajo es gran parte gracias a ti. GRACIAS.

Abstract

Due to the climate crisis, there is a need to find alternative energy sources for space heating, cooling, and domestic hot water (DHW) production. Heat pumps are an excellent alternative to substitute current boilers to reduce gas emissions. A liquid source heat pump is highly recommended in new buildings with access to land or water due to its significant advantages.

The main problem with this technology is that it uses a refrigerant inside, and there is no refrigerant with good performance, cheap and safe to handle.

The near future trend in heat pumps used for space heating is to use pure refrigerants such as natural refrigerants and HFOs. These refrigerants (except CO_2) have safety issues (flammability or toxicity); consequently, a maximum amount of refrigerant is allowed without considering extra safety measures.

This PhD presents an experimental work with a ground source heat pump (GSHP) with a low R290 refrigerant amount. This experimental campaign is helpful to know the current achievable performance derived from the limitation of refrigerant amount, to develop refrigerant charge reduction strategies and to improve existing simulation software based on refrigerant charge prediction.

The experimental campaign was divided into two parts to focus separately on normal annual behaviour and refrigerant charge reduction strategies. In each test campaign, performance data was recorded during the test, and the refrigerant charge amount in each component was extracted and weighed after the end of each test. The installation had the tools to acquire data from the vapour compression circuit, isolate the components, and extract and weigh the refrigerant to know how much refrigerant was inside each section.

With the data collected, it was observed that the differences in refrigerant charge prediction in the components with the software used were significant, and some causes of these differences have been identified, correcting the prediction model. So, a compressor model has been developed, and a dead volume has been added to the refrigerant charge calculation in heat exchangers. With these changes, the refrigerant prediction has greatly improved in the model used and could be a reliable approximation.

Resumen

Debido a la crisis climática, es necesario encontrar fuentes alternativas para la climatización de locales y la producción de agua caliente sanitaria (ACS). Las bombas de calor se presentan como una alternativa excelente para sustituir a las calderas y así poder reducir las emisiones de gases contaminantes. En obra nueva, si se dispone de acceso al terreno o a una masa de agua, las bombas de calor agua-agua o salmuera-agua son altamente recomendadas debido a sus numerosas ventajas.

El principal problema que presentan las bombas de calor es el refrigerante que contienen, ya que en la actualidad no existe refrigerante que sea a la vez barato, seguro y con propiedades termodinámicas óptimas. La tendencia en el futuro cercano en bombas de calor utilizadas para la calefacción de locales es volver al uso de refrigerantes naturales como los hidrocarburos y las hidrofluorolefinas. Estos refrigerantes presentan problemas de seguridad debido a su inflamabilidad o toxicidad y es por eso que, en caso de carecer de medidas de seguridad adicionales, la cantidad de refrigerante está limitada.

En esta tesis se presenta un trabajo experimental sobre una bomba de calor salmuera-agua trabajando con poca cantidad de R290. La campaña experimental fue pensada para obtener resultados beneficiosos sobre cuál es el actual potencial de este tipo de tecnología tras la limitación de la carga de refrigerante, para desarrollar formas de reducción de carga de refrigerante en los sistemas y para mejorar las simulaciones de predicción de la cantidad necesaria de refrigerante.

La campaña experimental está dividida en dos partes, cada una enfocada en uno de los siguientes objetivos: la primera en conocer el actual comportamiento anual de esa bomba de calor y la segunda para desarrollar estrategias de reducción de carga de refrigerante. En cada campaña experimental se almaceno tanto los datos de funcionamiento como la cantidad de refrigerante que había en cada uno de los componentes. La instalación estaba equipada con las herramientas necesarias para la toma de datos durante el funcionamiento de la bomba de calor y también era capaz de sectorizarla asilando cada uno de los componentes para poder extraer y pesar el refrigerante y así conocer que cantidad había en cada zona.

Con los datos recogidos, se ha podido observar diferencias entre la predicción de carga de refrigerante en los diferentes componentes y la medida experimentalmente, y también se ha encontrado alguna de las causas de esa discrepancia, pudiendo así corregir el modelo. Para ello, se ha desarrollado un modelo de compresor y al modelo existente de intercambiadores de calor se le ha añadido un volumen muerto de refrigerante. Con estos cambios la predicción ha mejorado notablemente en el modelo utilizado y en la actualidad se puede utilizar para conocer una aproximación del refrigerante necesario.

Resum

A causa de la crisi climàtica, és necessari viienden fonts alternatives per a la climatització dels locals i la viiendenciavii d'aigua calenta sanitaria (ACS). Les bombes de calor es presenten com una alternativa excel·lent per a substituir a les calderes i així poder reduir les emissions de gasos contaminants. En obra nova, si es disposa d'accés al terreny o a una massa d'aigua, les bombes de calor aigua-aigua o salmorra-aigua són viiendencia recomanades a causa dels seus nombrosos avantatges.

El principal problema que presenten les bombes de calor és el refrigerant que contenen, ja que en l'actualitat no existeix refrigerant que siga alhora barat, segur i amb propietats termodinàmiques òptimes. La tendencia actual en bombes de calor utilitzades per a la calefacció d'espais, és tornar a l'ús de refrigerants naturals com els hidrocarburs i les hidrofluorolefines. Aquests refrigerants presenten problemes de seguretat a causa de la seua inflamabilitat o toxicitat i és per això que, en cas de mancar de mesures de seguretat addicionals, la quantitat de refrigerant està limitada.

En aquesta tesi es presenta un treball experimental sobre una bomba de calor salmorra-aigua treballant amb poca quantitat de R290. La campanya experimental va ser pensada per a obtindre resultats beneficiosos sobre quin és l'actual potencial d'aquesta mena de tecnologia després de la limitació de la càrrega de refrigerant, per a desenvolupar formes de reducció de càrrega de refrigerant en els sistemes i per a millorar les simulacions de predicció de la quantitat necessària de refrigerant.

La campanya experimental està dividida en dues parts, cadascuna enfocada en un dels següents objectius: la primera a conéixer l'actual comportament anual d'aqueixa bomba de calor i la segona per a desenvolupar estratègies de reducció de càrrega de refrigerant. En cada campanya experimental s'emmagatzeme tant les dades de funcionament com la quantitat de refrigerant que hi havia en cadascun dels components. La instal·lació estava equipada amb les eines necessàries per a la presa de dades durant el funcionament de la bomba de calor i també era capaç de sectoritzar-la asilant cadascun dels components per a poder extraure i pesar el refrigerant i així conéixer que quantitat hi havia en cada zona.

Amb les dades recollides, s'ha pogut observar diferències entre la predicció de càrrega de refrigerant i la mesura experimentalment, i també s'ha trobat

alguna de les causes d'aqueixa discrepància, podent així corregir el model. Per a això, s'ha desenvolupat un model de compressor i al model existent de bescanviadors de calor se li ha afegit un volum mort de refrigerant. Amb aquests canvis la predicció ha millorat notablement i en l'actualitat es pot utilitzar per a conéixer una aproximació del refrigerant necessari.

Contents

List of Figures

List of Tables

Nomenclature

Symbols

Symbol	Description	Unit
A	Air	
a	Length	m
A_w	Heat exchanger area	m^2
B	Brine	
b	Random standard deviation	
b	Width	m
C	Cooling	
Cc	Charge specific capacity	kW/kg
Cp	Specific heating capacity	kW/kg K
d	Depth	m
dT	Temperature approximation	K
E	Electrical energy	kJ
$\dot{E}$	Electrical power	kW
f	Function	
H	Heating	
m	Mass	kg
$\dot{m}$	Mass flow	kg/s
n	Compressor speed	Hz
Nplates	Number of plates	
P	Pressure	bar
pp	Plate pitch	mm
Q	Heating (or cooling) energy	kJ
$\dot{Q}$	Heating (or cooling) capacity	kW
s	Systematic standard deviation	
s	Slip ratio	
T	Temperature	ºC
U	Uncertainty	

Symbol	Description	Unit
u	Standard deviation of the sample	
V	Volume	m^3
W	Water	
x	Measured variable	
x	Vapour quality	

Greek symbols

Symbol	Description	Unit
α	Void fraction	
β	Compactness	m
δ	Approximation	
Δ	Difference	
η	Efficiency	
ω	Refrigerant mass fraction	
Φ	Diameter	m
π	Pi	
ρ	Density	kg/m^3
σ	Standard deviation	

Subscripts

Symbol	Description
95	With 95% of confidence
b	Brine
c	Cylinder
comp	Compressor
cond	Condenser
consummed	Consummed
dis	Discharge
evap	Evaporator
ext	Extracted
h	Heating
i	Zone i=1 compressor...
in	Inlet
ins	Inserted
liq	Liquid
N	Nitrogen
oil	Oil sump
on	On
out	Outlet
r	Receiver
ref	Refrigerant
rem	Remaining
sec	Secondary fluid
suc	Suction
useful	
vap	Vapour
w	Water

Acronyms and abbreviations

Symbol	Description
3WV	Three way valve
ASHP	Air Source Heat Pump
BPHE	Brazed Plates Heat Exchanger
CFC	Chlorofluorocarbon
COP	Coefficient of Performance
CP	Circulation pump
DHW	Domestic Hot Water
EEV	Electronic Expansion Valve
EG	Ethylene Glycol
ErP	Energy-related product
GSHP	Ground Source Heat Pump
GWP	Global Warming Potential
HC	Hydrocarbon
HCFC	Hydroclorofluorocarbon
HFC	Hydrofluorocarbon
HFO	Hydrofluorolefin
IR	Infrared
LFL	Lower Flammability Level
LN2	Liquid Nitrogen
Loc	Location
MCHE	Microchannel Heat Exchanger
MV	Manual Valve
NZEB	Near Zero Energy Building
ODP	Ozone Depletion Potential
PCM	Phase Change Material
POE	Polyol Ester
QCV	Quick Closing Valves
QCVT	Quick Closing Valves Technique
Ref	Reference

Symbol	Description
Refr	Refrigerant
RTD	Resistance temperature detector
RWT	Remove and Weight Technique
SC	Subcooling
SCOP	Seasonal Coefficient of Performance
SEER	Seasonal energy efficiency ratio
SH	Superheat
SPF	Seasonal Performance Factor
Var	Variable
WSHP	Water Source Heat Pump

Chapter 1: Introduction

1.1. Prologue

Due to climate change, there is a need to reduce global warming gas emissions. For this reason, political strategies and regulations are trying to minimise energy consumption by increasing energy efficiency and reducing non-renewable primary energy consumption. In this direction, the heat pump results in a great solution since its primary power consumption is electric, and they have high efficiency. They need less primary energy needs than most of the classical technologies. However, heat pumps have some concerns, specifically with the refrigerant. One of the most promising refrigerants for domestic appliances, due to its null ozone depletion potential (ODP), almost zero global warming potential (GWP), and good performance behaviour, is propane (R290).

Nevertheless, for safety reasons, as it is a flammable refrigerant, the amount of refrigerant charge inside a heat pump should be limited. This thesis aims to help create a heat pump with high efficiency and low refrigerant charge amounts. Below is detailed all the information exposed in more depth, justifying the need for the work performed along with this doctoral thesis.

1.1.1. Europe 2030 and Europe 2050

As it is commonly known, the planet's temperature is rising, which is highly related to human activity. This increment started with the industrial revolution (0.08 ^{o}C/decade), and since 1980 it has become even more critical (0.18 ^{o}C/decade) [1]. This tendency and the current situation can be observed in Figure 1. Currently, the temperature anomaly approaches 1 ^{o}C. If the increment reaches 1.5 ^{o}C, it will become an irreversible problem [2]. For this reason, the UN settled the Paris Agreement, establishing a common objective to limit the global temperature increase to 1.5 ^{o}C.

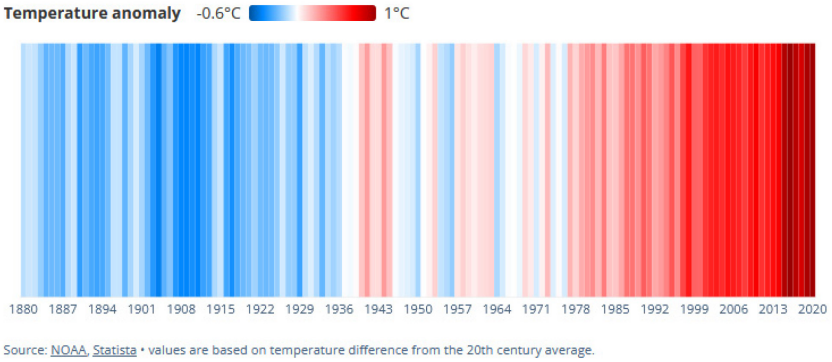

Figure 1: Global annual land and ocean surface temperature anomalies from 1880 to 2020 [1].

To accomplish this objective of 1.5 ^{o}C or at least to try to be as near as possible, the European Commission adopted a set of proposals to reduce greenhouse gas emissions [3]. These proposals took the form of objectives and milestones to be accomplished by the EU members in 2020 and 2030. They are defined in the eight types of activities, which are:

- Climate
- Energy
- Agriculture
- Industry
- Environment and oceans
- Transport
- Finance and regional development
- Research and innovation

However, as this work is focused on the Energy and Climate sectors, only the objectives of these areas will be written in this document. These key targets are listed in Table 1.

	2020	2030
Cuts in greenhouse gas emissions from 1990 levels	20 %	40 %
Share for renewable energy	20 %	32 %
Improvement in energy efficiency	20 %	32.5 %

Table 1: Energy and Climate key targets EU 2020 and 2030. [3]

These key targets align with the long-term strategy for 2050, aiming to achieve a climate-neutral society while ensuring social fairness [4].

European households account for 26.3 % of the total energy consumption, and 78.8 % of this energy is used mainly for space heating, cooling, and domestic hot water production [5]. Additionally, 75 % of the energy

employed for space heating and domestic hot water production in buildings is produced by burning fossil fuels directly in the household or indirectly because of the electricity mix [6]. These effects are intended to be corrected by constructing new buildings under new energy performance directives and renovating the existing ones following energy reduction guidelines. Nonetheless, the renovation rate of buildings should increase and be at least double the current one [7].

To reduce the emissions of buildings, new buildings must accomplish the near-zero energy building (NZEB) norm defined by every country. Still, all of them have to achieve the following requirements [8]:

- To have a very high energy performance.
- To fully cover the energy required by energy from renewable sources either generated on-site or from a renewable energy community or district heating or cooling using renewable energy or waste heat.
- To not have non-renewable primary energy use.
- To not cause on-site carbon emissions from fossil fuels.

From 2020, all new buildings constructed must be NZEB and from 2018, all new public buildings as well. However, in Europe, in 2016, the market penetration of NZEB was far from the objectives set [9]. If these requirements are met and the renovation rate increases, the final energy employed for space conditioning and the total energy per capita used for this purpose shall be reduced. In contrast, the demand for domestic hot water (DHW) is not easy to reduce, as it can mainly be decreased only by reducing water waste. Some tips can be used to reduce the water used, such as employing the grey waters for plants or secondary uses, not using DHW until the water gets warm in the tap, etc. Consequently, the energy utilised to heat the water from the water system to the final temperature would be similar and only depend on the number of people living.

These measures limiting building energy consumption shouldn't only be a European initiative. In Europe, last year, there was slow demographic growth compared to the rest of the world, with average values of 0.2 % of growth. The problem is that the rest of the world's population is increasing considerably. In 1900 Europe accounted for 25 % of the total population, this value is currently 10 %, and it is expected that in 2070 this percentage will get a value of 4 %. This growth must be followed with a higher

efficiency increment in every aspect, or the finite resources on the planet will rapidly disappear.

Summarising all the information mentioned, the EU needs to be carbon neutral by 2050. Buildings' heating and cooling energy demand will be reduced as their efficiency increases. As most of the buildings present in 2050 are already constructed, there will still be a need to provide heating and cooling in buildings and a similar DHW demand in households. Both heating and DHW production can be covered using the current boilers. To substitute them, heat pumps powered by renewable sources acquire great importance since part of the valuable energy is obtained from the source (mainly air or ground), and other consumption to work is electrical energy. Electrification is also an essential step towards decarbonisation, as well as increase the increase of electricity production from renewable sources.

Heat pumps use a fluid, the so-called refrigerant, to transfer absorbed heat from a low-temperature level called source to the sink, driving the fluid mechanically with an electrically driven compressor.

Suppose the annual ratio between the delivered heat to the sink and the electrical energy consumed in the compressor is higher than 2.5. In that case, some supplied thermal energy (power) is considered renewable [10]. This ratio is called the seasonal performance factor (SPF) or the seasonal coefficient of performance (SCOP). It is calculated as the division of the useful energy (heating or cooling) divided by the energy consumed, as shown in equation(1).

$$SCOP_{on} = SPF = \frac{\sum_{j=1}^{n} Q_{useful}}{\sum_{j=1}^{n} E_{consumed}} \quad (1)$$

1.1.2. Water-water heat pumps

Heat pumps represent an excellent alternative to substitute current boilers to reduce gas emissions regarding heating and DHW. In new or existing buildings with access to the land or a water source, using a liquid source heat pump, i.e., ground-source heat pump (GSHP) or water source heat pump (WSHP), is highly recommended.

These systems have a significant advantage: the source temperature fluctuates less along the year, having less seasonal effect than the air source heat pumps. This temperature remains almost constant throughout the

year. It also stays nearer to the operative temperature, lowering the condensation temperature when cooling is required and the evaporation temperature higher when heating is required. This effect reduces the pressure ratio and increases the SCOP and seasonal energy efficiency ratio (SEER).

In GSHP, the seasonal temperature fluctuation of the ground decreases with the depth, as shown in Figure 2 from the work of [11].

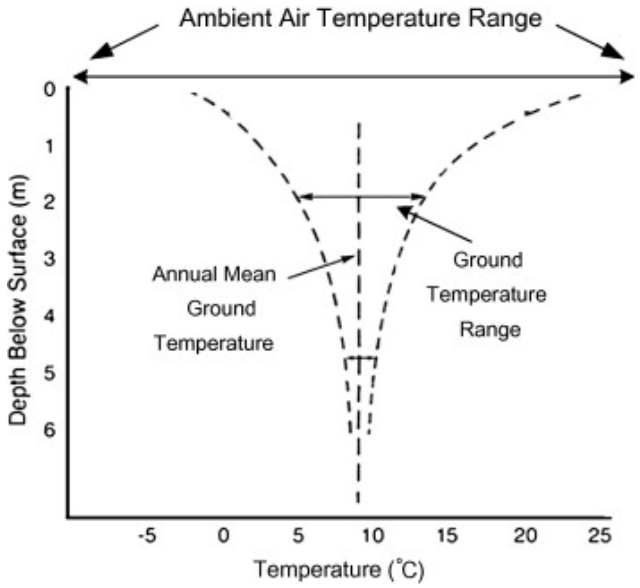

Figure 2: Ottawa's annual ground temperature [11]

GSHP, as air source heat pumps (ASHP), can work directly with their source and sink or with secondary loops. This work considered only GSHP with secondary loops for several reasons. The heat transfer from/to the ground is obtained using long pipes in different possible configurations (horizontal, trenched, spiral, vertical [12]). Owing to the low heat transfer coefficient of the ground, this piping must be extended. If the fluid inside the pipes is the refrigerant, this means a considerable volume and significant amount of refrigerant are needed, which means a tremendous initial investment.

Additionally, the pressure loss in the pipelines would affect the behaviour of the heat pump, and this pressure loss is easier to save if the fluid is pumped instead of compressed. Also, if the secondary loop is installed, the

heat pump gains compactness and can have better heat exchangers for charge specific capacity (kW/g). Lastly, if there is a leakage or need for maintenance in the ground heat exchanger, all the refrigerant would not be lost, and it is easier to operate with other secondary fluids.

Seeing the other part (demand), it is interesting to add a secondary loop too. In heating systems, using a radiant floor or water radiators, comfort is achieved with less energy consumption or pressure levels that directly make heat pumps work using heat transfer between the air and the refrigerant. For DHW production, the secondary loop prevents refrigerant and sanitary hot water from being in contact. Also, secondary loops help to improve the system compactness and, consequently, reduce the refrigerant charge.

In summary, using secondary loops instead of direct expansion makes the system need less refrigerant charge amount, have a more compact design, use less energy due to pressure losses and have less operational and investment costs. However, as a negative point, it must be said that the COP obtained is higher with direct expansion if the effect of the pressure drop in the lines is lower to the effect of temperature difference derived from the addition of the secondary loop.

1.1.3. Refrigerants

As mentioned before, heat pumps use a refrigerant to transfer heat from the source to the sink. The selection of this refrigerant is essential because it extensively affects the results obtained and the components to be used. A set of properties must be considered when selecting the refrigerant to use. One of the properties is the environmental impact. There are two things to consider in this aspect: the ODP and GWP values. Because of this impact, some refrigerants are forbidden or encouraged not to be used [13]. In the EU, this limitation are defined in the F-gas Regulation 2014

The next thing to consider is the refrigerant's thermophysical properties: mainly freezing point, critical properties, and specific heat, among others.

Then, possibly one of the most important properties is the performance. The theoretical performance of a simple cycle, infinity capacity source, and sink with a constant temperature is typically used to evaluate and compare refrigerant performance. However, the sink and source have a finite capacity in real applications. The application provokes a temperature difference between the inlet and the outlet of the secondary fluids. [14]–[16].

Regarding safety, refrigerants are classified according to their flammability and toxicity. Refrigerants are classified into four categories in the flammability classification according to the flame propagation and lower flammability level (LFL): Class 1, Class 2L, Class 2, Class 3 being non-flammable, slightly flammable, mildly flammable and highly flammable respectively. In terms of toxicity, the classification is A or B, being non-toxic and toxic depending on whether the occupational exposure limit is greater or lower than 400 ppm [13].

Higher Flammability	A3	B3
Lower Flammability	A2	B2
	A2L	B2L
No Flame Propagation	A1	B1
	Lower toxicity	Higher Toxicity

Table 2: Safety class of refrigerants [13].

It is also essential that the refrigerant selected is compatible with all the system elements. The first important materials are metals. Refrigerants usually can work with metals, and the piping is mainly made of copper. However, ammonia is incompatible with this material, brass or other copper alloys. Magnesium alloys and aluminium are not recommended if water may appear, and zinc is not recommended with R113 [13]. The following important compatibility is with lubricants. The function of oils is to increase moving surfaces' life by reducing the contact between solids or the friction between them. In the compression chamber, the oil has other functions, such as sealing between the high-pressure and the low-pressure sides, limiting the internal leakages and increasing the volumetric and issentropic efficiency, reducing the noise and transferring heat from the mechanisms to the crankcase. The refrigerant and lubricant must be chemically compatible. Its miscibility must be high enough to ensure that it returns to the compressor but must not be excessive, as it decreases the heat pump performance [17].

Due to the aforementioned, the refrigerants employed varied considerably along the history of mechanical refrigeration. The first refrigerants used were the ones that mechanically worked but were not necessarily the best. In 1932, R-12 or freon-12 was created, replacing the former refrigerants. Then, in the mid-30s, other chlorofluorocarbons (CFCs) R11, R113 and the

HCFC R22 were produced on a large scale due to their stability, non-flammability, non-toxicity and excellent compatibility. Then, it was discovered that some substances (including this family of refrigerants) were depleting the ozone layer. Consequently, in 1987, the Montreal Protocol took place to protect the ozone layer. The refrigerants employed at this moment contained chlorine particles that reacted with the ozone and destroyed the layer.

For this reason, CFCs and HCFCs were replaced by HFCs without ODP. Later, in 1994, Kyoto Protocol was thought to reduce greenhouse gas emissions, leading to a slow substitution of refrigerants, taking more into account their GWP. Nowadays, the refrigerant needs to have a low value of GWP and a null value of ODP. The refrigerants that are used currently are hydrocarbons (HCs), inorganics, HFC blends and hydro-fluoro olefins (HFOs) [18].

For this reason, there is an attempt to recover the natural refrigerants, which have shown excellent performance in vapour compression cycles. Its main problem is safety concerns. Most natural refrigerants are hydrocarbons which are highly flammable, or ammonia which is toxic, or CO2, which has a low critical temperature [16], [19]–[21]

Because of these safety concerns, if the refrigerant is flammable, the maximum amount of refrigerant charge allowed without extra safety measures is 150g [22].

1.2. Subject

After everything mentioned before, it is clear that it is interesting to firstly reduce all the energy consumption of the buildings (among others) as possible and cover the energy employed for heating, cooling and DHW that could not be reduced using heat pumps with natural refrigerant. However, as the maximum refrigerant charge is 150 g, in the case of flammable refrigerants, which are the most suitable pure refrigerants for domestic heating and DHW production application in households, it remains the doubt if it would be a feasible renewable alternative to substitute the heating boilers.

1.3. State of the Art

Due to the problems mentioned, many authors started to study the refrigerant amount in refrigeration systems and strategies for charge reduction. Poggi et al. [23] made in 2006 a bibliographical synthesis of the knowledge about the refrigerant charge at that date. Firstly, they started by collecting statistical data on the refrigerant charge required for each kW of heating capacity, using the variable of charge specific capacity described in equation (2). They pointed out that for air conditioning, the maximum C_C calculated from their sources was 20 kW/kg, 7 kW/kg for commercial refrigeration, 3 kW/kg for domestic refrigeration and 2 kW/kg for industrial refrigeration. However, all the systems they mention in the study are cooling applications.

$$C_C = \frac{\dot{Q}}{m} \quad in \quad \left(\frac{kW}{kg}\right) \tag{2}$$

Despite being focused on the present thesis in heating applications, the statistical study and the variable used to compare refrigerant charge in systems are interesting.

Using this parameter, comparing different works where vapour compression cycles are used can give us a background of at which point of refrigerant charge reduction we are, and strategies already performed for refrigerant charge reduction.

Starting with cooling applications, three main applications were found in this domain: refrigerators, water chillers and air conditioners. For the last two, some data were found regarding refrigerant charge reduction, and from the data obtained, it has been possible to calculate the C_C value. In 2008, Hrnjak and Litch presented in [24] a water chiller which uses ammonia as the refrigerant. In this work, a value of 55 kW/kg was obtained. There is data from two types of machines for air conditioning: domestic air conditioning and automotive air conditioning. In the first group, Mulroy and Didion [25], Xu et al. [26], Tang et al. [27], Chen et al. [28] and Wang et al. [29] presented their works and from them, C_C values of 2.3 kW/kg, 16.6 kW/kg, 15 kW/kg, 8.5 kW/kg and 7.1, respectively, were calculated. Lastly, in automotive air conditioning, using R290 (propane), Hrnjak and

Hoehne [30] reported a value of C_C of 10.8 kW/kg; alternatively, Peuker [31], using R134a, obtained 4.15 kW/kg.

There are three main groups in heat pump systems: air conditioning, space heaters and water heaters (where the difference between air conditioning and space heaters is the heat sink medium, air or water). Han et al. obtained in [32] a value of 4.57 kW/kg for air conditioning units, and Li et al. [33] 13.14 kW/kg. In space heating, which is the application more important for this study, using R410A, Kim et al. [34], Boahen et al. [35] and Chae and Choi [36] obtained values of 4.62 kW/kg, 0.64 kW/kg and 0.15 kW/kg with aerothermal, geothermal, and geothermal with cascade systems respectively. Using R290, Fernando et al. in 2004 [37] achieved a value of 25.7 kW/kg, Corberán et al. [38] got as well almost the same value in 2008, and Andersson et al. [39] in 2018 reached a value of 100 kW/kg in a geothermal installation using automotive components. Lastly, using other HFCs, Choi et al. [40] obtained a value of C_C of 1.35 kW/kg with R134a and Sieres et al. [41] 8 kW/kg with R407C.

Unfortunately, it was impossible to find much information about this value for refrigerators or DHW production. In this type of vapour compression cycle, stationary heating capacity is not that easily calculated and not as important as other parameters, such as the time needed to heat a water tank from an initial to an objective temperature or to cool down the food stored, face the water consumption, etc.

Table 3 summarises the value of the charge specific capacity mentioned in the literature. As told before, the focus was set more on heating systems, more concretely, liquid-to-water heating systems, to see the precedencies in this technology. However, currently, there is more information in the literature about split units and automotive air conditioners. In some cases, the value of charge specific capacity was not provided by the article itself, but it was calculated with the data found in them.

H/C	Description	C_C (kW/kg)	Refr charge (g)	Refr	Test condition	Ref
Cooling	Air-cooled chiller	55.5	234	R717	A35W7	[24]
	Air conditioner	2.3	3700	R22	A30A2	[25]
		16.62	190	R290	A35A27	[26]
		15	350	R290	A31A26	[27]
		8.5	365	R290	A35A27	[28]
		7.14	700	R744	A35A27	[29]
		20	-	-	-	[23]
	Automotive air conditioner	9.55	115	R290	A15A28	[30]
		4.15	1000	R134a	A35A35	[31]
	Refrigeration	7	-	-	-	[23]
		3	-	-	-	
		2	-	-	-	
Heating	Automotive air conditioner	4.57	1050	R410A	A7A15	[32]
	Split unit	13.14	360	R290	A7A20	[33]
	Air-water	4.62	1300	R410A	A7W30	[34]
	Brine-water	1.35	5200	R134a	W12W25	[40]
	Brine-water and water heater	8	813	R407C	B10W35	[41]
	Water-water	25.71	245	R290	A6W40	[37]
		25.5	550	R290	W10W45	[38]
		100	100	R290	B10W40	[39]
		0.64	4700	R410A	W5W40	[35]
	Cascade water-water	0.15	13200	R410A/ R134a	W5W40	[36]

Table 3: Charge Specific Capacity found in the literature.

Besides, it is also helpful to see the current situation to know the values of actual machines in the market. Luckily, in 2007, B. Palm revised these data [42], as shown in Table 4. This information must be updated to know the real market situation, but it is helpful as an initial figure.

Model	Type	H/ C	Capacity (kW)	Charge (kg)
LW 80N-I	Air water	H	7.8	1.4
LW 110H-I	Air water	H	11.7	1.9
Aeroheat 10l	Air water	H	8.5	1.4
Aerotec 3	Air water	H	6.3	1.7
Several models	Air conditioning	C	3.2	0.1-0.5
LA 9 PS	Air water		7.1	1
LA 12 PS	Air water		9.4	1.4
LA 18 PS	Air water		14.1	2
LA 22 PS	Air water		16.7	2.2
LA 26 PS	Air water		18.8	2.5
Aerotop 10l	Air water	H	8.5	1.4
HWS serie E	Brine water		3.9	0.3
HWS serie E	Brine water		7.2	0.48
HWS serie E	Brine water		12.6	0.8
HWS serie E	Brine water		18.2	1.25
HWS serie E	Brine water		27	2.1
LI10P	Air water	H	8.5	1.4
LI 10P	Air water	H	8.5	1.4
HLP90a	Air water		7.1	1
HLP120a	Air water		9.4	1.4
HLP180a	Air water		14.1	1.6
LW 110H-I	Air water	H	11.7	1.9
Pro-D 5/10 WI	Brine water		11.4	3
Pro-D 9/18 Wi	Brine water		15.6	4.5
Fighter 100P	Air-air		0.75	0.3
Fighter 200P	Air-air		1.42	0.42
Fighter 360P	Air-air		1.93	0.49
Siemens LI8H	Air water		7.8	1.4
Siemens LI11H	Air water		11.7	1.9
SuPRO Therma	Brine water		7.98	2.25
SuPRO Therma	Brine water		14.1	3.25
SuPRO Therma	Brine water		23.1	5.5
LI10P	Water-water	H	8.5	1.4
Futura HSWP 40EVU	Water-water	H	8.6	1.6
Futura HSWP 81EVU	Water-water	H	17.2	2.3
Tw 2 1/2	Water-water	H	5.3	0.35
Tw 3	Water-water	H	6.7	0.4
Tw 3 1/2	Water-water	H	7.5	0.5
Tw 4	Water-water	H	9	0.65

Model	Type	H/C	Capacity (kW)	Charge (kg)
Tw 4 1/2	Water-water	H	10.5	0.75
Tw 5	Water-water	H	0.85	0.85
Tw 6 1/2	Water-water	H	1	1

Table 4: Revision of commercial products using propane as refrigerant[42].

Summarising all the information in one graph, Figure 3 shows all the values from Table 3 and Table 4, with the heating capacity (in kW) in the abscises and the inverse of charge specific capacity, specific charge (in $g \cdot kW^{-1}$), in the ordinates. Additionally, in the chart, three auxiliary lines representing the lines of a specific amount of refrigerant charge have been added, more concretely, 150 g, 500 g and 1 kg. The target capacity between 7.5 kW and 12.5 kW has been added as vertical red dashed lines. This target heating capacity is the typical demand for single-family houses in the centre of Europe [43]. It can be seen that only one unit is in the optimum zone, and the others which have the amount required for heating capacity have more than 500 g of refrigerant charge. Unfortunately, the one heat pump that accomplishes both requirements was not ideally tested (it was already installed in one facility and not in a controlled setting [39]).

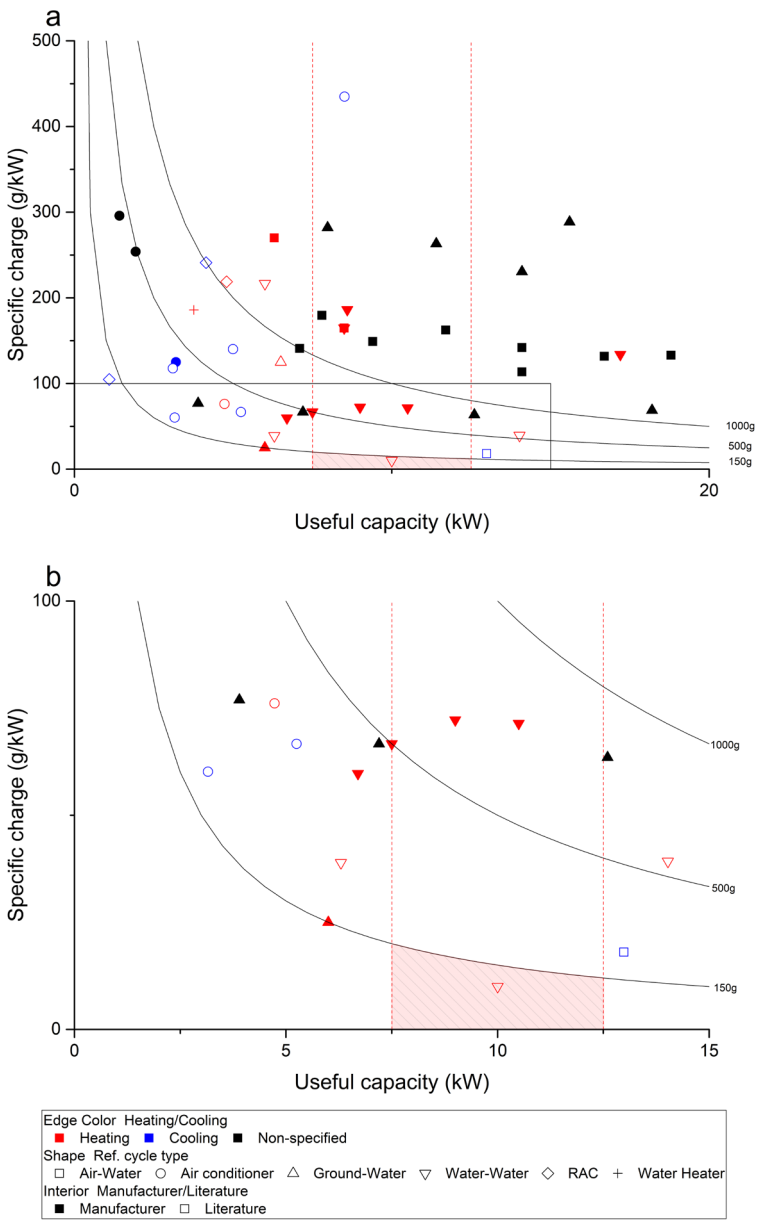

Figure 3: Summary of specific charge values found in the literature and manufacturers' data. a) all the information, b) zoomed

In Figure 3, it can also be seen that most of the heat pumps from the manufacturers have a heating capacity higher than the inferior limit of 7.5 kW said before. This information strengthens the hypothesis of having this value as the reference for a typical household. In the bottom part of the figure, there is a graph with information on the vapour compression cycles with less than 100 g/kW to see more in detail if there is anyone near this limit. Only a few machines enter this limited graph, indicating that many have a large amount of refrigerant.

To sum up, almost all the heat pumps with the required heating capacity to satisfy the needs of a regular household in Europe have more than 500 g. Also, the heat pumps with a refrigerant charge between 150 g and 500 g (being 150 g, the maximum allowed without adding additional safety measures such as a degasser, forced ventilation in case of leakage, etc.) have a heating capacity of less than 7.5 kW. Consequently, it is necessary to search for strategies for refrigerant charge reduction.

When speaking about refrigerant charge reduction, there are two main points of view: (i) to study the minimum charge that can make the system work without losing performance (a common point of view when the aim is to substitute a current system); and (ii) to study the maximum performance that can be achieved with a certain amount of refrigerant charge. Both points of view have the same objective, maximising the charge specific capacity of the system.

In our case, the objective inherits from both points of view. The first point of view is related to the limitation of 150 g of refrigerant charge for flammable refrigerants[22] and secondly, a minimum heating capacity of 8 kW that must be satisfied [43], and a minimum SCOP of 2.5 that makes the heat pump consider part of this heating capacity as obtained from a renewable source [10].

Poggi et al. [23] already mentioned refrigerant charge reduction strategies in their work. They focus on the system architecture, the refrigerant, diameters and lengths of pipes, receiver sizing and expansion devices. Other authors added other parameters to focus on.

Also, the manufacturers were focused last years on this matter. Aligned with this purpose, compressor manufacturers have designed compressors with less oil or even without lubricant. Also, heat exchanger manufacturers

are designing asymmetrical heat exchangers and non-conventional geometries for refrigerant charge reduction.

Seeing the heat pump components separately, it can be divided into the compressor, the heat exchangers, the piping, the receiver, and the expansion device. In the compressor, the most important amount of refrigerant is dissolved in the oil, so the points to consider are the amount of oil and solubility. The minimum amount of oil is the addition of the amount that makes the compressor work properly, plus the amount circulating or trapped through/in the circuit. The refrigerant oil solubility follows a trend, as shown in Figure 4.

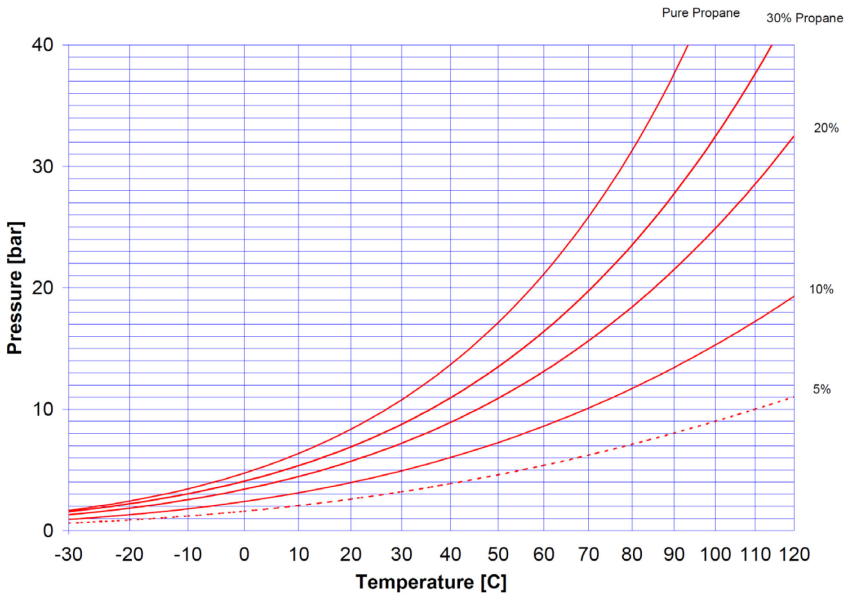

Figure 4: Example of refrigerant-oil solubility [30].

Then the following components are the heat exchangers. Compact heat exchangers shall be used to reduce the refrigerant amount without losing performance. Compactness, β, is defined as the wet surface divided by internal refrigerant volume, as shown in equation (3). The desirable compactness value would be the highest possible to reduce the refrigerant charge amount. This value is inversely dependent on the hydraulic diameter used.

$$\beta = \frac{A_w}{V_{ref}} \tag{3}$$

The heat exchangers with higher compactness values are microchannels heat exchangers (MCHE) to exchange with air and brazed plates heat exchangers (BPHE) to exchange heat with a liquid. Also, in the literature are found some different geometries to reduce refrigerant charge [37], [44], [45].

The length of the pipes could also be a significant since the liquid line can store a considerable amount of refrigerant charge in systems with long lines like split systems and direct expansion commercial systems. This problem was reported in the summary made by Poggi et al. [23] about work from David [46].

1.4. Objectives and Scope

Accordingly, to the statements mentioned in this chapter, the main objective of this Doctoral Thesis is to study the refrigerant charge experimentally to provide the tools and information to develop new heat pumps that can replace current gas boilers in households, becoming a renewable alternative to provide heating, cooling and to satisfy the DHW demands.

To achieve this global objective, different sub-objectives have been defined. These objectives are:

1. To prove that it is possible to have a ground-source heat pump able to provide enough heating capacity for domestic space heating with less than 150g of R290.
2. To obtain experimental data about refrigerant charge distribution and performance of ground source heat pumps at different conditions, geometries and control strategies.
3. To analyse the performance data and refrigerant distribution to understand how the condition variations affect to the refrigerant charge in each component and also the variations due to the change in geometry.
4. To develop strategies for refrigerant charge reduction.

To achieve these objectives, the subsequent actions have been taken place:

1. To design and build a ground-source heat pump of about 8 kW of heating capacity for experimental analysis.
2. To design an experimental campaign wide enough to consider different scenarios of working conditions. Considering compressor speed, external conditions, and sizing of the components.
3. To perform experimental tests
4. To analyse the data.

As it has been said, the scope of this thesis is limited by ground-source heat pumps for domestic heating. However, part of this study can be used for other refrigeration cycles or refrigeration cycles used for other purposes.

1.5. IUIIE's Thermal Area and LC150 Project

The IUIIE was founded in 2001 at UPV to study all the energy fields in a multidisciplinary way and to evaluate trends in this field. It is divided into five different areas, and this thesis was framed in the Thermal area, which tackles the following knowledge areas:

1. Basic research about heat transfer and heat exchangers.
2. InfraRed thermography.
3. Refrigeration equipment and heat pump development and optimisation.
4. Refrigeration and air conditioning modelling and software development.
5. Alternative refrigeration systems.
6. Building air conditioning with low enthalpy geothermal systems.
7. Energy efficiency in buildings
8. Complex energetic systems analysis and optimisation.

This Doctoral Thesis is aligned mostly with knowledge areas three and four (Refrigeration equipment and heat pump development and optimisation, refrigeration and air conditioning modelling and software development.).

Also, during the development of this doctoral thesis, there was a partnership between IUIIE and Fraunhofer ISE, which meant a collaboration of the IUIIE inside the project LC150. I was also part of the project LC150 internally in Fraunhofer ISE during a six-month international stay in Freiburg im Briesgau.

1.6. Thesis structure

This thesis is organised as follows. In Chapter 1, the motivation is explained. Also, state of the art is located here trying to answer if it is possible to achieve the heating capacity needs with the safety limitations, if this has been achieved before, which refrigerant charge reduction techniques have been used in the past, and in which way this work can fulfil the needs.

Then in Chapter 2, the methodology employed in the work is explained. This consists of two different methods. Firstly, there is the experimental part, where the prototype, instrumentation and control loops are described, and secondly, the tools and techniques used in the data analysis.

In the following chapter, Chapter 3, the results obtained are shown. This chapter corresponds to the experimental results, both performance and refrigerant charge distribution, analysing and comparing with the simulation software.

Lastly, the final chapter, Chapter 4, exposes the conclusion and a thought on future work.

References

[1] M. J. Menne, C. N. Williams, B. E. Gleason, J. Jared Rennie, and J. H. Lawrimore, "The Global Historical Climatology Network Monthly Temperature Dataset, Version 4," *J Clim*, vol. 31, no. 24, pp. 9835–9854, Dec. 2018, doi: 10.1175/JCLI-D-18-0094.1.

[2] O. Hoegh-Guldberg *et al.*, "Impacts of 1.5°C of Global Warming on Natural and Human Systems," V. Masson-Delmotte, P. Zhai, H. -O. Pörtner, D. Roberts, J. Skea, P.R. Shukla, A. Pirani, W. Moufouma-Okia, C. Péan, R. Pidcock, S. Connors, J.B.R. Matthews, Y. Chen, X. Zhou, M.I. Gomis, E. Lonnoy, T. Maycock, M. Tignor, and T. Waterfield, Eds., Cambridge: Cambridge University Press, 2018. doi: 10.1017/9781009157940.005.

[3] "A European Green Deal | European Commission." https://ec.europa.eu/info/strategy/priorities-2019-2024/european-green-deal_en (accessed Jan. 20, 2022).

[4] "2050 long-term strategy." https://ec.europa.eu/clima/eu-action/climate-strategies-targets/2050-long-term-strategy_en (accessed Jan. 20, 2022).

[5] "Energy consumption in households - Statistics Explained." https://ec.europa.eu/eurostat/statistics-explained/index.php?title=Energy_consumption_in_households#Energy_products_used_in_the_residential_sector (accessed Jul. 28, 2021).

[6] European Commission, "Heating and cooling | Energy." https://ec.europa.eu/energy/en/topics/energy-efficiency/heating-and-cooling (accessed Feb. 04, 2019).

[7] European Commission, "Building and renovating," *The European Green Deal*, 2019, doi: 10.2775/466559.

[8] "Nearly zero-energy buildings | Energy." https://ec.europa.eu/energy/topics/energy-efficiency/energy-efficient-buildings/nearly-zero-energy-buildings_en (accessed Dec. 27, 2021).

[9] "ZEBRA 2020-NEARLY ZERO-ENERGY BUILDING STRATEGY 2020 Strategies for a nearly Zero-Energy Building market transition in the European Union," 2016.

[10] European Comission, "DIRECTIVE 2009/28/EC OF THE EUROPEAN PARLIAMENT AND OF THE COUNCILof 23 April 2009on the promotion of the use of energy from renewable sources and amending and subsequently repealing Directives 2001/77/EC and 2003/30/EC," *Official Journal of the European Union*, 2009.

[11] S. J. Self, B. V. Reddy, and M. A. Rosen, "Geothermal heat pump systems: Status review and comparison with other heating options," *Appl Energy*, vol. 101, pp. 341–348, Jan. 2013, doi: 10.1016/J.APENERGY.2012.01.048.

[12] A. Mustafa Omer, "Ground-source heat pumps systems and applications," *Renewable and Sustainable Energy Reviews*, vol. 12, no. 2, pp. 344–371, Feb. 2008, doi: 10.1016/J.RSER.2006.10.003.

[13] American Society of Heating Refrigerating and Air-conditioning Engineers, *ASHRAE Handbook - Fundamentals*. 2017.

[14] L. Sánchez-Moreno-Giner, E. López-Juárez, J. Gonzálvez-Maciá, and A. H. Hassan, "Thermodynamic Assesment of Ultra-Low-Global Warming Potential Refrigerant for Space and Water Heaters," *Heat Transf Res*, vol. 51, no. 14, pp. 1317–1335, 2020, doi: 10.1615/HEATTRANSRES.2020035317.

[15] G. Nellis and S. Klein, *Heat Transfer*, vol. 1, no. 69. Cambridge University Press, 2009.

[16] M. Pitarch, E. Navarro-Peris, J. Gonzálvez-Maciá, and J. M. Corberán, "Evaluation of different heat pump systems for sanitary hot water production using natural refrigerants," *Appl Energy*, vol. 190, pp. 911–919, Mar. 2017, doi: 10.1016/j.apenergy.2016.12.166.

[17] American Society of Heating Refrigerating and Air-conditioning Engineers, *ASHRAE Handbook - Refrigeration*. 2018.

[18] S. Kujak and K. Schultz, "Insights into the next generation HVAC&R refrigerant future," *Sci Technol Built Environ*, vol. 22, no. 8, pp. 1226–1237, 2016, doi: 10.1080/23744731.2016.1203239.

[19] G. Lorentzen, "The use of natural refrigerants: a complete solution to the CFC/HCFC predicament," *International Journal of Refrigeration*, vol. 18, no. 3, pp. 190–197, Mar. 1995, doi: 10.1016/0140-7007(94)00001-E.

[20] P. A. Domanski, R. Brignoli, J. S. Brown, A. F. Kazakov, and M. O. McLinden, "Frigorigènes à faible GWP pour les applications à moyenne et haute pression," *International Journal of Refrigeration*, vol. 84, pp. 198–209, Dec. 2017, doi: 10.1016/j.ijrefrig.2017.08.019.

[21] M. O. McLinden, J. S. Brown, R. Brignoli, A. F. Kazakov, and P. A. Domanski, "Limited options for low-global-warming-potential refrigerants," *Nat Commun*, vol. 8, Feb. 2017, doi: 10.1038/ncomms14476.

[22] European Committee for Standardization, "EN 378-1:2016 Refrigerating Systems and Heat Pumps - Safety and Environmental Requirements - Part 1: Basic Requirements, Definitions, Classification and Selection Criteria," 2016.

[23] F. Poggi, H. Macchi-Tejeda, D. Leducq, and A. Bontemps, "Refrigerant charge in refrigerating systems and strategies of charge reduction," *International Journal of Refrigeration*, vol. 31, no. 3, pp. 353–370, May 2008, doi: 10.1016/J.IJREFRIG.2007.05.014.

[24] P. Hrnjak and A. D. Litch, "Microchannel heat exchangers for charge minimization in air-cooled ammonia condensers and chillers," *International Journal of Refrigeration*, vol. 31, no. 4, pp. 658–668, Jun. 2008, doi: 10.1016/J.IJREFRIG.2007.12.012.

[25] W. J. Mulroy and D. A. Didion, "Refrigerant Migration in a Split-Unit Air Conditioner.," *ASHRAE Transactions*, vol. 91, no. pt 1A. pp. 193–206, 1985. Accessed: Feb. 26, 2021. [Online]. Available: https://www.nist.gov/publications/refrigerant-migration-split-unit-air-conditioner

[26] B. Xu, Y. Wang, J. Chen, F. Li, D. Li, and X. Pan, "Investigation of domestic air conditioner with a novel low charge microchannel condenser suitable for hydrocarbon refrigerant," *Measurement (Lond)*, vol. 90, pp. 338–348, Aug. 2016, doi: 10.1016/j.measurement.2016.04.034.

[27] W. Tang, G. He, D. Cai, Y. Zhu, A. Zhang, and Q. Tian, "The experimental investigation of refrigerant distribution and leaking characteristics of R290 in split type household air conditioner," *Appl Therm Eng*, vol. 115, pp. 72–80, Mar. 2017, doi: 10.1016/j.applthermaleng.2016.12.083.

[28] R. Chen, J. Wu, and J. Duan, "Performance and refrigerant mass distribution of a R290 split air conditioner with different lubricating oils,"

Appl Therm Eng, vol. 162, p. 114225, Nov. 2019, doi: 10.1016/j.applthermaleng.2019.114225.

[29] A. Wang, X. Yin, J. Fang, and F. Cao, "Refrigerant Distributions and Dynamic Migration Characteristics of the Transcritical CO2 Air Conditioning System," *International Journal of Refrigeration*, Jun. 2021, doi: 10.1016/j.ijrefrig.2021.06.009.

[30] P. S. Hrnjak and M. R. Hoehne, "Charge minimization in systems and components using hydrocarbons as a refrigerant," *ACRC TR-224*, vol. 61801, no. 217, 2004.

[31] S. Peuker, "Experimental and analytical investigation of refrigerant and lubricant migration," University of Illinois at Urbana-Champaign, 2010. doi: 10.1007/978-3-319-30602-5_43.

[32] B. Han, G. Yan, and J. Yu, "Refrigerant migration during startup of a split air conditioner in heating mode," *Appl Therm Eng*, vol. 148, pp. 1068–1073, Feb. 2019, doi: 10.1016/j.applthermaleng.2018.11.126.

[33] T. Li *et al.*, "Measurement of refrigerant mass distribution within a R290 split air conditioner," *International Journal of Refrigeration*, vol. 57, pp. 163–172, Sep. 2015, doi: 10.1016/J.IJREFRIG.2015.05.012.

[34] D. H. Kim, H. S. Park, and M. S. Kim, "The effect of the refrigerant charge amount on single and cascade cycle heat pump systems," *International Journal of Refrigeration*, vol. 40, pp. 254–268, Apr. 2014, doi: 10.1016/J.IJREFRIG.2013.10.002.

[35] S. Boahen, K. H. Lee, and J. M. Choi, "Refrigerant Charge Fault Detection and Diagnosis Algorithm for Water-to-Water Heat Pump Unit," *Energies 2019, Vol. 12, Page 545*, vol. 12, no. 3, p. 545, Feb. 2019, doi: 10.3390/EN12030545.

[36] J. H. Chae and J. M. Choi, "Evaluation of the impacts of high stage refrigerant charge on cascade heat pump performance," *Renew Energy*, vol. 79, no. 1, pp. 66–71, Jul. 2015, doi: 10.1016/J.RENENE.2014.07.042.

[37] P. Fernando, B. Palm, P. Lundqvist, and E. Granryd, "Propane heat pump with low refrigerant charge: design and laboratory tests," *International Journal of Refrigeration*, vol. 27, no. 7, pp. 761–773, Nov. 2004, doi: 10.1016/J.IJREFRIG.2004.06.012.

[38] J. M. Corberán, I. O. Martínez, and J. Gonzálvez, "Charge optimisation study of a reversible water-to-water propane heat pump," *International*

Journal of Refrigeration, vol. 31, no. 4, pp. 716–726, 2008, doi: 10.1016/j.ijrefrig.2007.12.011.

[39] K. Andersson, E. Granryd, and B. Palm, "Water to water heat pump with minimum charge of propane," in *Refrigeration Science and Technology*, International Institute of Refrigeration, 2018, pp. 725–732. doi: 10.18462/iir.gl.2018.1264.

[40] H. Choi, H. Cho, and J. M. Choi, "Refrigerant amount detection algorithm for a ground source heat pump unit," *Renew Energy*, vol. 42, pp. 111–117, Jun. 2012, doi: 10.1016/j.renene.2011.08.055.

[41] J. Sieres, I. Ortega, F. Cerdeira, and E. Álvarez, "Influence of the refrigerant charge in an R407C liquid-to-water heat pump for space heating and domestic hot water production," *International Journal of Refrigeration*, vol. 110, pp. 28–37, Feb. 2020, doi: 10.1016/j.ijrefrig.2019.10.021.

[42] B. Palm, "Hydrocarbons as refrigerants in small heat pump and refrigeration systems - A review," *International Journal of Refrigeration*, vol. 31, no. 4, pp. 552–563, 2008, doi: 10.1016/j.ijrefrig.2007.11.016.

[43] J. Lund, "Geothermal heat pumps - An overview," *Geo-Heat Center Quarterly Bulletin*, vol. 22, no. 1, pp. 1–2, 2001, Accessed: Dec. 29, 2021. [Online]. Available: https://www.researchgate.net/publication/242159982

[44] R. Ghoubali, P. Byrne, and F. Bazantay, "Refrigerant charge optimisation for propane heat pump water heaters," *International Journal of Refrigeration*, vol. 76, pp. 230–244, Apr. 2017, doi: 10.1016/J.IJREFRIG.2017.02.017.

[45] A. Cavallini, E. Da Riva, and D. Del Col, "Performance of a large capacity propane heat pump with low charge heat exchangers," *International Journal of Refrigeration*, vol. 33, no. 2, pp. 242–250, 2010, doi: 10.1016/j.ijrefrig.2009.10.010.

[46] L. David, "Instrumentation et caractérisation du fonctionnement d'une installation frigorifique classique," Antony, 2002.

Chapter 2: Methodology

The methodology employed in this thesis to analyse the refrigerant charge is mainly experimental. The experimental campaign consists of two prototypes' performance and refrigerant distribution analysis. All the tests have to be precise and repeatable to be helpful. For this reason, the measured variables have to give valuable information with low uncertainty. This chapter will explain the methodology used, how to calculate the precision obtained, and the uncertainty committed.

The content of this chapter follows the following structure:

The first part, section 2.1, describes how the refrigerant extraction method was selected. To do it, previous theoretical and experimental work was performed.

Succeeding section, 2.2, describes the test prototypes. Here are defined the components of the heat pump with their main characteristics. Then, 2.3 explains all the sensors used and their location to know which variable is measuring and to see the error committed while measuring. Section 2.4 describes the uncertainty analysis.

Section 2.5 explains how the tests are performed, and section 2.6 describes which tests are performed.

The final section, 2.7, explains the analysis of the data obtained from the tests concerning the refrigerant charge distribution and how this data can improve the current predictions made with the software IMST-ART.

2.1. Refrigerant extraction methods

Before starting the test campaign to know the refrigerant distribution in heat pumps, it is crucial to know if the method employed in the different tests will provide the best results or at least with acceptable accuracy. In this case, the object of the study is the refrigerant charge system circulating inside each heat pump component under different working conditions.

To know how this information will be measured in the tests, a bibliographical study of refrigerant charge measurements and refrigerant charge extraction was done. Then, an experimental study was done to choose one of the methods from the literature, analysing their precision and feasibility.

Two methods are mainly used in the literature: (i)the online method and (ii)the quick closing valve method. All methods are summarised in Figure 5 from Peuker's Thesis [1].

Online methods consist of weighing the parts of interest in knowing the amount of refrigerant charge while the system is still running. Nevertheless, the Quick Closing Valve Technique (QCVT) must stop the test to evaluate the amount of refrigerant charge inside each component or part of the circuit.

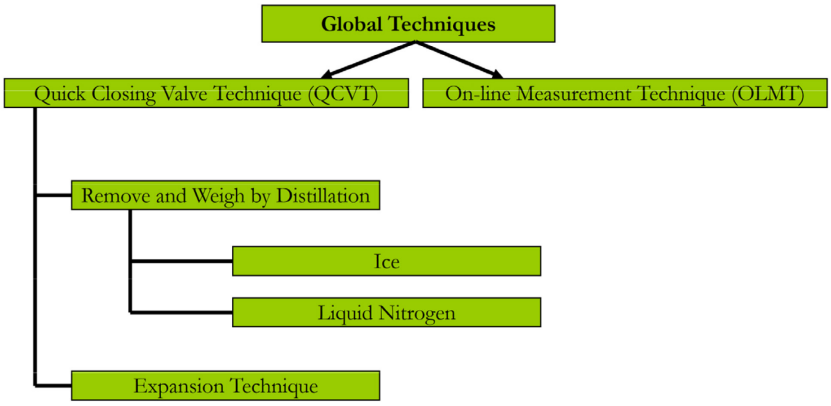

Figure 5: Techniques of measuring refrigerant charge. Source:[1]

Online methods are faster and less intrusive since they don't need to stop the refrigerant circuit from running and separate the elements from measuring or extracting the refrigerant charge from them. However, these methods are costly. They need expensive equipment, which is less precise than the alternative [2], [3]. Also, the component must be weighted with the refrigerant inside, and the weight of the refrigerant is much lesser than the weight of the element. This weight is sometimes about 2% of the total mass. Also, all the components are under vibration when the system runs, making the measuring more complex and less reliable or stable.

On the other hand, QCVT is much slower because the system has to be interrupted. Once the valves are closed and the system stops, the refrigerant must be measured. The most common approach to measuring the refrigerant is called the Remove and Weight Technique (RWT), done by distillation. This technique involves extracting the refrigerant from the section to be measured to a previously tared sample cylinder, generating a

pressure or temperature gradient. Tanaka et al. [4] were the first to mention this technique in 1982, and it has been widely used to know refrigerant distribution and migration. Examples of these uses are [5]–[8] and [1], [9]–[11], respectively. The sample cylinder is usually cooled down using liquid nitrogen; however, it is not the only option, P. Fernando [12] used liquified air instead. Bjork [2] proposed using a big tank to ensure the refrigerant expansion until reaching a superheated state. Once in the gas phase, it is easy to calculate the density by knowing the thermophysical properties. Ding et al. [3] proposed something similar to the liquid nitrogen method. And in the ASHRAE RP-1785 [13], they separated the components from each other and compared the weight to the tare weight to know the amount of refrigerant plus oil inside.

A previous study was performed to know which method would be suitable for the thesis to analyse the refrigerant charge distribution in the heat pump.

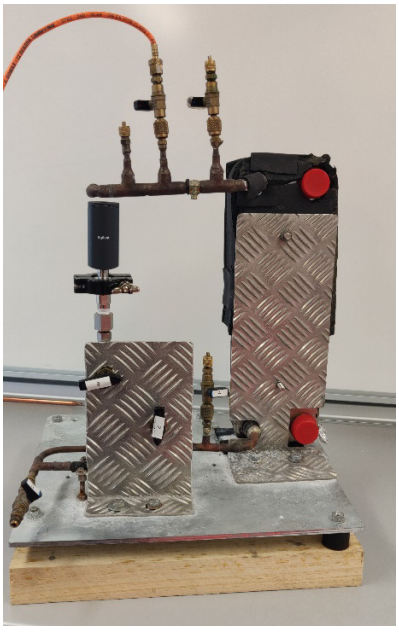

Figure 6: Prototype for refrigerant extraction.

Figure 7: Sample cylinder submerged in glycol with PCMs.

In this work, the extraction methods were studied using a prototype. This prototype consisted of a BPHE connected with closed tubes equipped with

quick connections to ball valves to attach equipment, such as pressure sensors, the sample cylinder to do the extraction, and the pure refrigerant cylinder, as shown in Figure 6.

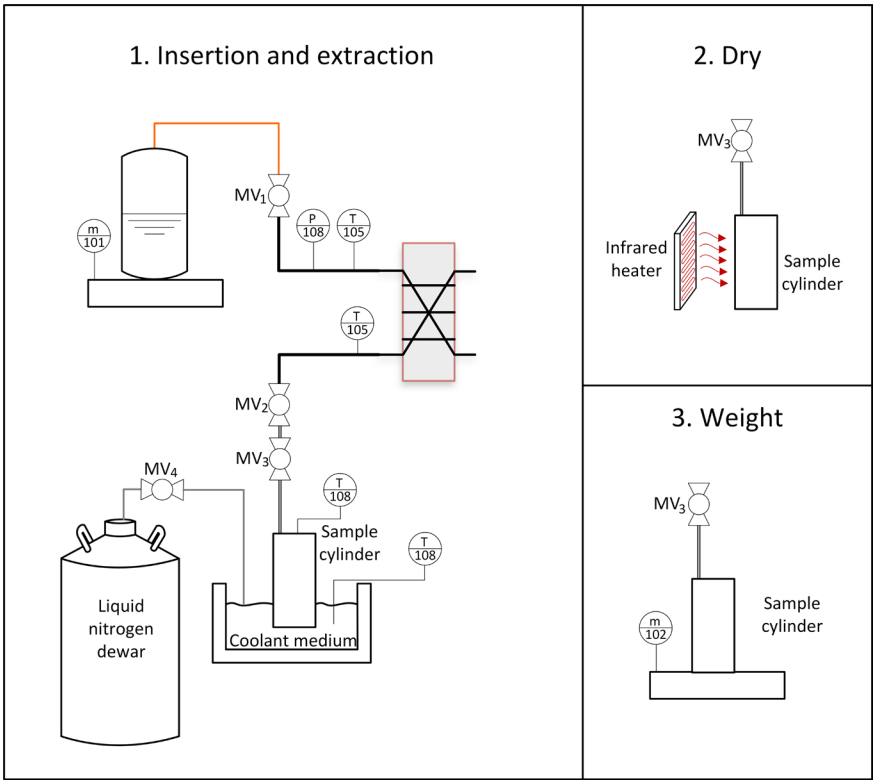

Figure 8: Scheme and procedure of refrigerant extraction study.

The study consisted in charging a controlled and measured amount of pure refrigerant into the prototype and extracting it by distillation with the sample cylinder submerged in different fluids, Figure 7. The scheme and the process explained can be observed in Figure 8.

Then to increase accuracy, using the final remaining pressure and the temperature, it was possible to calculate the theoretical remaining refrigerant charge inside the prototype and add it to the measured amount inside the cylinder. This remaining refrigerant, which is in the gas phase, is calculated with the density, equation(4), estimated using the pressure and temperature and the thermophysical properties of the refrigerant from the Refprop Database Version 10 database [14].

$$m_{rem,i} = V_i \cdot \rho_i(P_i, T_i) \tag{4}$$

This work compared the feasibility of using ice, phase-change material (PCM) with a melting temperature of -18^{o}C and liquid nitrogen (LN_2) as the chilling medium. The results can be seen in Figure 9, Figure 10, and Figure 11 (more details of this study can be found in [15]). In these figures, the addition of the refrigerant extracted with the calculated amount remaining inside with equation (4) is compared to the amount inserted.

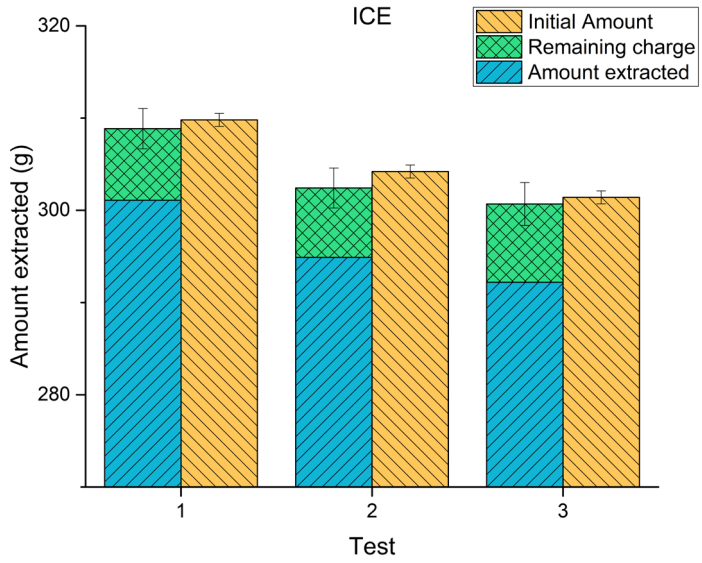

Figure 9: Results of extraction using ice.

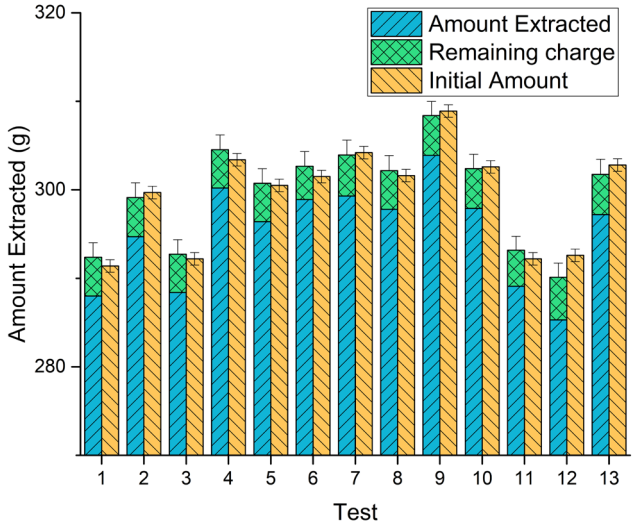

Figure 10: Results of extraction using PCM(18^{o}C).

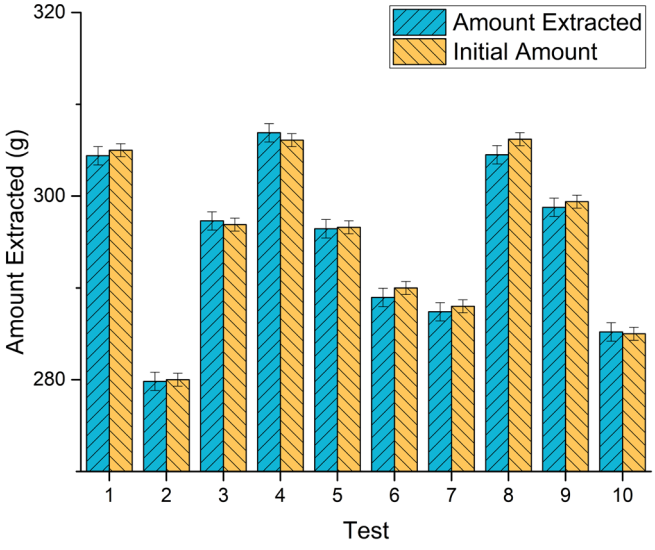

Figure 11: Results of extraction using LN_2.

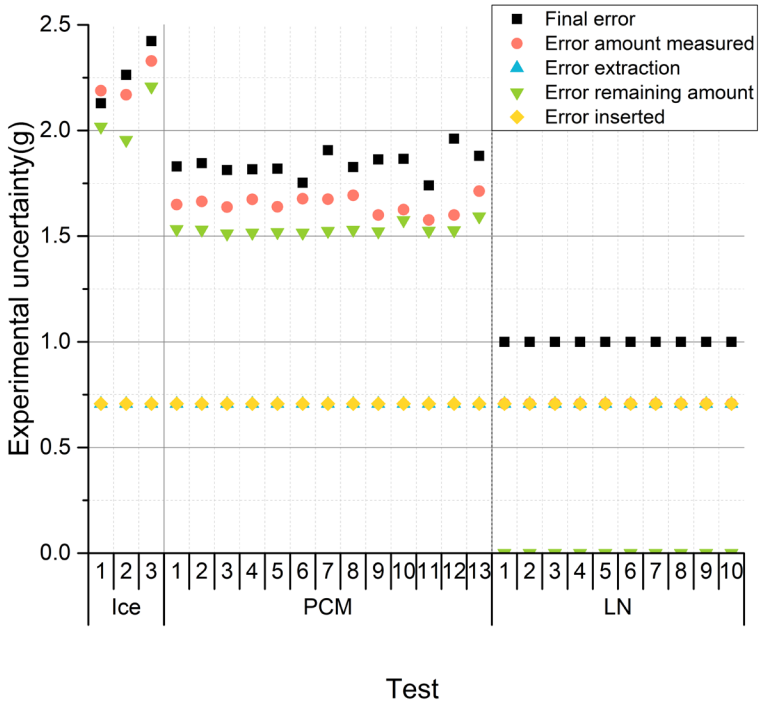

Figure 12: Errors committed in each test

Figure 12 shows the different tolerances in the steps performed on each test depending on the refrigerant extraction method used. The error of the amount extracted and inserted is the same, as the same scale was used and calibrated just before the test. It can also be seen that the tolerances of the extraction are directly related to the error of the amount measured, which also corresponds to the error in the calculation of the refrigerant amount remaining inside the prototype. The more refrigerant extracted, the more precise the method is.

Consequently, the best method to extract precisely is using LN_2. Still, if the remaining theoretical amount is added when using the PCM, the results are reliable, and the uncertainty is not much higher. After the results of this previous study, it was concluded to use liquid nitrogen to prevent adding uncertainties to the outcome. However, if we had used PCMs, similar results would have been obtained.

2.2. Test prototypes

Two prototypes were used to obtain data from different working conditions in the experimental campaign. Both were GSHP with a theoretical design heating capacity of 9kW approximately at the rating conditions, B0W35[1], from the standard EN 14511-2 [16] at full compressor speed (120 rps). The only difference between them is the BPHE working as the evaporator, which was changed from one bigger to another smaller.

The installation scheme can be seen in Figure 13, and as it shows, it is a GSHP connected to two secondary loops. On the secondary side connected to the condenser, water inside is used as a sink of the heat from the condenser that drives this heat to a chiller. By contrast, in the secondary loop connected to the evaporator, the fluid is a mixture of ethylene glycol (EG) and water with a concentration in the volume of EG of 39 %, i.e. a freezing temperature of -24 ºC. In the refrigerant circuit, the refrigerant used was propane (R290).

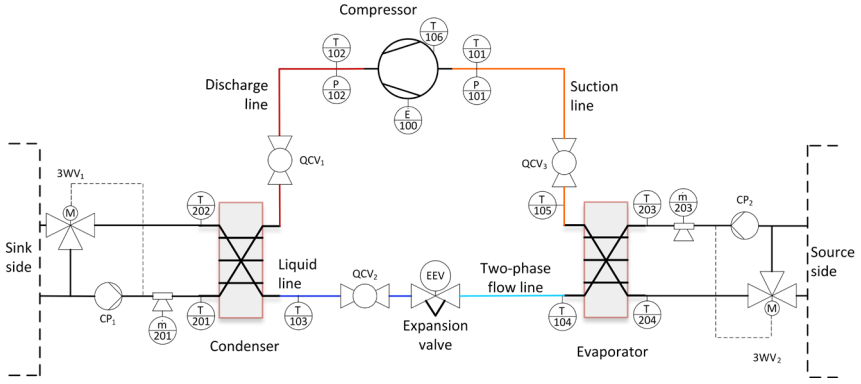

Figure 13: Installation scheme.

[1] first letter is the source type, first number is the source temperature, second letter is the sink type, second number is the sink temperature. Source/sink types are B: brine, W:Water, A:Air

Temperature				Pressure		Mass flow rate		Power absorbed	
Refrigerant side		Secondary fluid side		Refrigerant side		Secondary fluid side			
Loc	Var	Loc	Var	Loc	Var	Loc	Var	Loc	Var
101	$T_{comp,in}$	201	$T_{w,in}$	101	P_{suc}	201	$\dot{m}_w$	100	$\dot{E}_{comp}$
102	$T_{comp,out}$	202	$T_{w,out}$	102	P_{dis}	203	$\dot{m}_b$		
103	$T_{cond,out}$	203	$T_{b,in}$						
104	$T_{evap,in}$	204	$T_{b,out}$						
105	$T_{evap,out}$								
106	T_{oil}								

Table 5: Variables of the scheme and their location.

As shown in Figure 13, the GSHP configuration is a simple cycle with quick closing valves (QCV). That means the main components of this heat pump are the compressor, heat exchangers, electronic expansion valve, tubes, and QCV.

The compressor is a rotary compressor with a compression chamber of 30.6 cm^3. It has a small deposit to prevent refrigerant liquid from entering the compression chamber. The oil was in the crankcase where the refrigerant went after compression. It was polyvinyl ether, and the total amount was 0.4 dm^3. A summary of the compressor's characteristics can be found in Table 6. The internal volume of the crankcase was calculated from an isothermal gas test, explained further on.

Compressor type	Rotary
Swept volume (cm^3/ rev)	30.6
Speed range (rps)	20-120
Internal volume* (dm^3)	1.99
Oil type	POE
Oil amount (dm^3)	0.4
Weight (kg)	13.8
*Calculated with the isothermal gas method	

Table 6: Compressor characteristics

Heat exchangers, as mentioned before, are BPHE. The condenser is asymmetric, with an internal volume of the refrigerant side of 0.39 dm^3. Its dimensions are 75 mm in depth, 76 mm in width and 393 mm in height. Its number of plates is 38.

The evaporator of the first prototype is a symmetric BPHE with an internal volume of 0.66 dm^3, a total number of plates of 16 and dimensions of 69 mm length, 113 mm width and 529 mm height.

The evaporator of the second prototype is an asymmetric BPHE with 14 plates, an internal volume of 0.26 $dm^{3,}$ and dimensions of 56 mm length, 119 mm width and 376 mm height.

BPHE	Condenser	Evaporator v1	Evaporator v2
Type	Asymmetric	Symmetric	Asymmetric
Number of plates (including external)	38	16	14
Heat transfer area (m^2)	1.04	0.85	0.49
Internal volume refrigerant side (dm^3)	0.39	0.66	0.26
Dimensions Depth x Width x Height (mm)	75x76x393	69x113x529	56x119x376

Table 7: BPHE characteristics.

The expansion device is an electronic expansion valve which opens or closes the throttling area controlling the superheat (SH) value.

The pipes that connect the components were the same for both prototypes, and their diameter and length can be seen in Table 8. They were minimised in volume as much as possible to reduce the system's charge.

Line	External Diameter(mm)	Length (mm)
Suction line	18	1000
Discharge line	12	1060
Liquid line	12	200
Two-phase flow line	12	130

Table 8: Pipe sizing.

The QCV shut off the system and isolated one section from another. They were actioned mechanically with compressed nitrogen to close in less than one second and ensure no migration after the compressor stopped. For this

purpose, there was no leakage through the valve from one side to the other and neither to the ambient. This tightness was previously verified with a pressure test. The sections isolated by the quick closing valves are shown in Figure 13 and Table 9.

As done in the refrigerant extraction method study, the refrigerant distribution study's remaining refrigerant in each section is calculated using the estimated density value with the measured thermophysical properties and determining the volumes of each section previously. To calculate these volumes, isothermal gas tests were done before the campaign. In these isothermal gas tests, we charge each section with a controlled amount of nitrogen and measuring the pressure and temperature. Then, the volume can be calculated again with equation. (4) but converted into equation. (5).

$$V_i = \frac{m_{N,i}}{\rho_i\,(P_i, T_i)} \tag{5}$$

The value of the section volumes obtained with the isothermal gas test was compared with the volume calculated and the manufacturer's data, except for the compressor section, where there was no information about its internal volume from the manufacturers. The volumes of each section are shown in Table 9. The comparison agrees in order of magnitude, so the measured volume is valid.

	Section	1-Compressor + Discharge Line+ Suction line	2-Condenser + Liquid Line	3-Evaporator + EEV + Two-Phase Line
Prototype 1	Measured volume (dm^3)	2.48	0.48	0.85
	Calculated volume (dm^3)	-	0.44	0.82
Prototype 2	Measured volume (dm^3)	2.48	0.48	0.45
	Calculated volume (dm^3)	-	0.44	0.42

Table 9: Internal volume of different sections.

2.3. Sensors and control system

Figure 13 shows the location of the sensors used to measure the different variables during the tests while the heat pump was running. In the refrigerant circuit, the sensors employed are PT100 class B for temperature measures, pressure transducers for measuring absolute pressure at the suction and discharge of the compressor, and the compressor consumption is determined using a power analyser. The temperature sensors mentioned are in contact with the tube with thermal paste, except the one located in the condenser outlet, which is inside the stream, for increasing accuracy.

On the secondary fluid circuits, source and sink, the inlet and outlet temperature were measured using PT100 class A in the fluid stream, and their mass flow rates were measured using Coriolis mass flow meters.

A scale (scale A from Table 10) was used for refrigerant insertion in the system. Meanwhile, scale B from Table 10 was used to measure the refrigerant extraction. The mass inserted is measured only once, while scale B measures every second during the extraction. It is connected to the sample cylinder and isolated with ball valves. Additionally, a pressure transducer measures the pressure of the system connected to the sample cylinder to calculate the refrigerant remaining on each section after the extraction is performed. Lastly, a thermocouple was used to know the sampling cylinder's temperature due to its resistance at low temperatures.

All sensors and their associated systematic uncertainty can be seen in Table 10. The RTD's uncertainty is calculated using the standard IEC 60751:2022 [17].

Variable measured	Type of sensor	Systematic Uncertainty 2σ (95% Confidence)
Temperature	PT100 class B	±0.3+0.005T (ºC) (3σ)
Temperature	PT100 class A	±0.15+0.002T (ºC) (3σ)
Temperature	Thermocouple type T	±0.8 or 0.75 % of the measure (ºC)
Circuit Pressure	Pressure transducer 1	0.25 % of the span
Gas pressure	Pressure transducer 2	0.04 % of the span
Mass flow	Coriolis mass flow meter	0.10 % of the measure
Mass extracted	Scale A	0.15 (g)
Mass inserted	Scale B	0.01+0.002m (g)
Power absorbed	Power analyser	0.6 % of the span

Table 10: Sensors and their uncertainty.

All these sensors (except scale A) measure each variable every second during the tests to reduce the random uncertainty. Temperature and pressure sensors were checked before its use with a high accuracy sensor and the scales were calibrated.

Water and brine circuits are driven with variable-speed circulation pumps for the control system. These flow rates are adjusted according to the standard EN 14511-3 [18], having as constant the temperature difference between the inlet and outlet of 5 K (or 8K for high temperature heating) for the sink side and 3 K for the source side. To control the water or brine inlet temperature, a three-way valve (3WV) is located in the source/sink circuit to control the energy absorbed or removed from the secondary loops. These loops are also connected to different elements to absorb/release heat to maintain the conditions constant.

2.3.1. Infrared pictures

To get complete information about the behaviour of the components, infrared (IR) pictures were taken in many test conditions. The main objective of these IR was to see the maldistribution qualitatively in the evaporator. Also, IR pictures of the condenser were taken. Still, it usually is better distributed than the evaporator due to the single-phase nature of

the refrigerant at the inlet and outlet, while in the evaporator only single-phase is found in the evaporator outlet. Under some conditions, an IR picture of the compressor was taken to help understand this component's heat losses. As commented, the purpose of these IR pictures was purely to know qualitative the temperature gradients in the components. Still, the value of the actual measure is known to be inaccurate. The emissivity value of the surfaces measured was not corrected, but the elements were painted with a thin layer of chalk spray to improve the captions. The IR camera was VarioCAM high resolution from Infratech (Figure 14).

Figure 14: Infrared camera used.

2.4. Uncertainty analysis

Uncertainty analysis was executed for performance and refrigerant distribution measurements at every test. For this analysis, knowing the uncertainty associated with the sensors is essential. The systematic part is included in the sensors' list in Table 10, but the random part of the uncertainty must also be considered. The systematic uncertainty corresponds to errors that don't vary during the measuring period, while random uncertainty vary.

The only variable that was measured as a single point on every test was m_{ins}. However, the typical deviation is inferred from the sample uncertainty obtained from a previous test. In this previous test, the scale

used for m_{ins} was used to perform several measurements to calculate the random uncertainty of the scale with a significant sample. Then, as only one measure was possible, we assumed that the typical deviation was the same as the previous one obtained. Using the method explained in [19] to expand the uncertainty to our measurements, the expanded random uncertainty of m_{ins} is ±0.83 g was obtained. The rest of the measured variables were recorded once per second, reducing the random uncertainty.

Then, to calculate the overall uncertainty, systematic and random uncertainties are combined using the assumption of a large sample [19] as written in equation (6).

$$U_{95} = 1.96u = 1.96\sqrt{s^2 + b^2} \tag{6}$$

Where U is the uncertainty, its subscript is the acceptance level, u is the combined standard uncertainty, s is the random standard uncertainty, and b is the systematic standard uncertainty.

Table 11 shows the systematic random and overall uncertainty of the different variables considered in the results.

Variable	Systematic uncertainty from sensor and installation (95% confidence)	Random uncertainty (95% confidence)	Overall uncertainty (95% confidence)
$T_{w,in}$	±0.14 C	±0.01 C	±0.14 C
$T_{w,out}$	±0.15 C	±0.01 C	±0.15 C
$\dot{m}_w$	±0.87 kg h^{-1}	±0.25 kg h^{-1}	±0.90 kg h^{-1}
$\dot{E}_{comp}$	±16.2 W	±0.13W	±16.2 W
m_{ins}	±1.62 g	±0.83 g	±1.82 g*
m_{ext}	±0.15 g	±0.02 g	±0.15 g
V_{comp}	±0.077 dm^3**	±0.039 dm^3	±0.079 dm^3
V_{cond}	±0.077 dm^3**	±0.016 dm^3	±0.077 dm^3
V_{evap}	±0.077 dm^3**	±0.023 dm^3	±0.078 dm^3
P_{ref}	±1.55 kPa	±0.58 kPa	±1.65 kPa
T_{ref}	±0.8 C	±0.001C	±0.8C
*Expanded uncertainty of a single-point measure. **Calculated using error propagation of pressure and temperature to calculate the volume.			

Table 11: Uncertainty of the different variables for the nominal point of prototype 1.

There are some variables that are not measured but their value was obtained from measurements of other variables. The uncertainty of these calculated variables is obtained using the Taylor Series Method for the propagation of uncertainties (7). Examples of these variables are heating capacity ($\dot{Q}_h$), COP, section volumes, remaining mass in the sections, etc.

$$U_{95} = \sqrt{\sum_{i=1}^{N} \left(\frac{\partial f}{\partial x_i}\right)^2 U_i^2} \tag{7}$$

Where f is a function of the measured variables x_i.

As an example, the results of propagation of uncertainty in the nominal point of the first prototype are ±54 W in $\dot{Q}_h$ and ±0.1 in COP, ±0.19 g in remaining refrigerant charge for the compressor section, and ±0.18 g in remaining refrigerant charge for the condenser and the evaporator sections.

2.5. Test procedure

2.5.1. Refrigerant charge determination

Before every test, a test is performed to determine the refrigerant charge to be inserted. These previous tests consist in adding a certain amount of refrigerant charge, far from the objective but enough to start the machine and arrive at the desirable secondary conditions. Once in the test conditions, 10 g of refrigerant charge steps are added, with at least 15 minutes of steady-state between every step. Steady-state is defined in the standard EN 14511-3 [18] as no individual deviations from the mean (or objective value) of ±0.5 K in the inlet water/brine temperatures, ±0.6 K in the outlet water/brine temperatures, ±2.5 % in the mass flow rates, ±10 % in the static pressures and ±4 % in the voltage, and no deviations on the average values of ±0.2 K in the inlet water/brine temperatures, ±0.3 K in the outlet water/brine temperatures, ±1 % in the mass flow rates and ±4 % in the voltage.

When the refrigerant charge is near the objective (the expansion valve starts to be able to control the SH to the setpoint set), the steps of refrigerant charge increment are reduced to 5 g to gain precision. The test ends when the condensing pressure rises notably with the refrigerant charge

increase. Once analysed the data, the point where the maximum COP is selected. Examples of the results obtained in these tests are shown in Figure 15 and Figure 16.

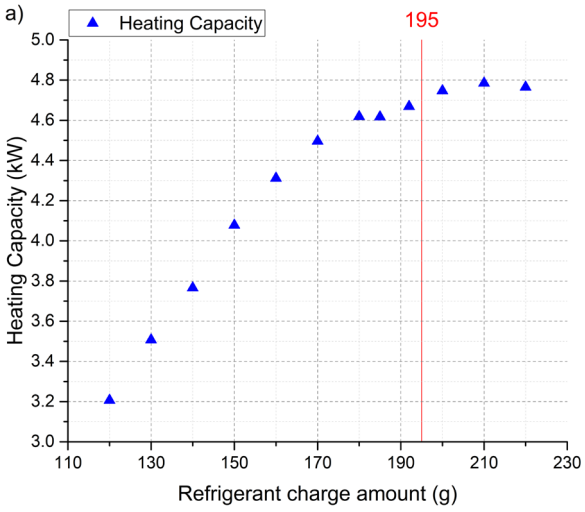

Figure 15: Heating capacity results of a refrigerant mass variation test at B0W35 at 60Hz of compressor speed.

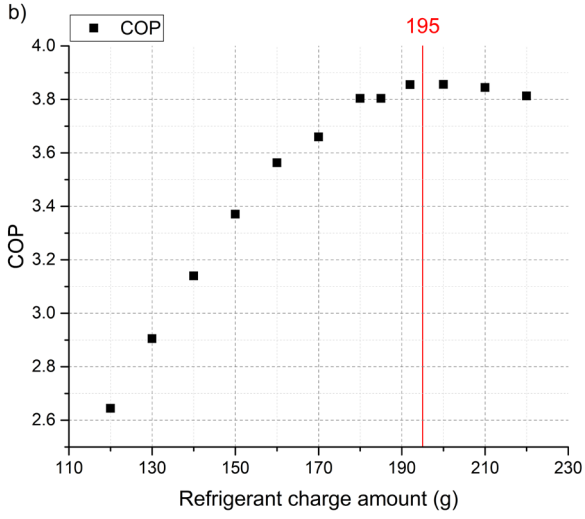

Figure 16: COP results of a refrigerant mass variation test at B0W35 at 60Hz of compressor speed.

2.5.2. Performance and refrigerant charge distribution

Given the previous test results, the test can be performed once the refrigerant charge amount is selected. Each test account for two differentiated parts: Performance results and refrigerant charge distribution results.

The process of each test is shown in Figure 17. Firstly, the heat pump is evacuated and tested to see if there is some leakage. A vacuum pump is operating for at least 2 hours to do it. The system is confirmed sealed if the pressure doesn't increase more than 0.1 mbar in one hour. Then the refrigerant charge is inserted into the system from a cylinder with pure propane (non-reused), measuring the mass with the scale A.

After this process, the heat pump starts at the setpoint compressor speed. The control loops are set to setpoint values, controlling SH, water inlet temperature, the temperature difference in the water circuit, the brine inlet temperature, and the brine circuit's temperature difference. Also, at this moment, the PIDs are reset to erase the previous data, which can affect the integrative part of the controller.

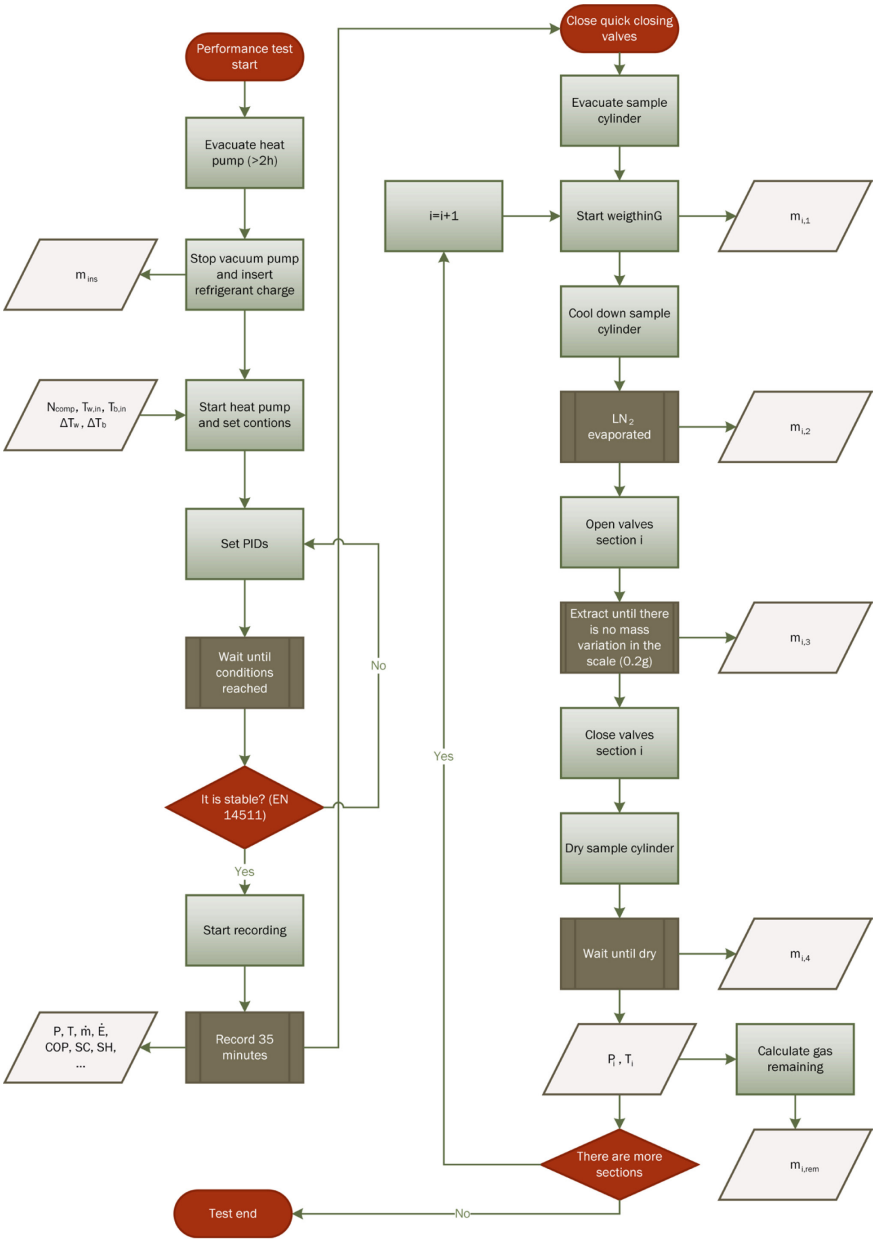

Figure 17: Test procedure

Once the stability is reached, as the steady state from the standard EN 14511-3 [18] the data is recorded for 35 minutes at least, and the performance part is finished. The results from this part are mainly heating capacity and COP calculated as shown in equations (8) and (9).

$$\dot{Q}_h = \dot{m}_w c_p \left(T_{w,out} - T_{w,in}\right) \tag{8}$$

$$COP = \frac{\dot{Q}_h}{\dot{E}} \tag{9}$$

All the variables measured in the refrigerant circuit will give additional information to correlate the simulation model with the tests and to understand better the root cause of the difference in refrigerant charge amount in each components between the tests, if this cause is linked with any of these variables.

Once finished the performance test, the QCV closed the sections suddenly (it actuates over all valves at the same time in less than one second), trapping the refrigerant inside each section and isolating them one from another. The compressor stops triggered by the pressure switches after the valves are closed to ensure that the charge distribution doesn't vary in this process.

For the refrigerant extraction, it is used the equipment shown in Figure 18. In this scheme, the sensors mentioned in Table 10 determine the remaining refrigerant charge.

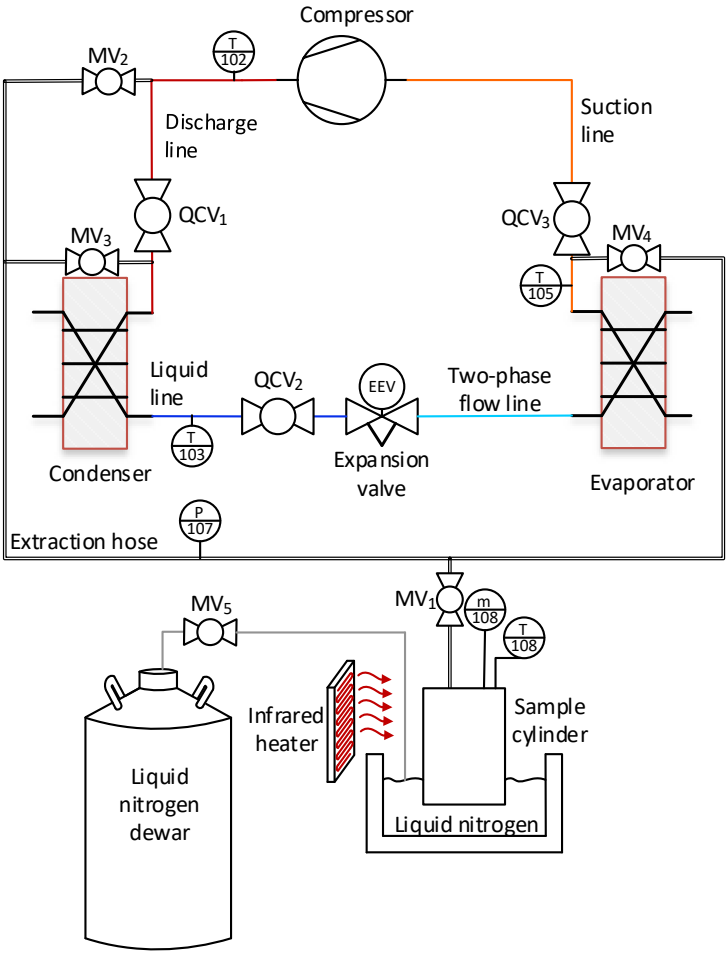

Figure 18: Refrigerant extraction scheme.

At the start of the second part of the test, the one regarding the refrigerant charge distribution, the sample cylinder and the extraction hoses are evacuated using the vacuum pump. This process is generally done simultaneously with evacuating the refrigerant circuit from the previous test. Then, the extraction is run for each section, one at a time. The process is the following. The first operation is taring the sample cylinder to obtain the first weight ($m_{1,i}$). In this state, the sample cylinder is dry and empty, i.e. there is no water condensed on the external surface and no refrigerant from the section inside the cylinder. Then the next step is cooling the sample cylinder using liquid nitrogen. It is possible to open the manual

valve two (MV_2) (if the section is the compressor one) if the MV_1 is closed. Once the sample cylinder is cooled enough and the liquid nitrogen is evaporated, to avoid the buoyancy effect, the sample cylinder would be with a bit of frost on the walls and empty, and its weight ($m_{2,i}$) would be a bit higher than ($m_{1,i}$). Then MV_1 is opened to start extraction, and it is stopped when it reaches equilibrium, defined as when the mass in the scale doesn't increase more than 0.2 g in 10 seconds. In this case, the MV_1 is closed again, and the weight ($m_{3,i}$) would be in a state of the cylinder full and the walls with frost. The last step consists in melting the ice from the walls. To do it, infrared heaters are powered to heat the sample cylinder. At this point, the sample cylinder would be dry and full of refrigerant, and its weight would be ($m_{4,i}$). This process and the weight at each point can be seen in Figure 19. In this figure, it can be seen how the cold surface of the sample cylinder absorbs moist from the ambient, and this moisture gets stuck to the wall during the cooling process, between $m_{1,i}$ and $m_{2,i}$, and how it is melted and dropped to the floor during the heating process, between $m_{3,i}$ and $m_{4,i}$.

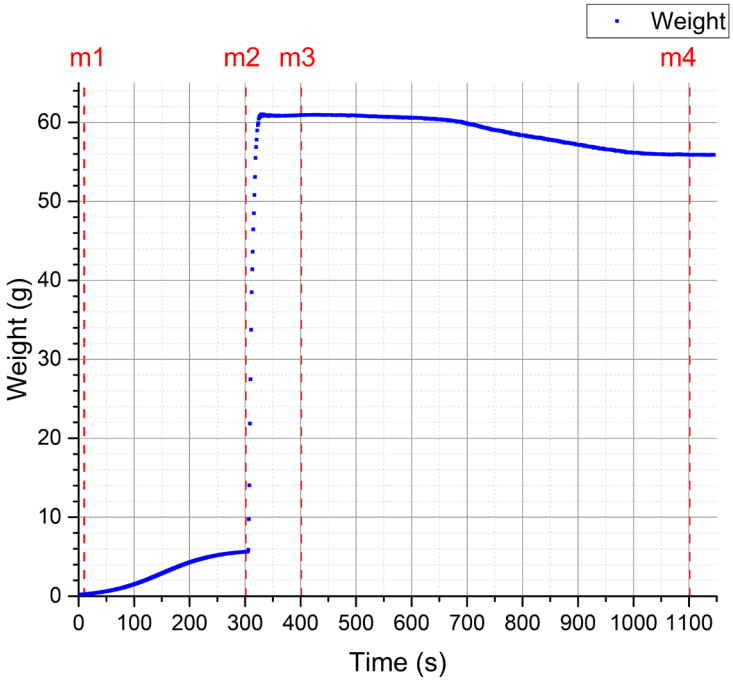

Figure 19: Example of the extraction process.

These measures of refrigerant extraction are used to check the extraction system. The correct value of refrigerant extracted from the section i is the result of $m_{4,i} - m_{1,i}$ and $m_{3,i} - m_{2,i}$ is only used to validate the former result. The test becomes invalid if the difference between these two substractions is greater than 3 g in any section. In addition to the result of the subtraction mentioned before and shown in equation (10), it has to be added the remaining refrigerant estimated with the values of pressure and temperature.

$$m_{ext,i} = m_{4,i} - m_{1,i} \tag{10}$$

The final value of the refrigerant that was in the section when the system stopped is the addition of this $m_{ext,i}$ to the estimated value obtained in equation (4). These estimated values are around 2 g for the compressor section and 0.3 g for the other sections. The reason for the compressor's amount is the slow evaporation of the refrigerant absorbed inside the oil. The final result is calculated as equation (11).

$$m_i = m_{ext,i} + m_{rem,i} \tag{11}$$

This process is done for all the sections and the refrigerant trapped inside the QCV, mainly in the QCV2 located in the liquid line. The typical values obtained of refrigerant charge amount inside these valves are 3 g, being 2.7 g trapped in the QCV2.

The extraction is done as if the QCV were another section. All sections and the QCV are opened to do it, and then the extraction process from Figure 17 is followed.

2.6. Test campaign

The test campaign performed had two primary purposes: (i) to test the feasibility of ground source heat pumps with the new components designed to reduce refrigerant charge and (ii) to provide data about refrigerant distribution in different conditions. Consequently, for each prototype, there are three groups of tests, considering the nominal situation. Firstly, the already mentioned nominal point will serve as a reference point for both test campaigns. The test conditions correspond to B0W35 at the nominal speed of the compressor, said by the manufacturer (60 rps) with an SH value of 10 K. This test will help to compare both prototypes to see

standard performance and a baseline to compare the refrigerant charge distribution when the conditions change.

The performance-focused campaign is based on the test conditions defined in the EN14825 standard [20] used for calculating the SCOP to be converted into a seasonal efficiency η which is used to calculate the labelling of the heat pump. In addition to the regular points to calculate the SCOP, two additional test conditions have been added to this campaign. These conditions are B0W32 and B0W29 and were added to have more intermediate points between the test conditions defined in the EN14825 standard to observe the tendencies more continuously.

The second campaign was focused on charge distribution and how it varied when some parameters changed. For this reason, the tests from this campaign were singular variations from the nominal point. In these tests, only one parameter is modified compared to the test considered baseline, the nominal point. These singular variations were the following:

- Different compressor speed: Nominal conditions, but the compressor was at the maximum speed allowed. In this case, it corresponded with a test from the performance campaign.
- Overfilled: Extra refrigerant charge was added to check towards which component it goes.
- SH variations: SH increase and reduction to see its impact.
- Crankcase compressor heated: To reduce the solubility of the oil
- Source or sink temperature variations: To analyse the impact of external conditions on refrigerant charge and refrigerant charge distribution.

Even though the different campaigns of one prototype have different purposes, the complete test, including performance and refrigerant distribution parts, described in section 2.5, were done for all the tests to save additional valuable information. Besides, performance results are essential for the refrigerant distribution to compare with the simulation model mentioned in section 2.7 and understand the behaviour and discrepancies.

For the performance campaign, the refrigerant charge was maintained constant at the value obtained at the nominal point. This value was obtained as mentioned in section 2.5, and it is the value that ensures a maximum COP. However, for the refrigerant distribution campaign, the

refrigerant charge that provides the maximum COP was determined in a test before performing every test, ensuring that the COP is maximized in the conditions where refrigerant distribution was determined.

	Test number	Test condition	Refr. charge (g)	Compressor speed (rps)	Comments
Nom	1	B0W35	195/170	60	
Performance	2	B0W35	195/170	120	
	3	B0W34	195/170	104	
	4	B0W32	195/170	90	
	5	B0W30	195/170	74	
	6	B0W29	195/170	60	
	7	B0W27	195/170	40	
	8	B0W24	195/170	20	
Refrigerant distribution	9	B0W35	255/220	60	Overfilled. SC=7
	10	B0W35	220/190	60	SH=5 K
	11	B0W35	160/160	60	SH=15 K
	12	B0W35	180/160	60	Compressor heated
	13	B7W35	195/185	60	
	14	B13W35	195/200	60	
	15	B0W55	195/185	60	
	16	B12W35	195/150	60	SH=24K

Table 12: Test conditions definition

All test definitions are shown in Table 12, and in Table 13, there are shown the test performed with each prototype. In the refrigerant charge column, the first number corresponds to the refrigerant charge of the first prototype and the second number of the second prototype. It can be seen that the first tests were repeated more times. It was done to confirm that the method and the results were consistent and confirm and be able to ensure future results by doing fewer repetitions.

	Test number	Prototype 1	Prototype 2
Nominal	1	x5	✓
Performance	2	✓	✓
	3	x2	✓
	4	✓	×
	5	x3	✓
	6	✓	×
	7	x2	✓
	8	✓	✓
Singular variations	9	✓	x3
	10	✓	✓
	11	✓	✓
	12	x3	✓
	13	✓	✓
	14	✓	✓
	15	✓	✓
	16	×	x2

Table 13: Tests performed on each prototype.

For test number 12, a heating wire was installed surrounding the oil sump in the bottom part of the crankcase of the compressor, as shown in Figure 20. This was done to heat the oil to force the desorption of the refrigerant from the oil, reaching another equilibrium condition where a less refrigerant amount is needed.

Figure 20: Placement of the heating wire around the compressor.

2.7. Refrigerant charge analysis

One of the most important results is the refrigerant charge amount of each component, also known as refrigerant distribution. Each component's behaviour is related to its thermophysical properties but is also associated with the system's dynamics.

Two main approaches will be followed to analyse measured refrigerant charge: (i) a comparative study between the different test conditions to extract conclusions about the necessary refrigerant charge and (ii) a detailed analysis through simulation software to know if refrigerant charge prediction would be possible. The first approach is more beneficial for detecting refrigerant reduction techniques, while the second one, if well performed, would provide a potent tool to help the heat pump designers.

To do the second method, the first approach was done with the software IMST-ART v4.0. Some differences were observed in the components between the experimental refrigerant amount measured and the calculated with the software. As a second step, each component was corrected differently. The following subsections will explain the second method more in depth: section 2.7.1 presents how the refrigerant charge prediction is

currently made in the different components in the software used, and section 2.7.2 presents the adjustments done in the compressor and the heat exchangers models to have a more valuable result from the simulations.

2.7.1. Initial comparison

For the initial comparison with the simulation software, the professional version of IMST-ART v4.0 was used. The modelling of every component was done by filling in all the possible information in the software from the manufacturer's data.

It is crucial to fit the refrigerant cycle results, as the pressure and temperature conditions at the different stages of the components significantly affect the calculated refrigerant charge. To do it, the process shown in Figure 21 was followed. This figure shows how the simulation results are fitted before accepting any refrigerant charge result. The first parameters matched were the ones relative to the BPHEs, in this case, pressure drop enhancement factors, heat transfer coefficient enhancement factors, plate pitch and area enhancement factors. Once validated these values, they were fixed for all the tests, and the iterative process started for each test. This iterative process consists in running the simulation and comparing the results to the experimental ones. Some parameters can be changed to fit them if they don't match. These parameters are the SC, SH, compressor's and tubes' heat losses. Once checked, the refrigerant charge prediction can be compared with the experimental result.

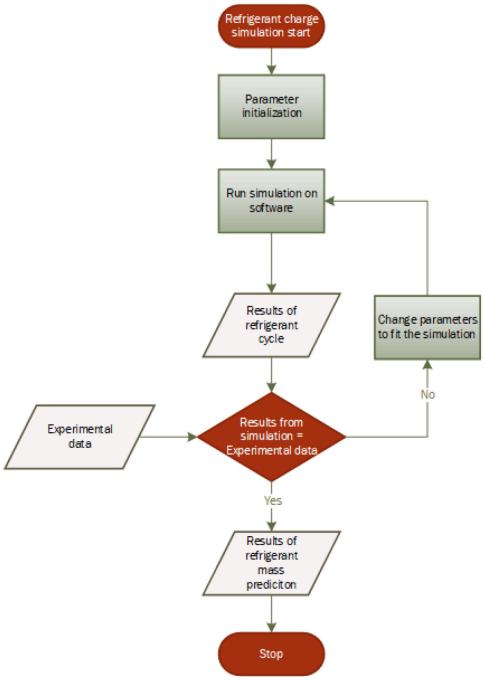

Figure 21: Initial simulation process.

In the following part of the section, it is going to be explained how refrigerant charge in the different components is calculated with the software.

Compressor

The compressor is defined by its displacement and efficiencies, which can be determined through catalogue data or the AHRI correlation. Knowing the compressor speed, suction conditions, condensation pressure and percentage of heat losses (which is adjusted to fit the experimental data), mass flow and electrical consumption can be calculated and, therefore, volumetric and overall efficiency.

Once known all the behaviour, the refrigerant charge is calculated with a standard solubility curve. The solubility curve was defined for every refrigerant using data from ASHRAE Handbook [21].

Heat exchanger

The heat exchangers are calculated using the finite volumes method. The heat transfer area is divided into small volumes, and in every small volume, the conservation equations are set to calculate the equilibrium conditions.

The main problem is that heat exchangers usually have counter-current flows; therefore, Figure 22 shows the equation system is non-linear and implicit.

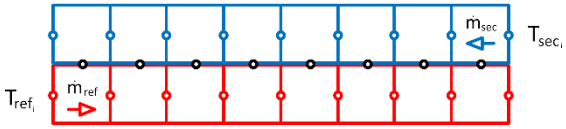

Figure 22: Example of finite volumes in a counter-current heat exchanger.

To avoid this problem, IMST-ART software uses conservation equations based on wall temperatures so that the equation system becomes a semi-explicit problem, easier to solve. The explanation can be found in an article [22].

Once the balance is achieved, the software calculates the refrigerant charge in each control volume knowing the pressure, temperature, mass flow, and quality. In cases of having single-phase flow, the density is easily calculated. However, the density must be calculated using the void fraction when there is a two-phase flow.

The void fraction is defined as the volumetric percentage of the space used by the vapour phase. This definition can be easily understood in Figure 23 and equation (12).

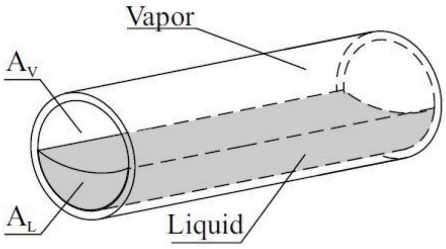

Figure 23: Void fraction explanation.

$$\alpha = \frac{A_v}{A_v + A_L} \tag{12}$$

The difference between vapour quality and void fraction stays in the densities and velocities of the different phases. There are a lot of different models regarding void fraction calculation. In this software, in BPHE, the

correlation is typically the Chisholm correlation [23]. This correlation is defined by equations (13) and (14).

$$\alpha = \frac{1}{1 + \frac{1 - x_{in}}{x_{in}} \frac{\rho_{vap}}{\rho_{liq}} s} \tag{13}$$

$$s = \sqrt{1 - x_{in}\left(1 - \left(\frac{\rho_{liq}}{\rho_{vap}}\right)\right)} \tag{14}$$

And therefore, the differential mass calculated in a control volume is as follows:

$$dm = \left(\rho_{vap}\alpha + \rho_{liq}\,(1 - \alpha)\right) A\, dL \tag{15}$$

2.7.2. Corrections in refrigerant charge prediction

Once refrigerant charge in the different components can be compared between the simulation and the experimental data, a revision in simulation calculations may be concluded as necessary. This correction shall be performed as proposed below.

Compressor

As mentioned before, the refrigerant charge in the compressor is calculated only by estimating the refrigerant charge amount that is dissolved in the oil. Still, refrigerant is also in the gas phase inside the crankcase and the deposit located in the compressor's suction. Additionally, the current solubility curve is a generic one.

The volumes mentioned were added to correct it. The density was calculated using equation (4), and the refrigerant amount dissolved in the oil was improved.

The results from the isothermal gas method were used to know the correct volume of the crankcase, as shown in Table 6. For the density calculation, the vapour in this part is at the discharge pressure, and the temperature is supposed to be at the discharge temperature. In the suction accumulator, the vapour is at suction pressure and temperature, measured during the test.

The manufacturer provided the solubility curve. It was fit using the equations presented by Seeton and Hrnjak [24]: This equation has the form shown in equation (16):

$$\log_{10}(P) = a_1 + \frac{a_2}{T} + \frac{a_3}{T^2} + \log_{10}(\omega)\left(a_4 + \frac{a_5}{T} + \frac{a_6}{T^2}\right) + \log_{10}^2(\omega)\left(a_7 + \frac{a_8}{T} + \frac{a_9}{T^2}\right) \quad (16)$$

a_1	4.549
a_2	-1148
a_3	24822
a_4	-0.1904
a_5	58.06
a_6	-15524
a_7	-0.9565
a_8	421.5
a_9	-75486

Table 14: Parameters of refrigerant-lubricant solubility.

The parameters for this specific mixture are shown in Table 14, and the results can be seen in Figure 24. In the equation, the pressure is in bar, the temperature in K, and the ω corresponds to the mass fraction of refrigerant, which is the refrigerant amount divided by the total amount (17):

$$\omega = \frac{m_{ref}}{m_{ref} + m_{oil}} \quad (17)$$

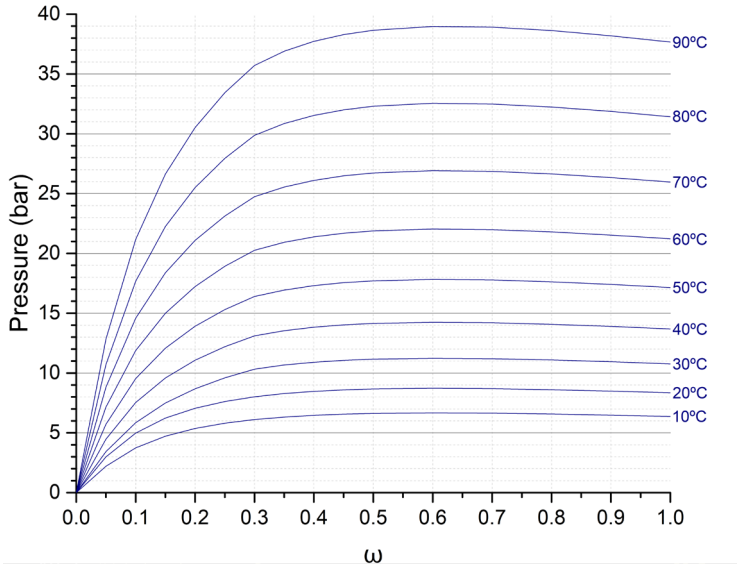

Figure 24: Solubility of the refrigerant-lubricant mixture.

Heat exchangers

In the experiments, it was observed that a portion of liquid refrigerant stayed in the bottom part of the heat exchangers, no matter the behaviour conditions.

The mass of this refrigerant in the liquid phase was added to the previously calculated refrigerant with IMST-ART. To do it, the volume was calculated geometrically. The refrigerant was supposed to be in the liquid phase in saturated conditions at the pressure measured in the suction or discharge line and correcting it with the pressure drop of the pipes and the heat exchanger.

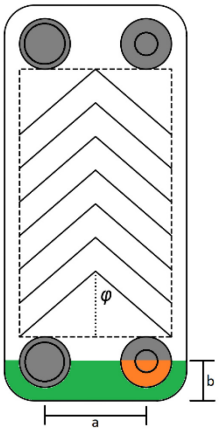

Figure 25: Geometrical assumption of refrigerant in the liquid phase.

For the geometrical assumptions, Figure 25 helps. The height of this liquid refrigerant stored in the heat exchanger was supposed to be half of the port after results observed from a colleague, Torsten Will, who was using the same BPHE with a sightglass in the inlet port. In the figure, it can be seen two differentiated parts in the zone of the BPHE. In the green part, the liquid is only in the refrigerant channels. Meanwhile, in the orange area, as the port has an opened zone where the refrigerant is distributed between the plates, as seen in Figure 26, the assumption is that the whole depth of the heat exchanger is filled with liquid refrigerant.

Figure 26: BPHE port cut.

Therefore, the volumes and mass added to the IMST-ART simulation can be calculated as shown in equations (18), (19) and (20).

$$V_{port,liq} = \pi \frac{\emptyset^2}{8} d \tag{18}$$

$$V_{plates,liq} = \left(a \cdot b + \pi \frac{b^2}{2} - \pi \frac{\emptyset^2}{4} \right) \cdot \left(pp_{ref} - e_w \right) \cdot \cdot \left(\frac{\mathrm{N_{plates}}}{2} - 1 \right) \tag{19}$$

$$m_{liq} = \rho_{liq,sat} \cdot \left(V_{plates,liq} + V_{port,liq} \right) \tag{20}$$

Where a is the distance between the distribution part of the ports, b is the height from the bottom until half of the port, pp_{ref} is the plate pitch, e_w is the plate thickness, $\mathrm{N_{plates}}$ is the number of plates, $\emptyset$ is the diameter of the distribution part of the hole, and d is the depth.

References

[1] S. Peuker, "Experimental and analytical investigation of refrigerant and lubricant migration," University of Illinois at Urbana-Champaign, 2010. doi: 10.1007/978-3-319-30602-5_43.

[2] E. Björk, "A simple technique for refrigerant mass measurement," *Appl Therm Eng*, vol. 25, no. 8–9, pp. 1115–1125, Jun. 2005, doi: 10.1016/J.APPLTHERMALENG.2004.09.008.

[3] G. Ding, X. Ma, P. Zhang, W. Han, S. Kasahara, and T. Yamaguchi, "Practical methods for measuring refrigerant mass distribution inside refrigeration system," *International Journal of Refrigeration*, vol. 32, no. 2, pp. 327–334, Mar. 2009, doi: 10.1016/J.IJREFRIG.2008.05.002.

[4] N. Tanaka, M. Ikeuchi, and G. Yamanaka, "Experimental Study on the Dynamic Characteristics of a Heat Pump," in *ASHRAE Transactions*, Toronto, 1982.

[5] R. Chen, J. Wu, and J. Duan, "Performance and refrigerant mass distribution of a R290 split air conditioner with different lubricating oils," *Appl Therm Eng*, vol. 162, p. 114225, Nov. 2019, doi: 10.1016/j.applthermaleng.2019.114225.

[6] P. S. Hrnjak and M. R. Hoehne, "Charge minimization in systems and components using hydrocarbons as a refrigerant," *ACRC TR-224*, vol. 61801, no. 217, 2004.

[7] S. Jin and P. Hrnjak, "Refrigerant and lubricant charge in air condition heat exchangers: Experimentally validated model," *International Journal of Refrigeration*, vol. 67, pp. 395–407, Jul. 2016, doi: 10.1016/J.IJREFRIG.2016.01.002.

[8] W. Li and P. Hrnjak, "Transient refrigerant and oil distribution in a residential heat pump water heater system: experiments and model," *International Journal of Refrigeration*, Apr. 2021, doi: 10.1016/j.ijrefrig.2021.04.012.

[9] B. Han, G. Yan, and J. Yu, "Refrigerant migration during startup of a split air conditioner in heating mode," *Appl Therm Eng*, vol. 148, pp. 1068–1073, Feb. 2019, doi: 10.1016/j.applthermaleng.2018.11.126.

[10] T. Li *et al.*, "Measurement of refrigerant mass distribution within a R290 split air conditioner," *International Journal of Refrigeration*, vol. 57, pp. 163–172, Sep. 2015, doi: 10.1016/J.IJREFRIG.2015.05.012.

[11] W. J. Mulroy and D. Didion, "Refrigerant Migration in a Split-Unit Air Conditioner," vol. 91, no. No. 1A. pp. 193–206. Accessed: Jul. 28, 2021. [Online]. Available: https://www.nist.gov/publications/refrigerant-migration-split-unit-air-conditioner

[12] Primal Fernando, "Experimental Investigation of Refrigerant Charge Minimisation of a Small Capacity Heat Pump Doctoral Thesis," 2007.

[13] A. J. Lee, C. K. Bach, and C. R. Bradshaw, "Differential mass evacuation sampling technique for measuring refrigerant charge and oil retention of round tube plate fin heat exchangers (ASHRAE RP-1785)," *Sci Technol Built Environ*, vol. 26, no. 6, pp. 790–804, 2020, doi: 10.1080/23744731.2020.1735262.

[14] E. W. Lemmon, M. L. Huber, and M. O. Mclinden, "REFPROP 9.1," *NIST standard reference database*. 2013.

[15] L. Sánchez-Moreno-Giner, F. Barceló-Ruescas, A. López-Navarro, and J. Gonzálvez-Maciá, "Experimental and Theoretical Analysis of Refrigerant Charge Extraction Methods," 2021. Accessed: Nov. 13, 2021. [Online]. Available: https://docs.lib.purdue.edu/iracc

[16] European Committee for Standardization, "EN 14511-2 Air conditioners, liquid chilling packages and heat pumps for space heating and cooling and process chillers, with electrically driven compressors - Part 2: Test conditions," 2019, Accessed: Mar. 03, 2022. [Online]. Available: https://www.techstreet.com/standards/din-en-14511-2?product_id=2076454

[17] I. E. C. IEC, " IEC 60751:2022 Industrial Platinum Resistance Thermometers and Platinum Temperature Sensors, International Standard," 2022.

[18] European Committee for Standardization, "EN 14511-3 Air conditioners, liquid chilling packages and heat pumps for space heating and cooling and process chillers, with electrically driven compressors - Part 3: Test

methods," 2019, Accessed: Sep. 21, 2021. [Online]. Available: https://www.techstreet.com/standards/din-en-14511-3?product_id=2076455

[19] H. W. Coleman, W. Glenn. Steele, and H. W. Coleman, *Experimentation, validation, and uncertainty analysis for engineers*. John Wiley & Sons, 2009.

[20] European Committee for Standardization, "EN 14825 - Air conditioners, liquid chilling packages and heat pumps, with electrically driven compressors, for space heating and cooling - Testing and rating at part load conditions and calculation of seasonal performance.," 2019, Accessed: Sep. 22, 2021. [Online]. Available: https://www.en-standard.eu/din-en-14825-air-conditioners-liquid-chilling-packages-and-heat-pumps-with-electrically-driven-compressors-for-space-heating-and-cooling-testing-and-rating-at-part-load-conditions-and-calculation-of-seasonal-performance/

[21] American Society of Heating Refrigerating and Air-conditioning Engineers, *ASHRAE Handbook - Refrigeration*. 2018.

[22] J. M. Corberán, P. F. De Córdoba, J. Gonzálvez, and F. Alias, "Semiexplicit method for wall temperature linked equations (sewtle): A general finite-volume technique for the calculation of complex heat exchangers," *Numerical Heat Transfer, Part B: Fundamentals*, vol. 40, no. 1, pp. 37–59, Jul. 2001, doi: 10.1080/104077901300233596.

[23] D. CHISHOLM, "Two-Phase Flow in Heat Exchangers and Pipelines," *Heat Transfer Engineering*, vol. 6, no. 2, pp. 48–57, Jan. 1985, doi: 10.1080/01457638508939624.

[24] C. J. Seeton and P. Hrnjak, "Thermophysical Properties of CO2-Lubricant Mixtures and Their Affect on 2-Phase Flow in Small Channels (Less than 1mm)," in *Purdue e-Pub*, 2006.

Chapter 3: Results

This chapter explains the results obtained during the thesis development.

The first part is dedicated to the test where the optimum refrigerant charge was obtained. This test consisted of a mass variation while maintaining the external conditions, as explained in section 2.5.1. This test was performed in both prototypes in every test condition. It serves to obtain not only the optimal charge that ensures the maximum COP but also to comprehend if the test condition is more or less charge-demanding than the nominal point.

The second part corresponds to the performance results of the test campaigns (SCOP and singular variation for each prototype). The objective of test performance campaigns is to analyse the behaviour of both prototypes in the seasonal performance campaign and obtain the virtual SCOP and heating capacity regarding the refrigerant charge needed. However, the objectives of knowing the performance data of the singular variation campaign are to compare the different charge reduction strategies, to see if the same approach affects equally for both prototypes and to obtain enough data on the refrigerant cycle to compare with the simulation.

Thirdly, results about refrigerant distribution are presented. This information is obtained from all test campaigns. With it, it can be observed how the different conditions directly affect the refrigerant charge of every component separately and know where the maximum discrepancy between the model and the experiment is observed.

Finally, all the data obtained during the experimental campaign is included in tables in Appendix D.

3.1. Refrigerant charge determination

Firstly, a preliminary test was performed to determine the refrigerant charge amount that makes the heat pump work in the optimal COP condition. This test was done in the nominal point (B0W35, at 60 rps of compressor speed, 10 K of SH) for determining the refrigerant charge of the nominal condition and the SCOP campaign and in every test condition of the singular variations campaign. This process was followed for both prototypes.

The refrigerant charge added to the system is always done using the gas connection of the refrigerant cylinder to reduce human error, as the velocity of the refrigerant is lower.

3.1.1. Nominal point

In the first test, in the first prototype, the initial charge to make the heat pump work was 120 g, and then steps of approximately 10 g were done to get the increment of COP and heating capacity. A steady state was reached in every step of the refrigerant charge to ensure the results were correct and the random uncertainty was low. In Figure 27, results of heating capacity (a), COP (b) increments, and charge specific capacity (c) at the nominal point for each step of refrigerant charge can be observed.

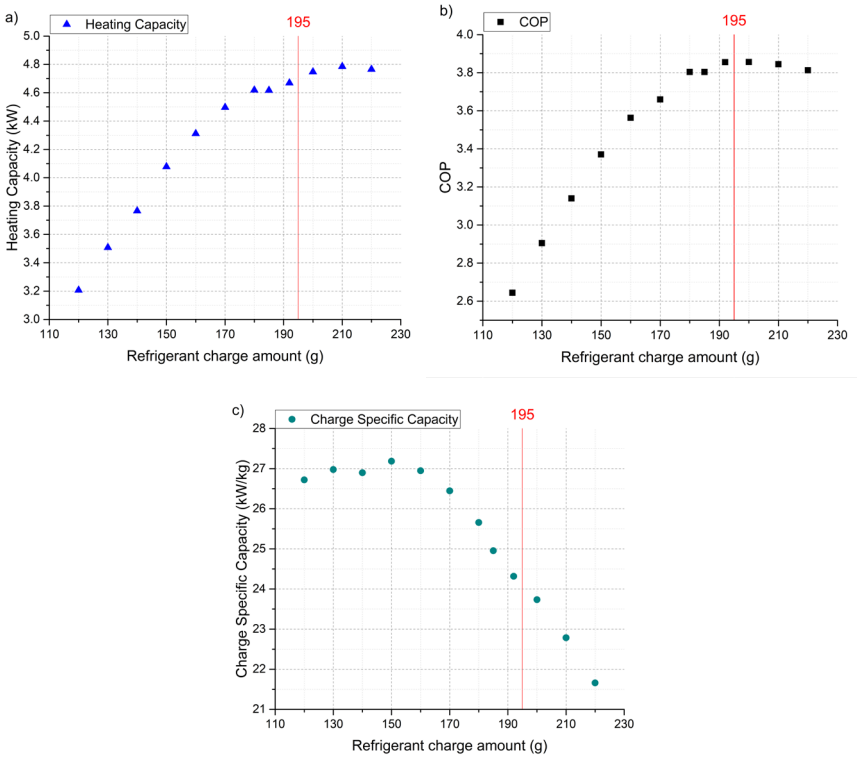

Figure 27: Mass variation test of prototype 1. Results of (a) Heating Capacity, (b) COP, and (c) Charge Specific Capacity.

In the test results, it can be seen that there are two differentiated parts for each variable. There is a quasilinear increment in heating capacity from the minimum charge (120 g) to 170 g. After the value of 170 g in this test, the heating capacity increases less when the refrigerant is added, but it still rises. Consequently, the charge specific capacity is nearly constant, with approximately 27 kW/kg and then starts decreasing sharply.

Focusing on the COP, the rise in the value in the first 170 g is almost linear, as the heating capacity increases without increasing the compressor power input. On the other hand, the COP increases as well until it reaches an optimum and then starts decreasing slightly.

Within this tendency, if more refrigerant charge steps were included, the heating capacity would have stayed at the same value, with little increments, resulting in a mild fall in COP and dramatic fall in charge specific capacity as observed in the work of Corberan et al.[1].

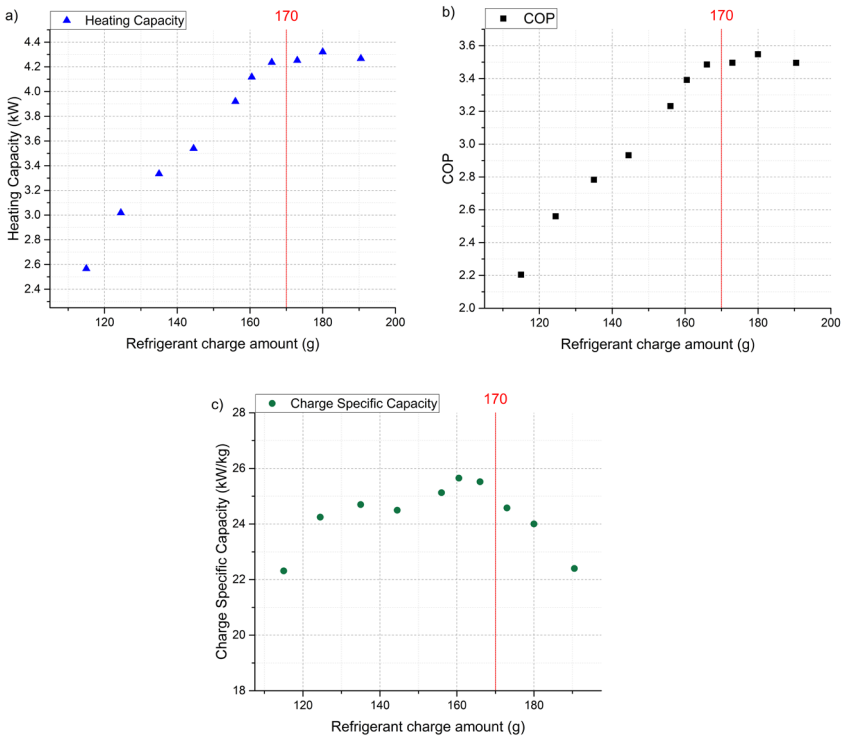

Figure 28: Mass variation test of prototype 2. Results of (a) Heating Capacity, (b) COP, and (c) Charge Specific Capacity

Similar behaviour is observed in the second prototype in Figure 28. In this case, the initial mass needed to start the heat pump was lower, around 115 g. The same strategy was followed: increase the charge with steps of 10 g and then reduce the steps to 5 g.

Seeing the graph of heating capacity and COP, each step's increment is sharper and reaches the optimum at a lower refrigerant charge. The optimum is achieved with lower heating capacity and lower COP.

The charge specific capacity graph shows a different behaviour than in prototype 1. In this prototype, an almost horizontal Cc is observed from the refrigerant charge value of 125 g to 170 g with a 25 kW/kg value. After this value, the Cc starts to decrease.

3.1.2. Variable study of the different tests

As mentioned before, this test was repeated for the different test conditions of both prototypes. This section shows the evolution of the variables affected mainly by the variation of the refrigerant charge while other variables are maintained.

COP

The first variable to be studied, since it was selected to be the one to be maximised in every test condition, is the COP. Figure 29 shows the COP results of the first prototype, and Figure 30 shows the same results from prototype 2. These figures have marked red vertical lines indicating the optimal refrigerant charge for each test. In prototype 1, four tests coincide with the optimal refrigerant charge: the nominal condition and the different source and sink temperature variations, which are B0W55, B7W35 and B13W35. Then increasing the SH from 10 K to 15 K reduces 35 g in this specific prototype, while decreasing the SH to 5 K increases 25 g. Lastly, heating the compressor with a heating wire leads to a refrigerant charge reduction of 15 g.

Focusing on the optimal refrigerant charge of prototype 2, it can be seen that there is more variability between the tests. The nominal point had an optimal COP at 170 g. Then, only source temperature increment was done in this prototype, which meant an increase of refrigerant charge needed, obtaining a value of 185 g for B7W35 and a value of 200 g in test B13W35.

In this case, when the SH was increased to 15 K, the refrigerant charge only decreased by 10 g, and when SH was reduced to 5 K, two local optima were observed. Still, regarding other test variables, such as EEV opening or SC, it was decided to select 185 g as the optimal refrigerant charge. Lastly, another test in this prototype was considered: increasing the superheat and the source temperature value and maintaining the

evaporation temperature. This test had the lowest value of refrigerant charge needed, 150 g.

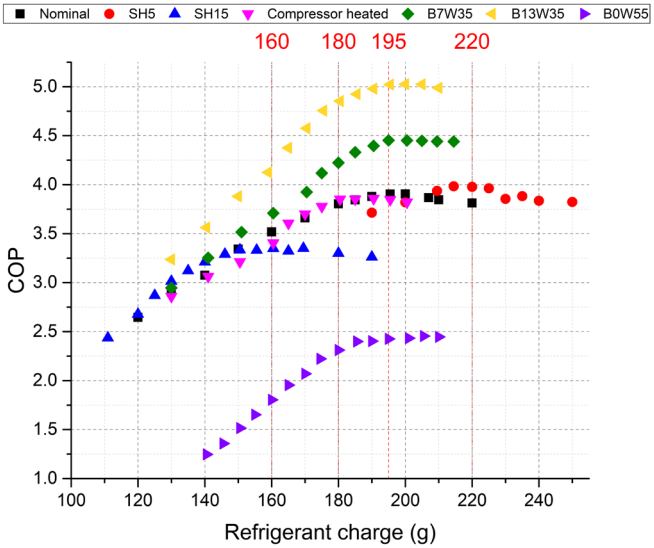

Figure 29: COP variation due to refrigerant charge of the different tests of prototype 1.

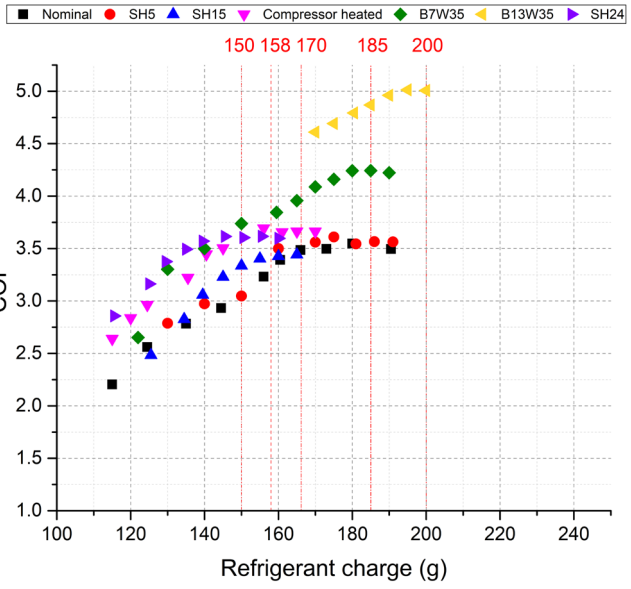

Figure 30: COP variation due to refrigerant charge of the different tests of prototype 2.

Comparing both graphs, it can be observed that SH level is the variable affected the most to the optimum refrigerant charge in the first prototype, while in the second prototype, it did not affect that much. However, while the source and sink temperature variations do not affect the first prototype, they have the most impact in the second.

Regarding the value of the COP, as in the second prototype, the evaporator was smaller; therefore, the absolute value of COP is lower in almost every case. The exception is the test with 15 K of SH. In this case, the evaporator size is unimportant for the COP value because the SH level and the brine return temperature limit the evaporation temperature.

Regarding both figures, the transition on each test after every step of the refrigerant charge is more predictable in prototype one than in prototype two. In this second prototype, in some conditions, the increase of COP is more linear until the optimum is achieved.

Heating Capacity

It is also necessary to look at the heating capacity for these tests since it is as essential as the COP. The heat pump must ensure a minimum heating capacity to reach comfort conditions.

Figure 31 and Figure 32 present the results of the heating capacity of both prototypes. These results show a tendency very similar to the results from COP values, with the main difference that, generally, a maximum is not observed in the test but a reduction in the growth of the heating capacity with the increase of refrigerant charge. This reduction is observed near the value where the maximum COP was obtained. After this value, the increase in compressor power consumption is higher than the increase in heating capacity.

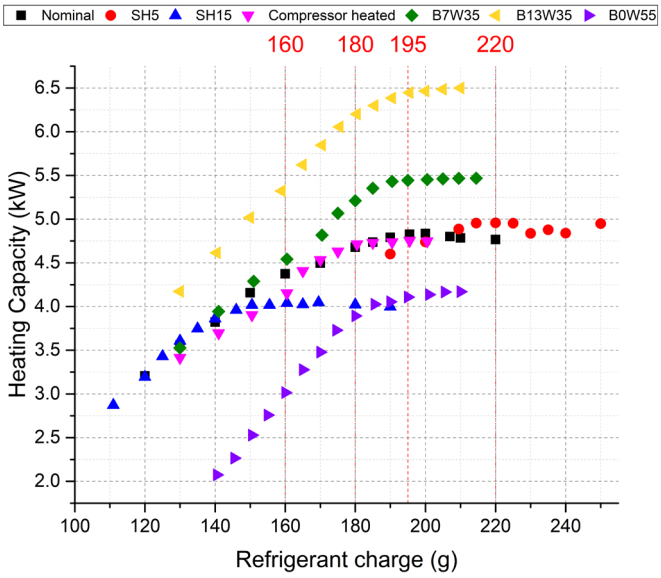

Figure 31: Heating capacity variation due to refrigerant charge of the different tests of prototype 1.

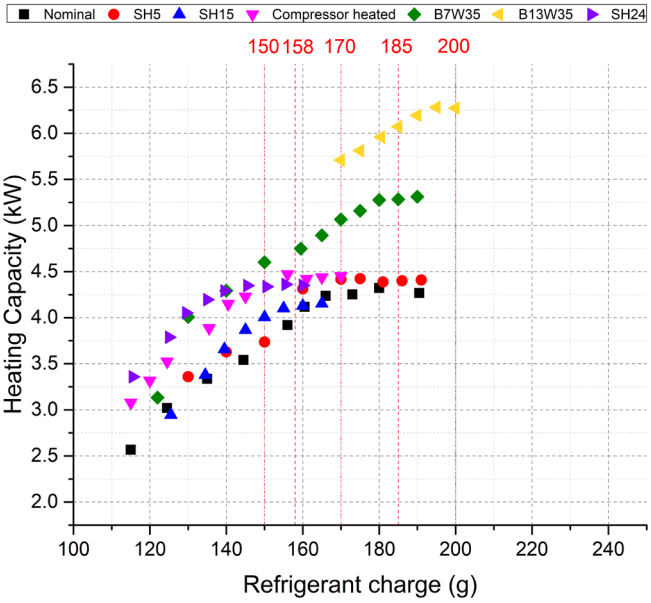

Figure 32: Heating capacity variation due to refrigerant charge of the different tests of prototype 2.

Comparing both prototypes, the first observation is that the heating capacity is reduced by 0.5 kW from prototype 1 to prototype 2 in the nominal conditions. This drop is caused by the decrease in evaporation temperature induced by the reduction of the evaporator heat transfer area. The same decline was observed comparing the tests with 5 K of superheat, as in this case, the evaporation temperature difference remained similar. Also, a similar distinction is observed in tests with source temperature variation, but half reduced the difference in these cases.

However, not all tests suffered a heating capacity degradation with the new heat exchanger. The test with 15 K of SH obtained a slightly higher heating capacity in the second prototype.

Charge Specific Capacity

Then, Figure 33 and Figure 34 show the variation in charge specific capacity of these tests. As mentioned in section 3.1.1, in all tests, the charge specific capacity starts rising until reaching an optimum and then drops. This optimum is always achieved at a lower refrigerant charge than the optimum COP, as it is the point where the heating capacity reduces the amount that increases each step, but it is still growing.

As with the heating capacity, prototype one has a higher charge specific capacity in the nominal point than prototype two. However, it is not the case in all tests. In B13W35, the value of Cc is still slightly higher. Still, in all other test conditions, B7W35, SH 15 K, SH 5 K and compressor heated, the second prototype achieves a higher value of the charge specific capacity.

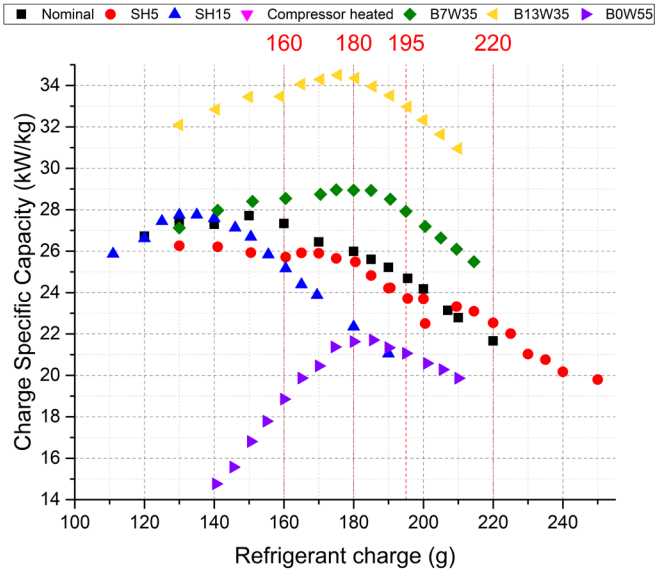

Figure 33: Charge specific capacity variation due to refrigerant charge of the different tests of prototype 1.

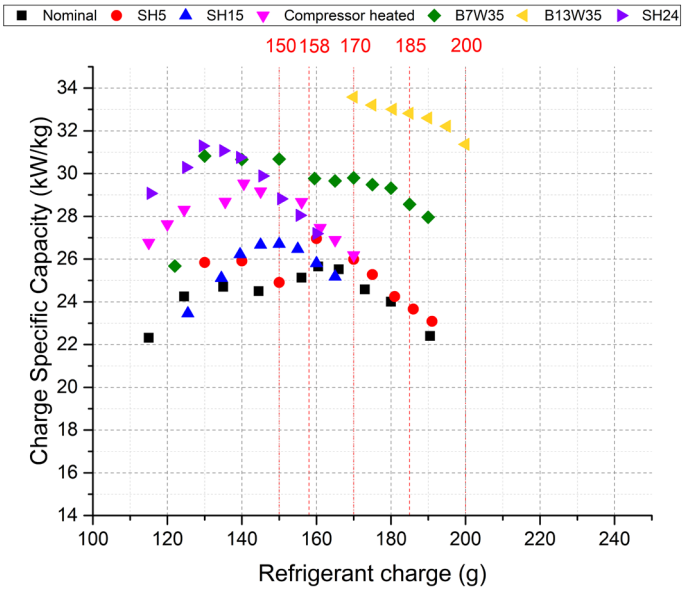

Figure 34: Charge specific capacity variation due to refrigerant charge of the different tests of prototype 2.

Subcooling

Regarding the subcooling, in the results, it can be seen either 2 or 3 regions with the increment of refrigerant charge. These results are shown in Figure 35 and Figure 36.

The first zone corresponds to the points where increasing the refrigerant charge doesn't affect the subcooling value much because of the refrigerant's lack in the system, and the steps of refrigerant charge are divided between the condenser, evaporator and compressor since the operation variables (pressures and temperatures) vary enormously with the refrigerant charge. The subcooling is almost flat in this first zone with a negligible increment.

In the first zone mentioned, the measured subcooling is always below 0K, which is impossible. Two main reasons can explain this phenomenon.

The subcooling is calculated as the difference between the temperature measured at the condenser outlet and the estimated condensation temperature obtained with the pressure measurement in the discharge line. This process is correct, but the pressure in the liquid line is different from the pressure measured in the discharge line. In the condenser outlet, a distributor is placed in case the cycle is reversed, which provokes a pressure drop which at high refrigerant mass flow rates could be significant.

Additionally, the sensors add uncertainty to the measurements, as explained in section 2.4, which can make some measurements not physically acceptable.

The second zone corresponds with the amount of charge that makes the heat pump works in optimal conditions. In these cases, a slight charge increase means a significant increase in subcooling value.

The last zone, which was not reached in all tests, is almost horizontal. In this case, the condenser is filled with liquid in the subcooling area, increasing the refrigerant charge in this zone. With it, the condensation pressure increases and another equilibrium point is reached.

In the second prototype, the same trend is observed, having three different zones but at lower values of refrigerant charge.

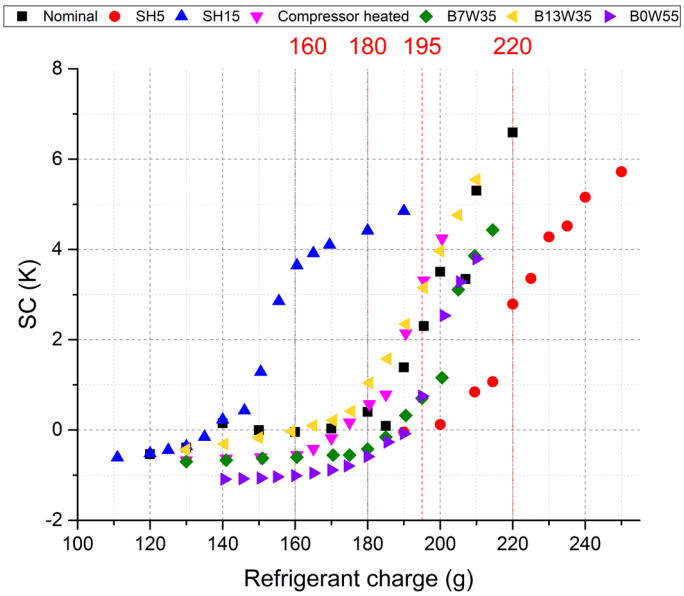

Figure 35: SC variation due to refrigerant charge of the different tests of prototype 1.

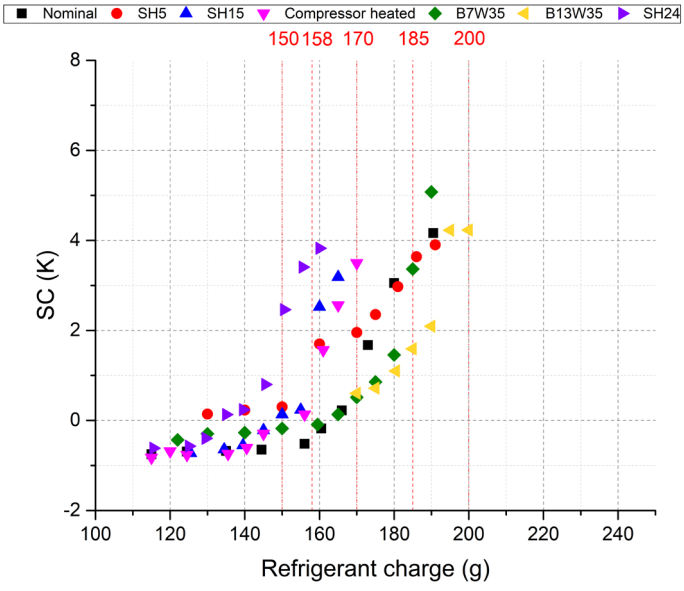

Figure 36: SC variation due to refrigerant charge of the different tests of prototype 2.

Electronic Expansion Valve

The expansion valve position can be a good indicator for locating the optimum refrigerant charge. As the refrigerant charge, three parts can be observed in the EEV.

The first zone is when the EEV is too small for the charge inserted due to the two-phase flow at the inlet of the expansion valve. When this happens, the valve is fully opened (100 %), the SH is not yet controlled, and it is higher than the target. The different refrigerant charge values at which the EEV starts controlling regarding the SH comparing the Nominal, SH5 and SH15 curves can be observed.

Then, the second zone is when the SH can be controlled. Still, an increase in refrigerant charge means a significant change in the expansion valve position since it means another equilibrium point in the refrigerant circuit.

The last zone corresponds to the equilibrium when increasing the refrigerant charge doesn't affect the conditions in the compressor and evaporator, and the extra refrigerant is stored in the condenser. In this case, the variation of the EEV position caused by the refrigerant charge increase is negligible.

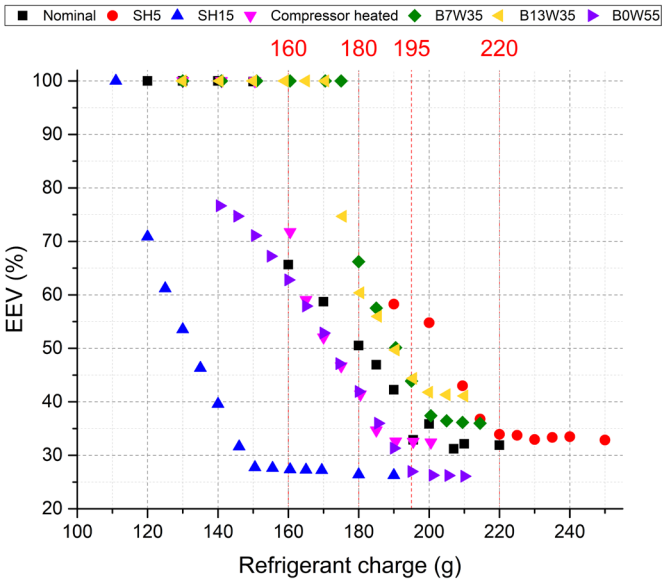

Figure 37: EEV variation due to refrigerant charge of the different tests of prototype 1.

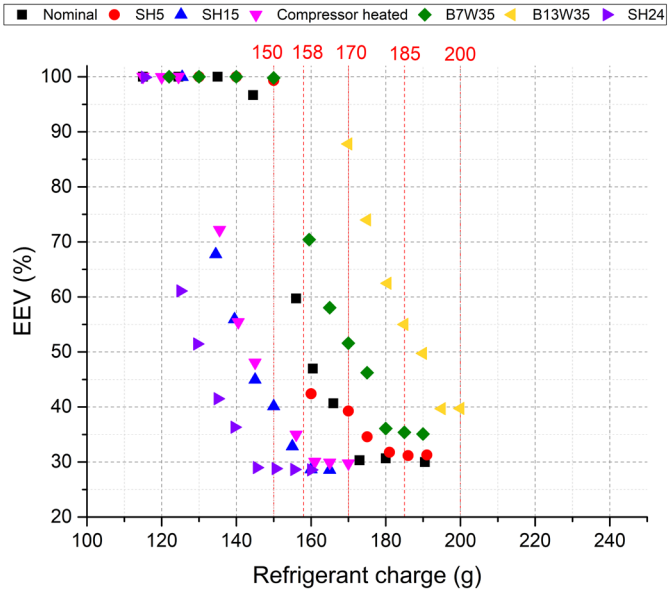

Figure 38: EEV variation due to refrigerant charge of the different tests of prototype 2.

3.2. Performance results

In this section, the performance results of all tests will be explained. These results were obtained while the heat pump was running. They were recorded during a steady state of at least 30 minutes to reduce random uncertainty.

Firstly, the results of the nominal test condition are presented. Then the focus will change to the test of the SCOP campaign, allowing us to obtain the hypothetical averaged COP during a standard year.

Thirdly, for the second campaign, every test is compared with the nominal point, analysing the main differences in the test variables.

Once all three analyses are done in the first prototype, the process is repeated in the second prototype.

Lastly, the comparison between both prototypes' results is made to end the section.

3.2.1. Prototype 1

Nominal Point

The starting point of the experimental campaign is the nominal point. This test corresponds to the test condition B0W35 at 60 Hz of compressor speed, having on the sink side a temperature difference of 5 K and 3 K on the source side.

This test was used to determine the refrigerant charge amount on the SCOP campaign and as a reference to study the singular variations of the second campaign. In this second campaign, each test presents variations in only one input variable compared to the nominal point.

In the first prototype's nominal test, a heating capacity of 4.6 kW with a COP of 3.8, i.e. an electric consumption of 1.21 kW.

The condensation temperature measured is around 34 ^{o}C, having a temperature difference to the secondary fluid (approach temperature) of almost zero, which means that it is the physically lowest temperature possible for this application, considering that the secondary fluid temperatures inlet and outlet are 30 ^{o}C and 35 ^{o}C, respectively. It also means that the condenser is oversized for this condition, and a possible reduction without losing performance could be made, which also would

mean a refrigerant charge reduction. However, as the compressor speed is only at 60 Hz and the maximum compressor speed is 120 Hz, as it will be seen, with full compressor speed, the condenser is not oversized.

The evaporation temperature obtained is around -9 ºC, which also could mean an oversized heat exchanger at this test condition. In this case, the secondary fluid, a mixture of Ethylene Glycol (EG) (40 % in volume) and water, goes from 0 ºC to -3 ºC controlled with a 3WV. The superheating is controlled with the EEV using the temperature of the compressor's inlet with a value of 10 K. This means that it is not physically possible to evaporate at a higher evaporation temperature since the heat gains in the suction piping (with an uninsulated filter drier) makes the refrigerant increase the temperature 1 K in this test condition.

The discharge temperature measured was 63.4 ºC, and the oil temperature was 48.2 ºC, having a significant difference between both. In contrast, as it is a rotary compressor, it has all the crankcase downstream of the compression chamber, i.e. at discharge pressure. The difference is the energy the refrigerant absorbs when cooling down the compressor's motor.

SCOP campaign

In this test campaign, as mentioned previously, the refrigerant charge was already settled in the nominal test. The idea behind it was to have the exact refrigerant charge during the whole campaign with the amount that approximately makes the average of the entire campaign work at its best. Considering the results from Appendix D and comparing them with those observed in Figure 27, it can be stated that the nominal point results of refrigerant charge variation can be settled as a compromise solution with only one test. For this reason, the refrigerant charge in this campaign is 195 g.

Performance tests of the SCOP campaign determine the declared capacity (heating capacity that the household unit can supply in the worst-case scenario) and the SCOP (an averaged yearly efficiency). In brine-to-water heat pumps, the source doesn't change the temperature with the ambient temperature, but with the ground temperature whose fluctuations are slower and dependent with the extraction/impulsion of energy from/to the ground. However, the heating loads of the building are higher when the ambient temperature decreases. To achieve comfort, the temperature of the secondary loop used in the terminal parts in the buildings is higher with lower ambient temperatures. To manifest these facts, the sink conditions

and partial loads according to the ambient temperature are standardised in EN 14825 [2]. This first prototype has achieved a declared capacity of $\dot{Q}_h = 9.49\,kW$ without any electrical heater backup at the maximum compressor speed (120 Hz) at the ambient temperature of -10 ºC (B0W35), and the SCOP of this test campaign was $SCOP = 4.01$.

As commented previously, the refrigerant charge in the system was 195 g (regarding that the system has added equipment that increases the refrigerant charge slightly), which results in a charge specific heating capacity of $C_c = 48.72\,\frac{kW}{kg}$. With a similar heat pump and the limited refrigerant charge of 150 g of propane without having any additional safety precautions, the heating capacity obtained would be $\dot{Q}_h = 7.31\,kW$.

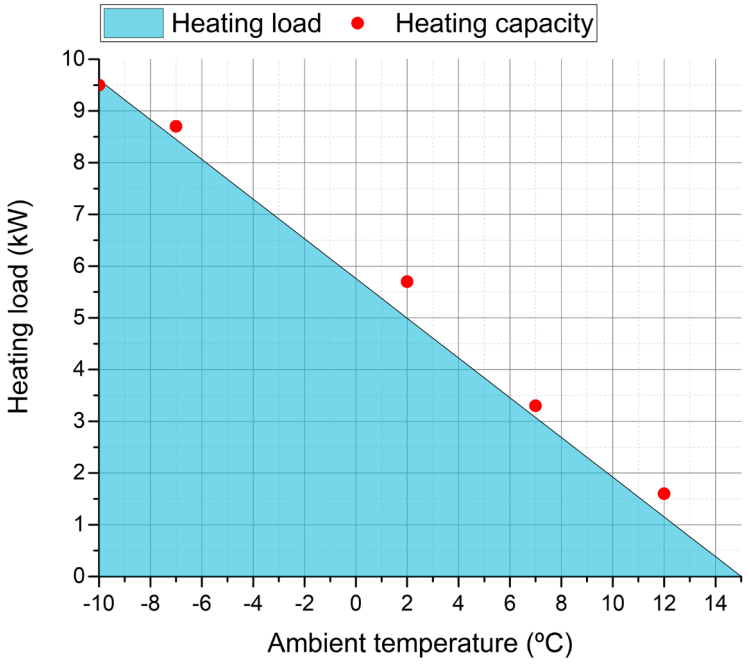

Figure 39: Heating load and heating capacity of prototype 1

Figure 39 shows the heating load from the hypothetical building where the heat pump would operate according to EN 14825 [2]. The heating capacity can be adjusted to the heating load required at each ambient temperature because the unit possesses an inverter driver able to modulate the compressor speed. This compressor speed has a minimum value set by the

compressor manufacturer, which would make the heat pump work with starts and stops to modulate the heating capacity. However, this would happen in ambient temperature greater than 12 ^{o}C. In the following figures, the test results will be shown with the compressor speed in the abscises. The tests correspond to the test conditions of the standard EN14825 with two extra tests added. The relationship between test condition and compressor speed can be seen in Table 15.

Test condition	Compressor speed (rps)
B0W35	120
B0W34	108
B0W32	90
B0W30	72
B0W29	60
B0W27	40
B0W24	20

Table 15: Compressor speed in SCOP campaign.

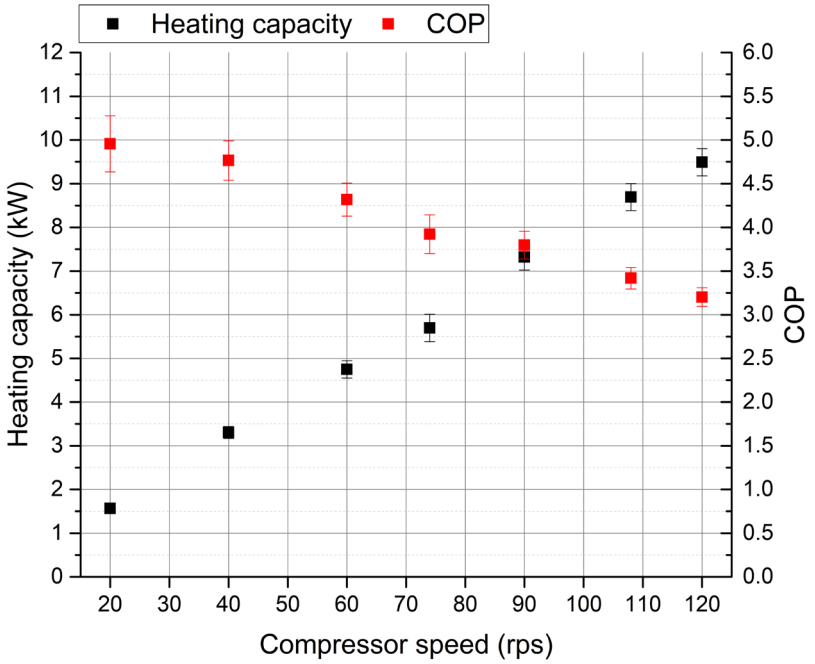

Figure 40: Heating capacity and COP of test campaign one first prototype.

As seen in Figure 40, as the compressor speed is reduced to fit the heating load, the heat pump works in a better condition, increasing its efficiency. This COP variation is quasilinear with the compressor speed, having the most efficient condition at 20 rps with a COP of 4.89 and the worst efficiency at maximum compressor speed (120 rps), obtaining a value of 3.21. Regarding the heating capacity, the behaviour is also almost linear with the compressor speed, but in this case, increasing. The minimum heating capacity is obtained with the minimum compressor speed $\dot{Q}_h = 1.56\,kW$ at $n = 20\,rps$ and the maximum value at maximum compressor speed, $\dot{Q}_h = 9.49\,kW$ at $n = 120\,rps$.

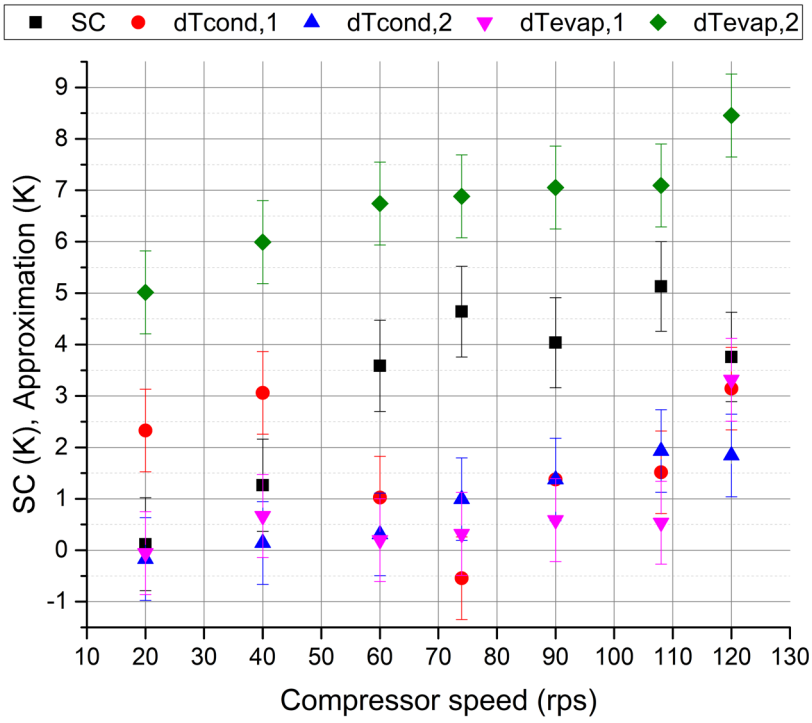

Figure 41: SC, approach temperature in the condenser and evaporator of test campaign one prototype 1.

Figure 41 shows the SC and the different approach temperatures in the condenser and evaporator. These are the minimum difference between the heat exchangers' refrigerant and secondary fluid temperatures. Three approach temperatures ($\delta T_{cond,1}$, $\delta T_{evap,1}$ and $\delta T_{evap,2}$) are easy to define and calculate, but the one concerning the condensation temperature is not that trivial, as seen in Figure 42. The $\delta T_{cond,1}$, $\delta T_{evap,1}$ and $\delta T_{evap,2}$ are defined in the equations (21), (22) and (23), respectively; and $\delta T_{cond,2}$ is calculated using a 3 zone model in the condenser, (superheated gas, two-phase, subcooled liquid) assuming ideal behaviour, without pressure drop. Figure 42 defines how the approach temperatures are measured in the condenser.

$$\delta T_{cond,1} = T_{cond,out} - T_{w,in} \tag{21}$$

$$\delta T_{evap,1} = T_{b,in} - T_{evap,out} \tag{22}$$

$$\delta T_{evap,2} = T_{b,out} - T_{evap,in} \tag{23}$$

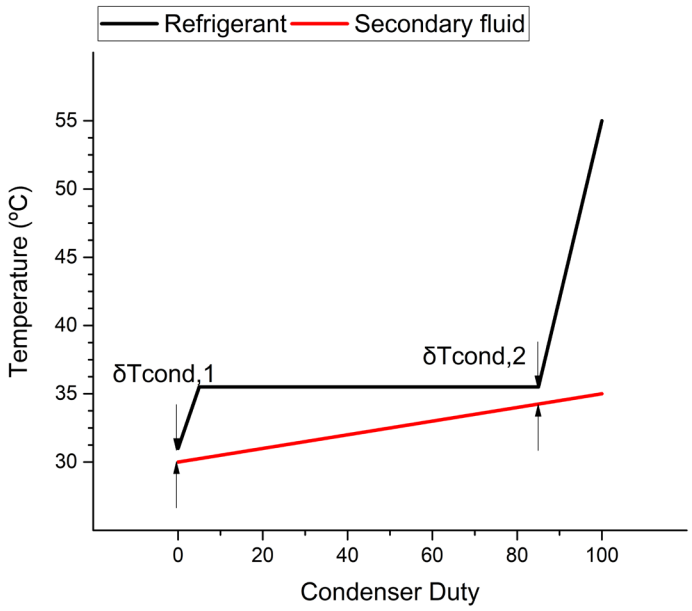

Figure 42: Temperature differences definition in the condenser.

Regarding the SC in Figure 41, the minimum values are observed at the minimum compressor speed, test B0W24. In this case, the subcooling value is almost 0 K which means that a little charge increase would have been possible, increasing the heating capacity without affecting the COP significantly. Then the next test with low SC is B0W27, which also corresponds to low compressor speed $n = 40\ rps$. The rest of the tests have a value of SC between 3.58 K and 5.13 K, and no more dependence on compressor speed can be found.

The different approaches in the condenser, $\delta T_{cond,1}$ are pretty variable, showing maximum value at the maximum and minimum compressor speeds and having it reduced in average speeds. A minimum is observed at 74 rps with an impossible negative value that the uncertainty of the measurements and the pressure drop inside the condenser and distributor can explain. Seeing the $\delta T_{cond,2}$, this variable is dependent on the compressor speed. This value expresses how oversized/undersized the condenser is, and being the maximum difference between the refrigerant and the secondary fluid of

1.93 K, the condenser size could have been reduced to reduce the refrigerant charge. This 1.93 K is relatively low for high compressor speed tests and indicates the condenser is oversized for the application. This oversizing is even more dramatic at low compressor speeds, and the heat exchanger volume reduction probably would not affect it. Also, in this case, impossible negative values are observed at low compressor speeds. The uncertainties in the measurements and pressure drop in the distributor in the port of the condenser and the condenser itself could explain these impossible values.

Changing the focus to the evaporator, seeing $\delta T_{evap,1}$ in Figure 41, the result is similar to $\delta T_{cond,2}$. In this case, all the tests but B0W35 have a $\delta T_{evap,1}$ nearly zero that indicates that the evaporation temperature is being determined by the SH level to avoid crossing temperatures. Only in the last test, the evaporator is not oversized, and a difference of 3 K appears. Additionally, similar conclusions can be extracted from $\delta T_{evap,2}$, as the evaporator inlet is already in phase change, the tests in which the evaporator temperature is only driven by SH, the $\delta T_{evap,2}$ is almost the same with the only difference in heat losses between the evaporator and the compressor.

Then, Figure 43 shows the discharge temperature, the oil temperature and the condensation temperature having as reference compressor speed and water outlet temperature.

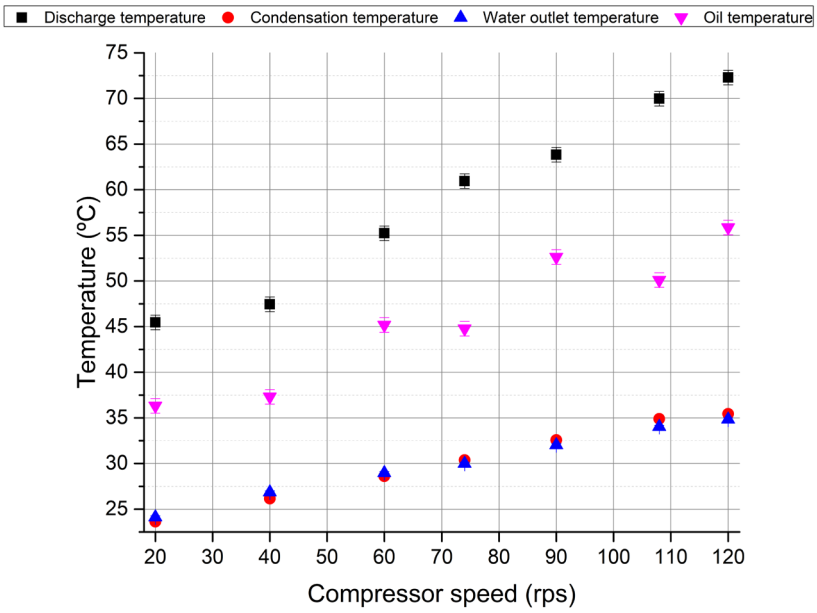

Figure 43: Discharge, condensation and oil temperature depending on compressor speed.

As can be seen, the discharge temperature rises with the compressor speed and the water temperature but also increases its difference with the condensation temperature, being this difference of 22 K at $n = 20\,rps$ and 36.9 K at $n = 120\,rps$. Oil temperature follows a similar trend, but it is less significant. The increase in oil temperature with compressor speed has a smaller slope, increasing the difference between oil temperature and discharge temperature. Consequently, the difference between the discharge and oil temperature increased from 9.2 K at $n = 20\,rps$ to 16.4 K at $n = 120\,rps$. Nevertheless, the increase of oil temperature is higher than the condensation temperature and the value of this difference is 12.7 K at $n = 20\,rps$ and 20.5 K at $n = 120\,rps$.

This last difference is mainly provoked by the increase of irreversibilities with the compressor speed and the rise in power consumption and heat losses inside the crankcase that heats the refrigerant while cooling the motor.

Lastly, in Figure 43, a slight difference between the outlet temperature of the water and the condensation temperature can be seen. This difference, DT_{cond} calculated as equation (24), starts being negative with a value of -0.49 K at n=20 rps and then becomes positive, with a value of 0.60 K at n=120 rps.

$$DT_{cond} = T_{cond} - T_{w,out} \tag{24}$$

Singular points campaign

The next test campaign refers to the singular variations from the nominal point. In this test campaign, the reference test condition is B0W35 with 10 K of SH with 195 g of refrigerant charge and 60 Hz of compressor speed. In the test of this campaign only one parameter is changed from the nominal test. Still, the refrigerant charge is calculated at every test condition with the same criterion used for the refrigerant charge selection as a reference, COP maximisation. Although, there are two exceptions for this refrigerant charge definition: test 2 (ErP E) and test 9 (overfilled). In test 2, the refrigerant charge is the same as the nominal point because it also belongs to the SCOP campaign, and in test 9, the test's purpose is to analyse the refrigerant charge excess. Consequently, there is more refrigerant charge than the optimal value.

Since the test campaign tries to analyse the effect of every variation alone, all tests will be compared with the nominal one. For this reason, in the different plots, the reference value is marked with a dashed horizontal line with the colour of the variable.

The first variables to analyse are the ones referring to the global performance of the refrigerant cycle. Figure 44 shows for these test conditions heating capacity, COP, and charge specific capacity.

Regarding the compressor speed increment, even though the compressor speed is doubled, the heating capacity increment is more than that. Volumetric efficiency increases at high compressor speeds [3]. Then, as the refrigerant charge is the same as in the nominal point, the charge specific capacity variation is equivalent to the heating capacity. Lastly, the COP is degraded due to inefficiencies (mainly mechanical and winding losses in the compressor).

When overfilling the system with refrigerant charge, the heating capacity still increases a bit, but the power consumption increases too, making the

COP remain or even decrease. As the heating capacity increment is insignificant, the charge specific capacity decreases.

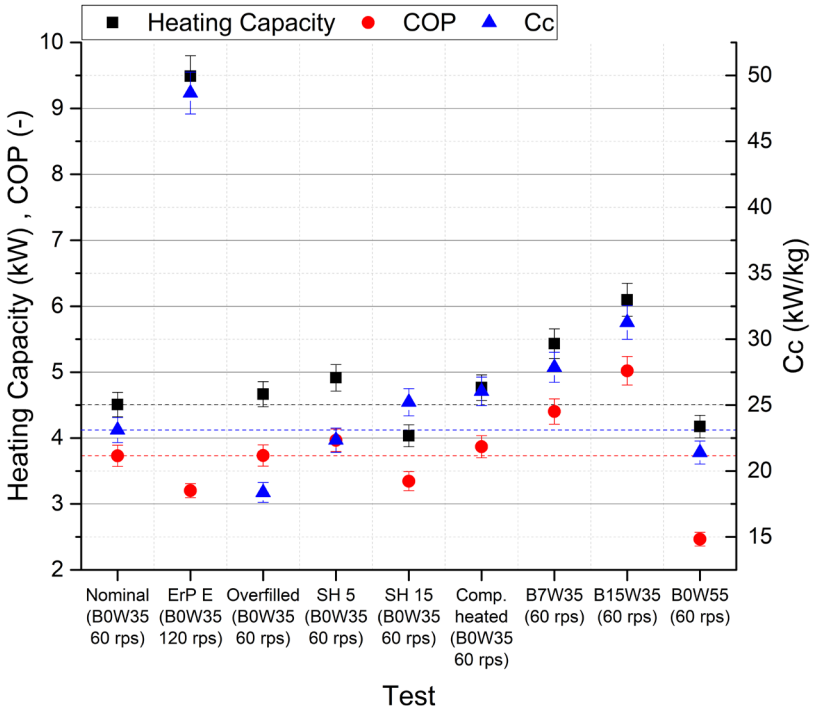

Figure 44: Heating capacity, COP and Cc of singular variations campaign in prototype 1.

When changing the superheat, its value affects inversely to the heating capacity, and an increment is seen in SH5 and a decrement in SH15 mainly due to the change of suction pressure and consequently suction density. However, as the refrigerant charge is involved too, the charge specific capacity is almost maintained in the case of 5 K and increased in the case of 15 K of superheat. The COP variations are similar to the heating capacity variations since the SH affects the suction conditions, pressure ratio, and compressor power input.

When the compressor is heated with a heating wire, there is a slight increment in the heating capacity and COP, but the COP value plotted does not consider the heating wire's power. If this consumption is considered, the global COP would be reduced to 3.41. Since the heating

capacity increases and the refrigerant charge needed is reduced, the Cc increases considerably.

Lastly, this comparison for source and sink temperature variations loses importance since the conditions are changed. When the source temperature increases, the compressor's suction gas density increases, increasing the heating capacity and the COP because of the reduction in pressure ratio and increase of refrigerant mass flow rate. The pressure ratio rises when the sink temperature increases, reducing compressor efficiencies, heating capacity, and COP.

In addition, Figure 45 shows the discharge and oil temperatures in this test campaign. It can be seen that increasing the compressor speed (ErP E) makes both temperatures rise since the motor has more heating losses and the crankcase gets hotter. However, when the system is overfilled, the discharge temperature increases without increasing the oil temperature. This increment is due to the increase in discharge pressure and, consequently, the pressure ratio.

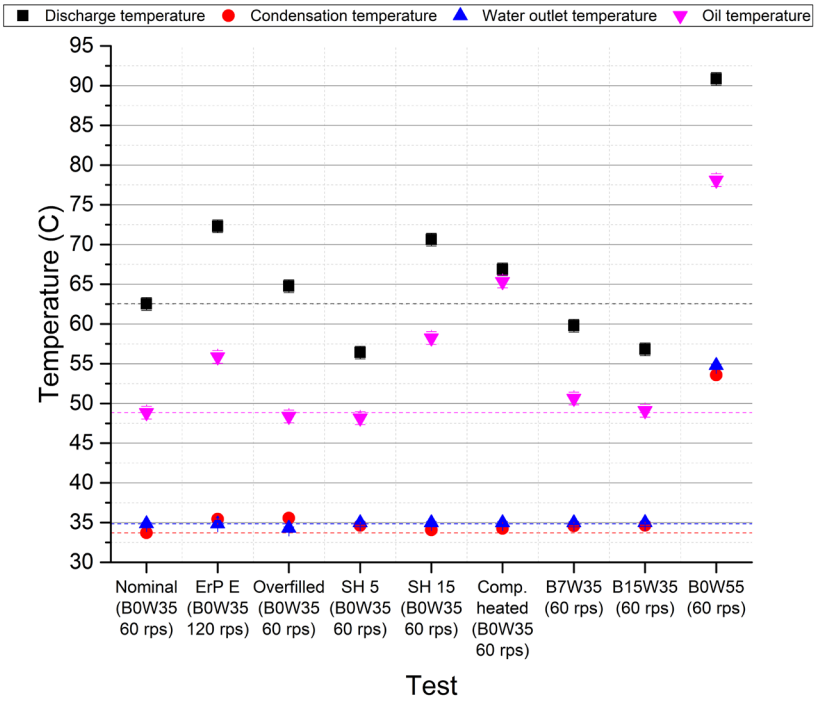

Figure 45: Discharge and oil temperatures in test campaign two prototype 1.

When the superheat is reduced, the discharge temperature decreases since the suction pressure increases and the suction entropy and pressure ratio are lower. Still, the drop in oil temperature is negligible. On the contrary, when the SH is increased, the discharge and oil temperatures rise.

In the test with the heating wire, the oil temperature increased, which was the main objective, and the discharge temperature increased too. The discharge temperature is always higher than the oil temperature but at certain point the difference between both temperatures become negligible.

When the source temperature increases, discharge temperature is reduced due to pressure ratio reduction and suction condition variations; however, the oil temperature remains almost constant, and no linear variation is observed.

Lastly, both temperatures rise when the sink temperature increases, and their difference to the saturated condensation temperature too.

3.2.2. Prototype 2

Nominal Point

As the previous prototype shows, the nominal point is the reference condition corresponding to the mentioned conditions. This condition is B0W35 at 60 Hz and 10 K of SH. This test was used again to determine the refrigerant charge in the SCOP campaign and as a starting point for further singular variations.

In the nominal point of the second prototype, the heating capacity obtained was 4.28 kW with a COP of 3.53 and electric consumption of 1.22 kW. The refrigerant charge used was 170 g which was settled for the first campaign.

As in the first prototype, the condensation temperature was near the physical limit, 34.18 ^{o}C. The water temperatures are between 30 and 35, and the refrigerant temperature must always be higher to ensure heat transfer. This is an expected result because the condenser didn't change between prototypes.

Regarding the evaporator, the evaporation temperature is -11.9 ^{o}C. Knowing that the superheat equals 10 K, the evaporator is a bit undersized for the application; in this case, the speed is only half the maximum allowed at the compressor.

The discharge temperature measured was 63.7 ^{o}C, and the oil temperature was 48.9 ^{o}C.

SCOP campaign

In this test campaign, the refrigerant amount used was the amount that made the nominal point work with the optimal COP (170 g).

In this prototype, with the refrigerant charge amount mentioned, the declared heating capacity is 8.15 kW and the SCOP value of 3.85.

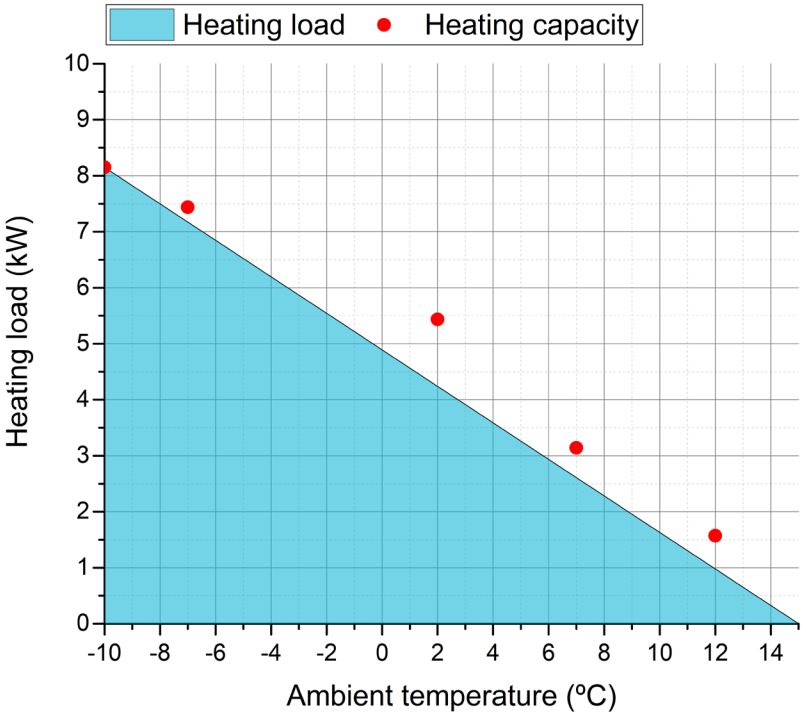

Figure 46: Heating load and heating capacity of prototype 2.

Figure 46 shows the heating load and capacity according to the ambient temperature. As mentioned before, as it is a variable speed compressor, the heating load easily fits with the heating capacity of any modulating compressor speed. This technology increases efficiency, obtaining a much better result than an On/Off system.

Then in Figure 47, the heating capacity and COP of the points mentioned in Figure 46 are presented. This figure shows how the COP decreases when the compressor speed increases, seeing the impact of the inverter technology on global seasonal efficiency. This variation is almost linear, having its

maximum of $COP = 5.00$ at 20 rps and the minimum value of $COP = 2.87$ at a compressor speed of 120 rps.

In this test campaign, it was decided not to add the two intermediate extra points and only perform the ones defined in the standard EN 14825.

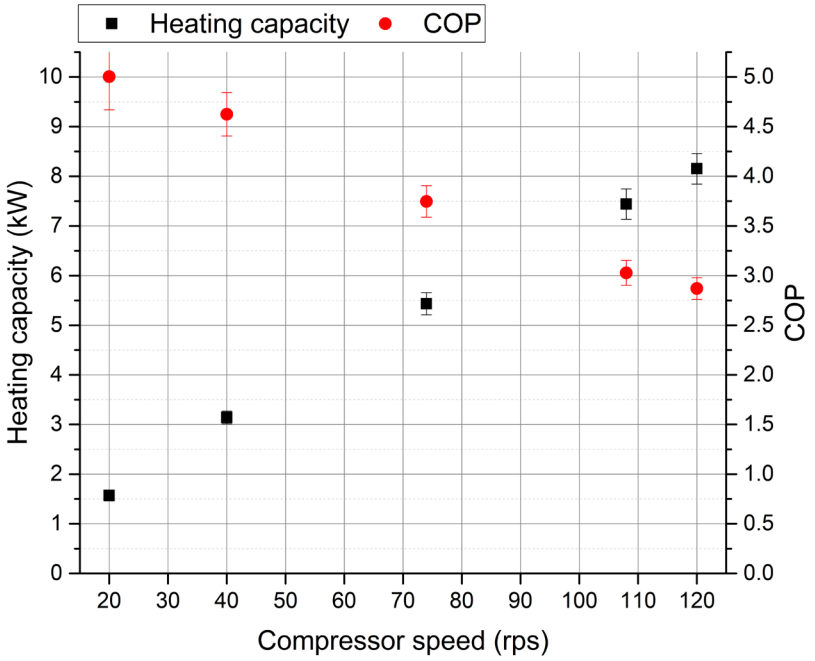

Figure 47: Heating capacity and COP of test campaign one prototype 2.

Heating capacity also shows a quasilinear increment with compressor speed, having its maximum of $\dot{Q}_h = 8.15\ kW$ at 120 rps and a minimum of $\dot{Q}_h = 1.57\ kW$ at 20 rps.

In addition, Figure 48 shows the value of SC and the different approach temperatures in heat exchangers. These approach temperatures are defined in equations (21),(22) and (23) and Figure 42 from section 3.2.1.

The SC has no linear relationship as it happened in the previous prototype. However, in the two tests with low compressor speed, the SC is lower than 2 K, and in the other three tests, the value oscillates between 3 and 5 K, 5.11 K more concretely. Seeing the approach temperatures in the condenser, $\delta T_{cond,2}$ shows that the condenser is oversized since its maximum value is 1.78 K at full compressor speed. A linear variation in this variable can be

seen, increasing with compressor speed, but the increment is minimal. The other approach temperature in the condenser $\delta T_{cond,1}$ shows that a bit more refrigerant charge could be added before the condenser works at its best point since its values remain between 1 K and 3 K in all tests of this campaign.

Moving to the evaporator, $\delta T_{evap,1}$ and $\delta T_{evap,2}$ show a quasilinear behaviour, increasing with compressor speed. $\delta T_{evap,1}$ values at low compressor speed conditions are approximately 0 K, meaning that in these tests, the SH forces the evaporation temperature to lower values. In contrast, high values are observed in other situations, suggesting that the component is undersized. The maximum value observed is 9.9 K which is non-negligible.

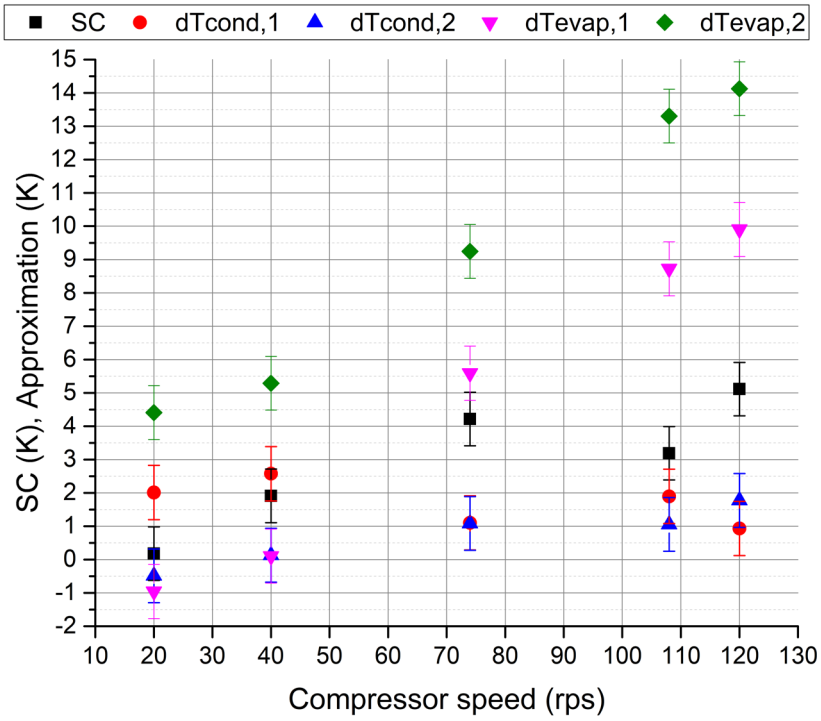

Figure 48: SC and approach temperatures in heat exchangers in test campaign one prototype 2.

Lastly, Figure 49 shows the discharge temperature, the oil temperature and the condensation temperature with the increasing compressor speed and adding to the plot as a reference the water outlet temperature.

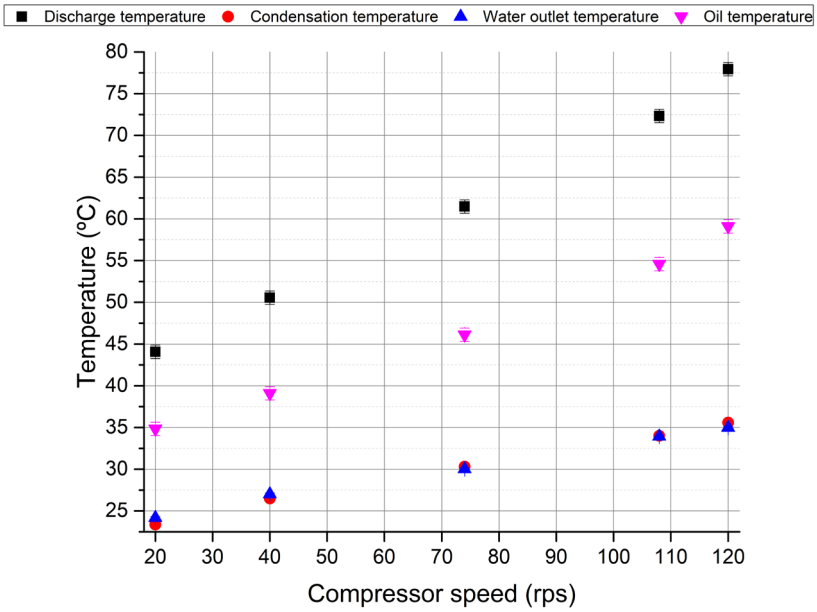

Figure 49: Discharge, oil and condensation temperatures in SCOP with prototype 2.

This figure shows a linear behaviour of the oil and discharge temperatures with the compressor speed. There is an increment in these temperatures and an increment in the difference between them. As the compressor speed increases, the isentropic efficiency decreases, increasing the heat losses that heat up the oil and the discharge. It can also be observed that the condensation temperature is below the water outlet temperature with low compressor speeds. When the compressor speed increases, the difference is reduced, and between 40 and 70 rps, there is a cross between the temperatures, and the difference starts to grow.

Singular points campaign

Like prototype 1, the next test campaign includes singular variations to the nominal point. This campaign added one test after seeing the importance of the refrigerant dissolved in the oil (SH24). This test tried to maintain the evaporation temperature at the same value but increase the suction

temperature. To manage it, the superheat and the source temperature were raised, making one variable compensate for the effect of the other in terms of evaporation temperature. In contrast, sink variation was not performed since it was less critical.

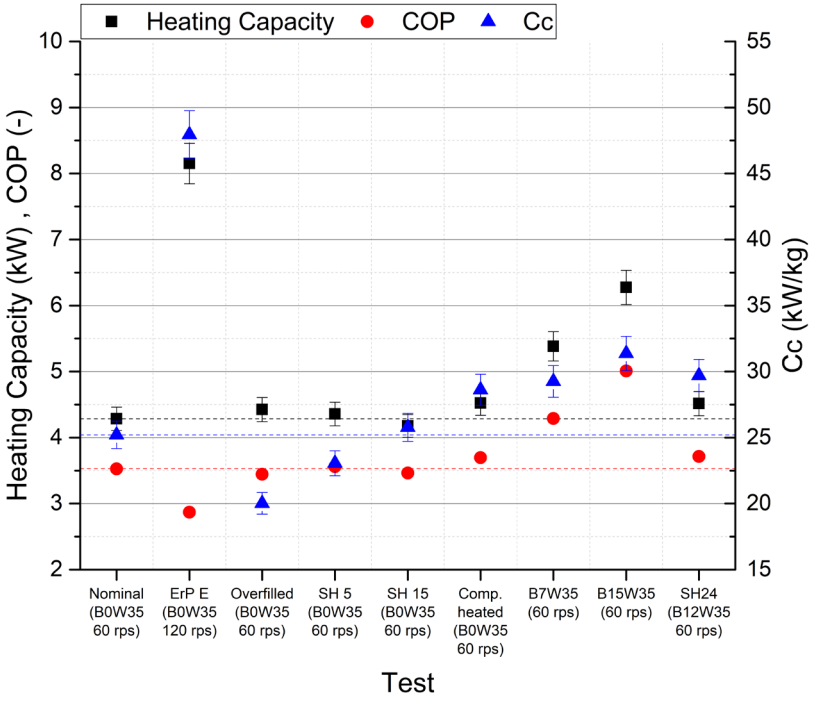

Figure 50: HC, COP and Cc of singular variation in prototype 2.

Figure 50 shows the heating capacity, COP and charge specific capacity in the different test conditions of this campaign. As it happened with the first prototype, as they are singular variations, the best form to understand it is by comparison to the nominal point.

Regarding the increment of compressor speed, in this case, the heating capacity obtained in the ErP E test is lower than double the reference value. This result is due to the change in evaporation temperature and, consequently, the suction density. Cc increases the same amount since the refrigerant charge remains invariant, and COP drops due to increased losses.

When overfilling, there is a minor increase in heating capacity, making the C_c drop due to the rise in refrigerant charge amount. Regarding the COP, there is a little decrement, which can already be observed in Figure 32.

The following tests are related to superheat variations. In these tests, the variations in heating capacity and COP are negligible since the evaporator is a bit undersized, and the superheat does not affect it as much as before. In this case, the variable most affected is the refrigerant charge and the charge specific capacity, increasing with high and decreasing with low superheat.

Then, some tests aim to heat the compressor crankcase to reduce the oil solubility. In the first test, a heating wire heated the compressor's bottom part, slightly increasing all variables shown in the Figure 50, however, the electric consumption of the heating wire has not be taken into account when calculating this COP. It is considered in section 3.4.

The second test warmed the compressor, increasing the superheat, and the heating capacity and COP results were very similar. However, the refrigerant charge needed was less in this second test, and the charge specific capacity increased more.

Lastly, seeing the source temperature variations, the heat pump works with a lower pressure ratio in a more efficient condition when the source temperature increases. A linear increase of all variables can be observed.

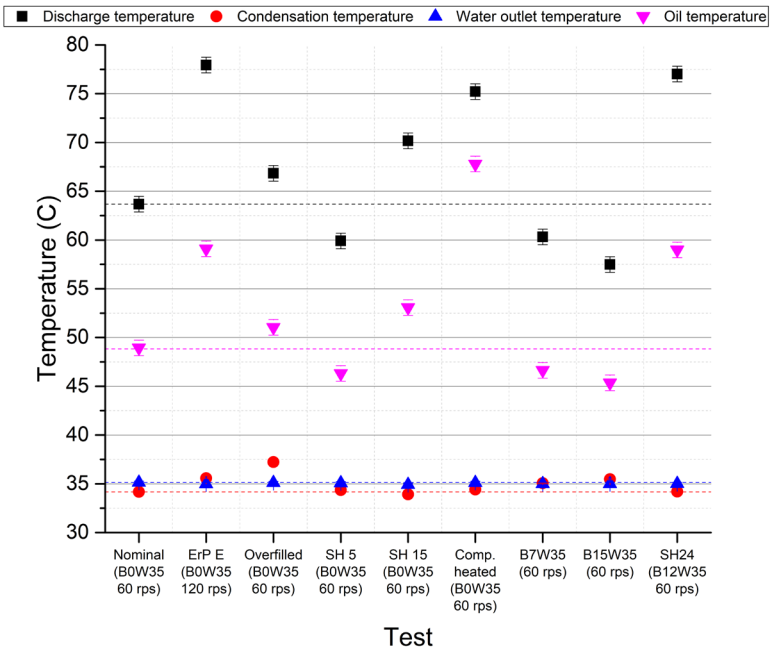

Figure 51: Discharge and oil temperatures in test campaign two with the second prototype.

Following with results of singular variations, Figure 51 shows these tests' discharge and oil temperatures. As seen in Figure 49, in test ErP E both discharge and oil temperature increased because of the pressure ratio and heat losses inside the compressor. When the system has too much refrigerant charge, the subcooling increases condensation pressure, and consequently, discharge and oil temperature rise due to the higher pressure ratio.

The superheat variations affect similarly with this prototype when its value increases and decreases. When the SH is reduced to 5 K, discharge temperature drops by 4 K and oil temperature by 3 K. When the SH is increased to 10 K, discharge temperature increases by 6 K, and oil temperature increases by 4K.

When the system is heated with a heating wire (250 W), the discharge temperature increases by 11 K and the oil temperature by 19 K. However, when heated with high SH, the discharge temperature increases by 13 K and the oil temperature by 10 K.

Lastly, when there is a source temperature variation, discharge and oil temperature decrease linearly with the source temperature increase due to the pressure ratio reduction. In the case of a sink temperature increase, both discharge and oil temperatures increase. However, the oil temperature difference from the condensation temperature is almost zero.

3.2.3. Prototype comparison

As seen in the previous sections, 3.2.1 and 3.2.2, the first prototype has both heat exchangers oversized for the compressor size, resulting in condensation and evaporation temperatures near the thermodynamic limit, due to external conditions, in almost all of the tests. Then going to the second prototype, changing the evaporator, as it has reduced the volume and the heat transfer area, it is not oversized. In this section, a comparison between both prototypes will be seen, and in the end, infrared pictures of both evaporators will be shown.

To start the comparison, the first analysis will be the nominal point. In this test condition, changing the evaporator has resulted in a 5 % decrease in heating capacity (220 W) and a 5 % decrease in COP since the compressor power input remains invariant. Refrigerant charge decreases by 13 % resulting in an increase of the charge specific heating capacity due to the lower decrease of heating capacity (5 %). The performance deterioration is explained because there is a reduction of 3 K in evaporation temperature while condensation temperature is almost the same, with only a 0.1 K difference. The rest of the variables in these tests remain similar between them.

In the SCOP campaign, there is a reduction in the heating capacity declared of 14 % (1.3kW) and a SCOP reduction of 4 % because the decrease in performance is more affected when the compressor speed is higher, as seen in Figure 52.

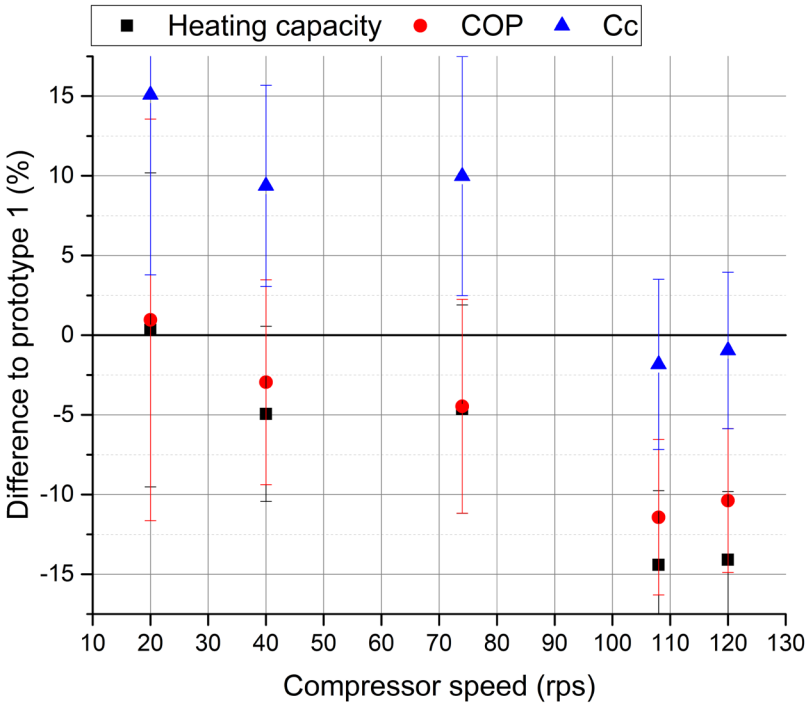

Figure 52: Performance variables differences between prototypes.

Regarding the variables of the thermodynamic circuit, the most affected parameter is the evaporation temperature difference, which is 1 K higher in second prototype at the lowest compressor speed and varies to 5.71 K lower at the almost highest compressor speed, as shown in Figure 53.

This difference in evaporation temperatures provokes a change in the pressure ratio since the condensation temperature remains the same. This change in pressure ratio also induces a variation in discharge and oil temperatures, having linear differences depending on the compressor speed, as shown in Figure 53.

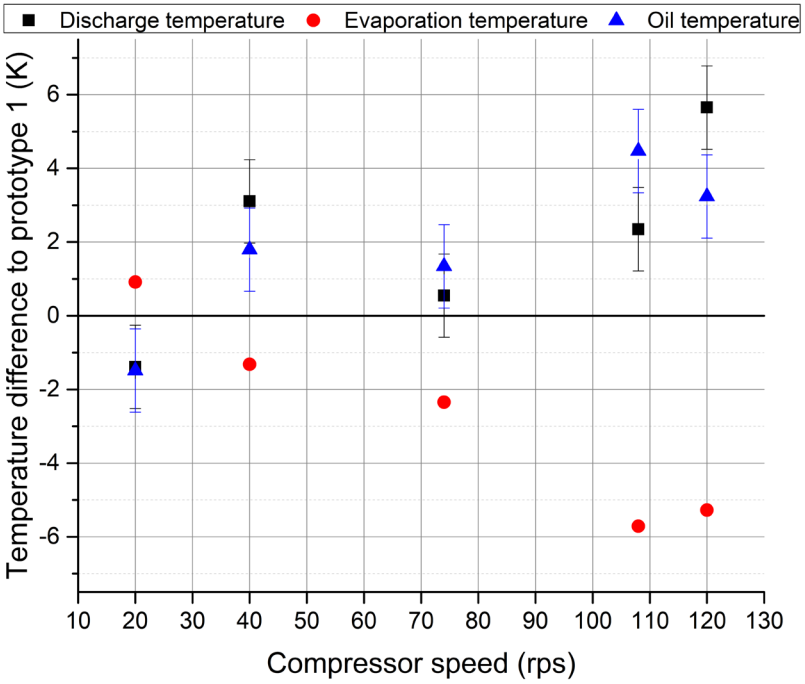

Figure 53: Temperature differences between prototypes.

In the singular variations campaign, in Figure 54 and Figure 55, it can be seen that the changes from the nominal point affect differently to the different prototypes. Heating capacity has decreased in almost all the tests of the second campaign with the second prototype. There are only three tests where the heating capacity has been maintained, SH 15, B7W35 and B15W35. In the rest of the tests, the relative difference is between -14 % to -3.5 %.

The COP variation in these tests is also negative, having values of COP reduction between 0 and -10 %. Only in the test SH15 the second prototype obtained a higher COP.

Regarding the refrigerant charge, in five of the tests, changing the evaporator has supposed to result in a refrigerant charge reduction of more than 25 g. Then in B7W35, the reduction decreased to 10 g, and in the tests B15W35 and SH15, a slight increment in refrigerant charge is needed.

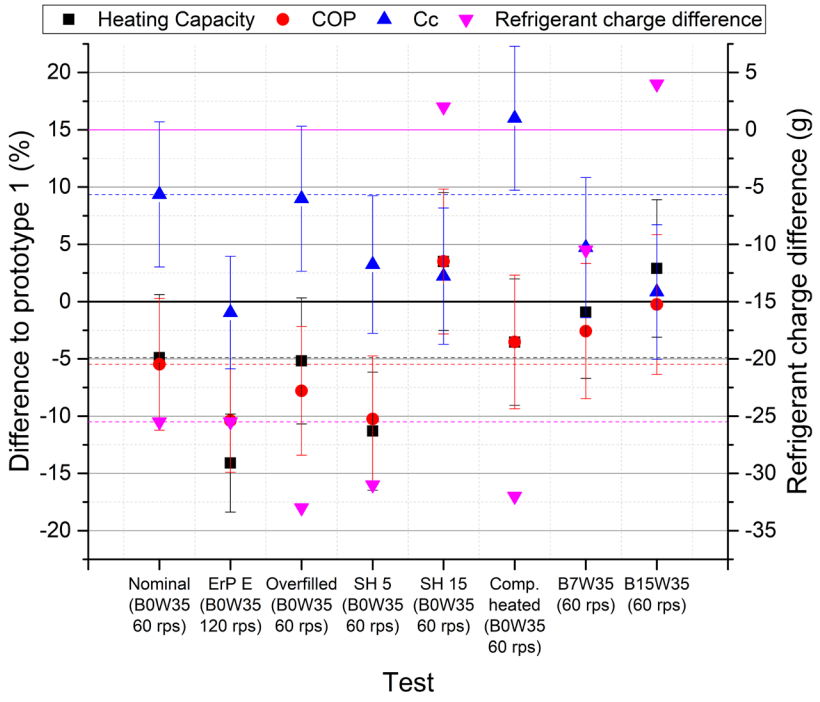

Figure 54: Differences from overall results in test campaign two.

Figure 55 shows the differences in the thermodynamic variables that changed the most between prototypes. Focusing on evaporation temperature, there is an overall behaviour of 2.5 K decrement after the evaporator change. The exceptions of this variation are: ErP E, which has the compressor speed doubled, and consequently, as the new evaporator is undersized, the lack of effective area is translated into an even lower evaporation temperature; SH5, due to the same undersize problem, there is no increase of evaporation temperature when the superheat is decreased; and SH15, increasing the superheat does not affect as much to the evaporation temperature as it happened in the first prototype.

Also, this figure shows a relationship between the difference in evaporation temperature and discharge temperature. A reduction in evaporation pressure means an increase in discharge temperature because of the rise in the pressure ratio. The only exception is the case of heating the compressor. This relationship is not maintained in oil temperature since other factors affect this temperature.

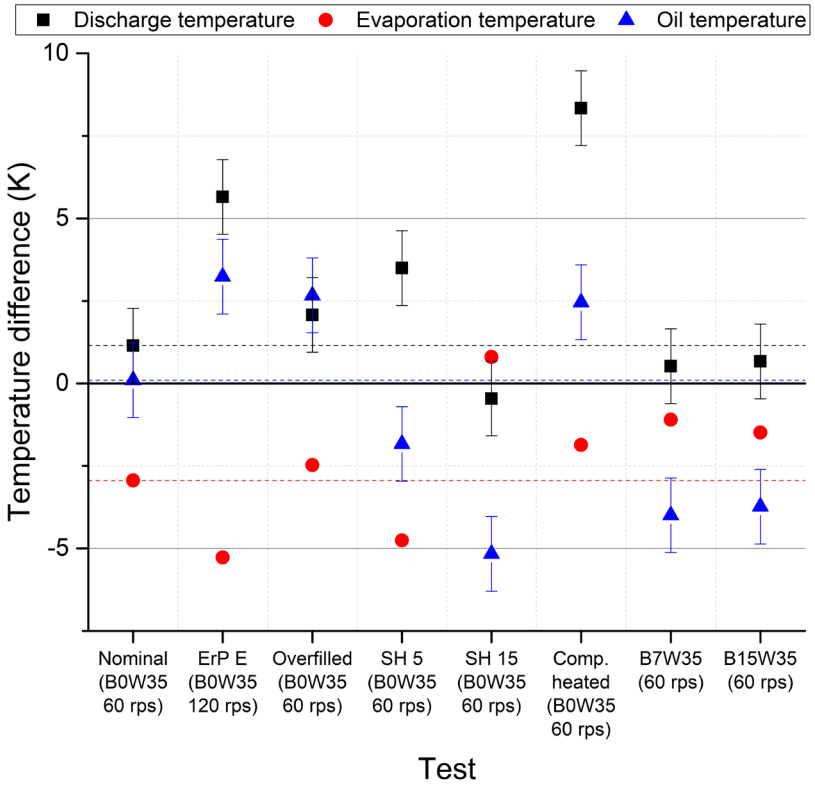

Figure 55: Temperature differences in test campaign two.

To understand the difference in the evaporator, this component's infrared (IR) pictures were obtained in all the tests performed. With them, it can be observed that maldistribution appears in both heat exchangers but is stronger in the second one.

All IR pictures can be seen in Appendix F. However, to illustrate the previous words, Figure 56 and Figure 57 show the worst test condition for the maldistribution effect in both heat exchangers. This test condition is test 2 (ErP E, B0W35 at 120 rps)

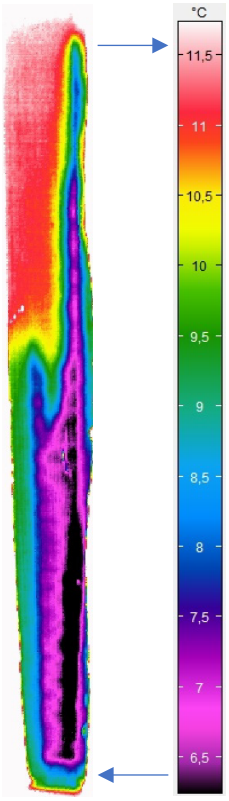

Figure 56: IR picture ErP E prototype 1

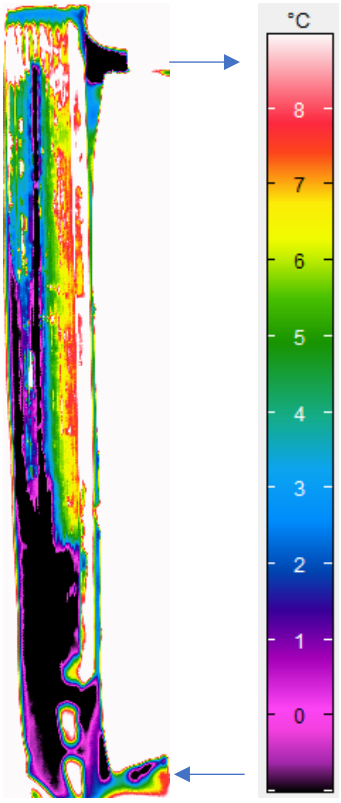

Figure 57: IR picture ErP E prototype 2

3.3. Refrigerant charge distribution

This section presents the refrigerant distribution in the different components when the heat pump was running in steady-state operation. After the data acquisition during the tests, the refrigerant was trapped in the different sections and extracted to be weighted.

The structure of the section is similar to the previous one. Firstly, the results of the first prototype will be exposed, starting with the nominal point, focusing on the charge distribution and the impact of every component. Then using the results of the SCOP campaign, the difference between the conditions that generally appear yearly will be studied, seeing the variations according to the compressor speed. And finally, a set of tests

with singular variations from the nominal point are shown, looking at the effect of these singular variations on the impact of the refrigerant charge on each component.

Once all the tests are studied in the first prototype, the same studies are performed in the second prototype, with a lower evaporator volume and refrigerant charge needed in almost all test conditions.

With all the results, a comparison between both prototypes is presented to see how it affects the singular variation on each of them.

The last part of the section will compare the refrigerant in each component and the result of the refrigerant prediction made in IMST-ART v4.0. An improvement in each component will be proposed, seeing the new refrigerant charge prediction results.

3.3.1. Prototype 1

Nominal point

As mentioned, the first point would be the nominal point, as this test condition determines the refrigerant charge of the SCOP campaign and the reference point for the singular variations. This test in the first prototype was made with 195 g of propane.

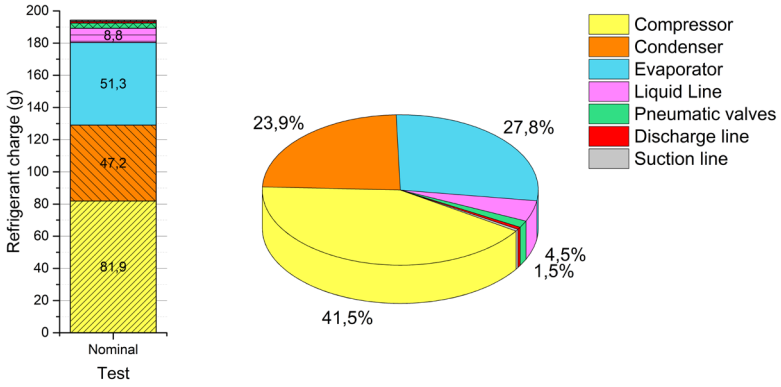

Figure 58: Nominal refrigerant charge distribution prototype 1

Figure 58 shows the amount of propane inside each component (left) and their percentages from the total (right). As can be seen, almost half of the refrigerant charge is inside the compressor (41.5 %). Then the rest is almost evenly distributed in the heat exchangers, 27.8 % in the evaporator and 23.9 % in the condenser. These numbers contrast the amount in the

literature, where the condenser plays a more significant role in the refrigerant charge amount. For example, in [4], the amount in the condenser gets from 33 % to 66 % in heating mode and 37 % to 53 % in cooling mode. These numbers are more commonly observed in the literature or even more percentage in this component. There are two reasons for the difference: (i) the vapour compression cycles in the literature where the refrigerant distribution has been studied are in a high proportion air-to-air heat pumps, being either domestic split air conditioning or automotive systems; and (ii) the subcooling employed in the literature is higher, usually going in the overfilled operation mode. This system is a brine-to-water heat pump with the refrigerant charge just on the border between regular operation and underfilled operation mode. These differences are mainly observed in the heat exchangers and, more in-depth, in the condenser.

The significant percentage in the compressor is due to the amount of refrigerant dissolved in the compressor's oil. In this case, the compressor's oil amount is 0.4 l (approximately 400 g). The typical solubility in the operation conditions is around 10 % (mass of refrigerant divided by the mass of the mixture), making the refrigerant dissolved in the oil and, therefore, useless for the application, approximately 44 grams (varying on the test condition).

The reason for the larger amount in the evaporator than in the condenser is not obvious, it has a bigger volume, but the proportion of liquid fraction in the heat exchange area is lower. Liquid refrigerant stored in the port or maldistribution effects can explain this fact.

Pipes and accessories store the remaining 6.8 % of the refrigerant charge. It is a small amount. However, as the system is a brine source heat pump, the liquid and two-phase lines are short to reduce as much refrigerant charge as possible in these lines. Even though the small dimensions, they account for 4.5 % of the total refrigerant charge and 66 % of the lines and accessories. The following important elements in this group are the QCVs, which trap inside their sphere the refrigerant that is flowing through at the activation moment. From these QCVs, the only one with a non-negligible refrigerant charge is located in the liquid line, with 1.5 % of the total amount. Considering it, the liquid line and two-phase line with its accessories store 88 % of the remaining refrigerant charge amount, making the rest of the lines negligible because they carry refrigerant charge in the gas phase.

SCOP Campaign

After the nominal point, the focus moves to the campaign to obtain the yearly performance. As mentioned, the refrigerant charge amount in this test campaign is obtained at the nominal point, 195 g. For this reason, some points may have excess or defect of refrigerant charge. The test conditions correspond to the ones defined in the standard EN14825 [2], and two extra tests were added between the conditions to have a smoother transition between them.

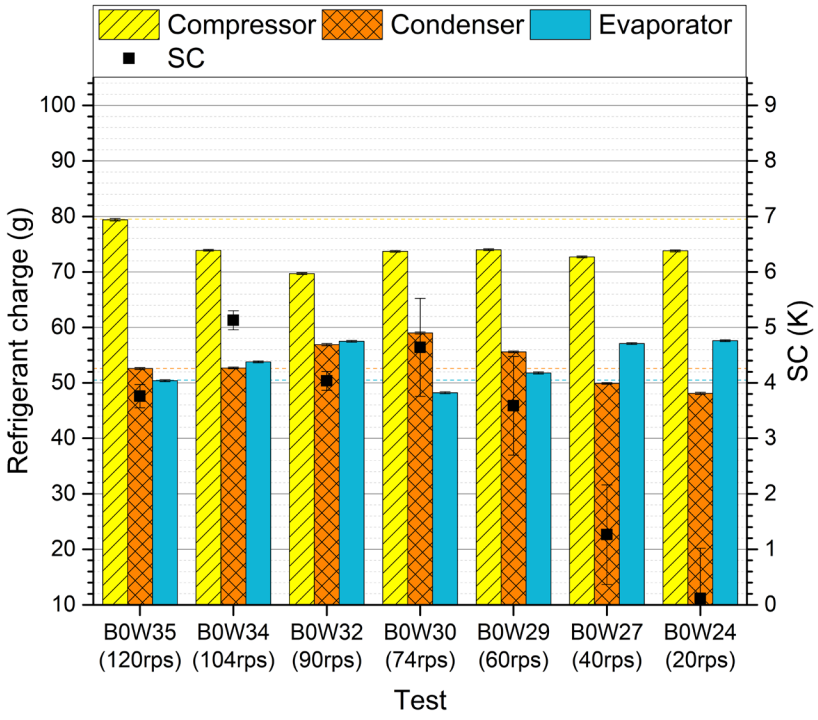

Figure 59: Refrigerant charge distribution in SCOP campaign prototype 1

Figure 59 shows the refrigerant distribution in the first campaign of prototype 1. No linear variations can be observed in any of the components. Looking at the compressor, as was mentioned, the most crucial part is the refrigerant dissolved in the oil. As the compressor's technology is rotary, this kind of compressor usually has the refrigerant in the crankcase after the compression chamber, i.e. at discharge pressure and temperature. The main variables affecting the solubility (as with any other mixture) are the

pressure and temperature, in this case, condensation pressure and oil temperature. As seen in Figure 43, these two variables increase with the compressor speed, making each other the opposite effect. The density of the refrigerant in the crankcase is also affected similarly by these two variables. All this explains the lack of linear regression between refrigerant charge and compressor speed in this test campaign (as the water outlet temperature also varies).

Then, focusing on the evaporator, there is also a lack of relationship between the tests and the refrigerant charge in this component.

Lastly, the condenser refrigerant charge amount depends on the refrigerant needed in the other components because the total amount of refrigerant charge is constant during the whole test campaign. In Figure 59, it has been added the SC amount to help understand the condenser refrigerant charge. The last two tests (B0W27 and B0W24) have a low value of SC, 1.26 K and 0.12 K, respectively and also present the minimum values of the amount of propane in this component. The rest of the tests have values of SC higher than 3.5 K, but not all of them seem to respect the relationship between SC and refrigerant charge in the condenser. Test B0W34 have the highest SC value, 5.13 K, but only 52 g were extracted from the condenser, while in test B0W29, the SC was 3.59 K, and the refrigerant amount was 55 g. These are low discrepancies that the uncertainty may explain.

It must be mentioned that in the testing points where low subcooling was observed, the total refrigerant charge of the whole heat pump may be in the underfilled region, according to Tang et al.[5], all the components have the refrigerant charge reduced due to this effect.

Singular variations campaign

The second test campaign consisted of tests where only one difference from the nominal point was considered. As explained, in these tests, the refrigerant charge of propane to perform the test was previously determined via a test, with the premise of maintaining the criterion of COP maximisation. The two exceptions are the compressor speed increase and the system's overfilling.

This test campaign aims to detect where the refrigerant charge is and how it varies according to particular variations. These variations would help to put the focus on any specific component to reduce the propane amount.

Also, refrigerant charge reduction strategies can be thought of with the results obtained.

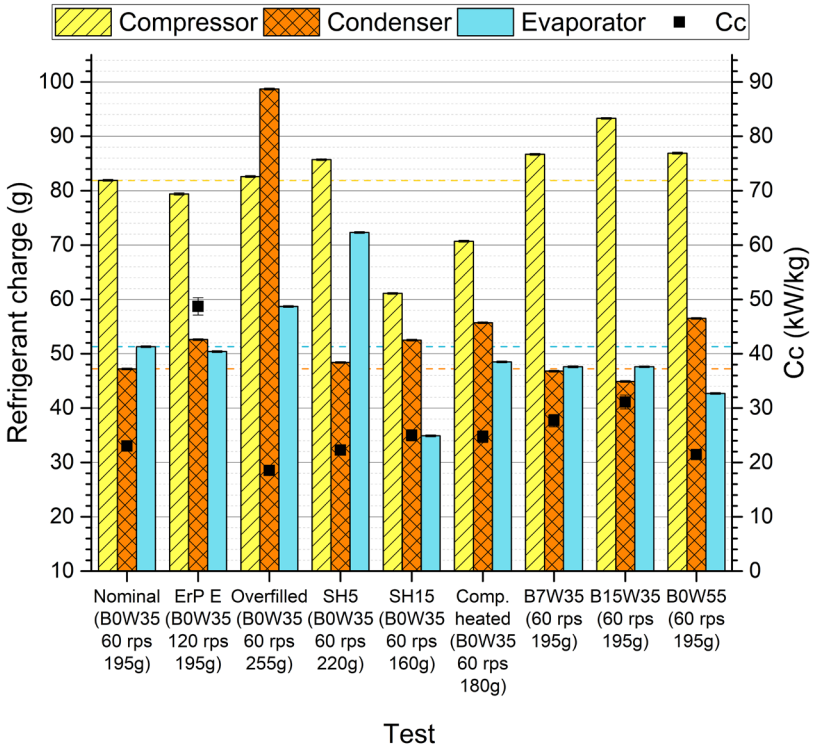

Figure 60: Propane distribution in singular variations of prototype 1.

Figure 60 shows the results of refrigerant distribution in this second campaign. In the figure, horizontal lines from the value of each component at the nominal point are displayed to help the visualisation.

In this case, increasing compressor speed (ErP E) reduces the refrigerant amount slightly in the compressor and evaporator, meaning a little increase in the condenser.

Then, analysing the overfilled tests, it was expected that all extra refrigerant had gone to the condenser. However, since the charge increase also meant a quality reduction in the evaporator inlet, the refrigerant charge in this component has also been affected, increasing by 6 g. The increase in the condenser was 51 g, more than 85 % of the amount added.

Analysing the superheating effect, reducing the superheat makes the compressor and evaporator increase the refrigerant charge needed. The SH reduction increases the suction pressure without changing the suction temperature, increasing the gas density in the little deposit in the suction inlet. Discharge temperature is also reduced due to the pressure ratio reduction, increasing gas density and oil solubility. By its side, in the evaporator, the SH reduction means the evaporation pressure already mentioned, and more heat exchanger volume is used for the evaporation of the refrigerant, increasing the average density and the refrigerant amount.

In contrast, increasing the SH provokes the opposite effect. It decreases the refrigerant charge in the compressor by increasing the discharge temperature and heating the oil with the pressure ratio increment. Evaporation pressure is reduced, reducing the refrigerant charge in the deposit and the solubility of the oil trapped in this piece. In the evaporator, the effect is the opposite; the evaporation pressure decreases, and the volume occupied for the phase-change is reduced, increasing the volume used by superheated gas, reducing notably the average density.

Heating the compressor had a similar refrigerant charge reduction in the compressor as increasing the SH because of the solubility reduction. Still, no effect is observed in the evaporator as was expected.

Lastly, with sink and source variations in this prototype, the refrigerant proportion changed slightly since the same refrigerant charge was obtained in the previous test. Increasing the source temperature increases suction pressure, which, as shown in the test with reduced SH, reduces the pressure ratio, reducing discharge temperature and increasing refrigerant in the compressor. However, unexpected behaviour is observed in the evaporator, where an increase in pressure should mean an increase in refrigerant charge, but in this case, it implies the opposite. Then, when the sink temperature increased, it also meant an increase in the refrigerant charge in the compressor driven by the rise of pressure in the crankcase. In this test, the refrigerant charge reduction in the evaporator can be explained by the increase in quality at the inlet of the evaporator.

3.3.2. Prototype 2

As in the first prototype and the previous results, the tests are divided into three campaigns: nominal, SCOP and singular points and the results.

Nominal point

As in the first prototype, the refrigerant charge that optimises the optimum COP in the nominal point was chosen for the SCOP campaign. This refrigerant charge amount was obtained in a previous test and reached a value of 170 g.

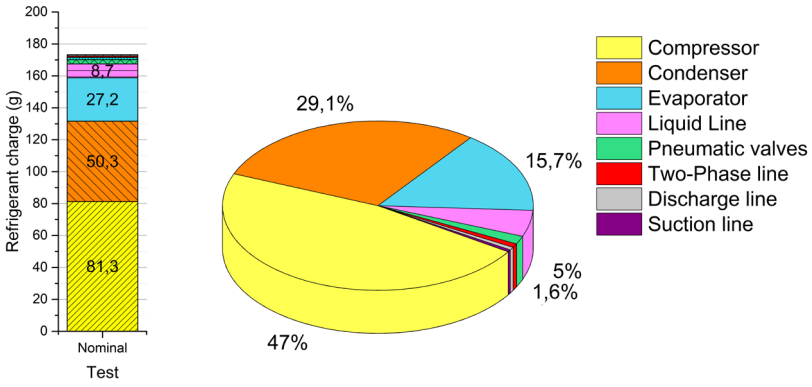

Figure 61: Refrigerant distribution in nominal point prototype 2.

Figure 61 shows the refrigerant distribution obtained with the second prototype at the nominal point. The compressor, as it happened in the first prototype, takes most of the refrigerant charge due to the high effect of the oil solubility. In this case, the refrigerant amount in the compressor is 81.3 g of the total 170 g, which corresponds to 47 % of the refrigerant charge, almost half of it. Then the condenser also plays a significant role in refrigerant charge amount needing 50.3 g, 29.1 % of the total. Lastly, as the internal volume has been reduced substantially in the evaporator, it has reduced the amount needed up to 27.2 g, 15.7 % of the total.

The explanation of the large amount in the compressor remains invariant from the results of the first prototype, the amount of oil (0.4 l) and the solubility of refrigerant inside the oil. The absolute number is also the same, but the proportion has increased as the total refrigerant amount has decreased. Seeing the heat exchangers, the condenser has an appreciably bigger internal volume than the evaporator, as the volume of the second one has been reduced. This difference has resulted in a more significant percentage of refrigerant charge in this heat exchanger. In this case, the proportion of refrigerant charge in the different heat exchangers is more similar to the studies observed in the literature. Still, the compressor takes

more importance in this study than the others because the heat pump has a lower total refrigerant amount.

In this test, pipes and accessories store the remaining 8.2 % refrigerant charge. The liquid and two-phase pipes are the principal volume where this refrigerant is stored.

SCOP Campaign

For the second prototype, the SCOP campaign was related to the standard EN14825 [2] without any extra points. These five tests have varied compressor speeds to fit the heating capacity demand required, according to ambient temperature. Also, the water temperature varies accordingly, making little variations in the discharge pressure.

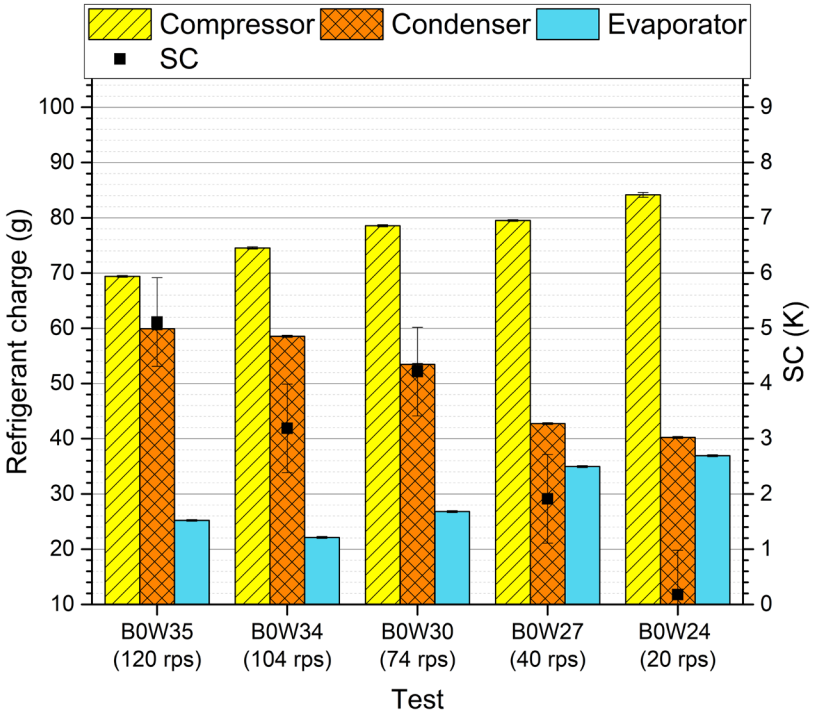

Figure 62: Refrigerant distribution in the SCOP campaign of the second prototype.

Figure 62 shows the refrigerant distribution and its variations during the first test campaign. A linear relationship can be observed between the compressor's refrigerant charge and the compressor's (inverse relationship)

speed. Since the evaporator is not oversized, increasing compressor speed decreases the suction pressure and increases the pressure ratio, raising discharge and oil temperature.

A quasilinear relationship can also be observed in the evaporator, decreasing the refrigerant charge with the increase of compressor speed. The reason is the same: since the evaporation pressure drops, this component's refrigerant charge should also decrease. Also, as the condensation temperature increases, caused by the water temperature increment, the quality at the inlet of the evaporator is higher, contributing to the refrigerant charge reduction in the component.

Once both compressor and evaporator reduce the refrigerant charge with the compressor speed, the condenser must absorb these differences by increasing the refrigerant charge in the component, which can be observed in the figure. Also, with this increment of refrigerant charge, the SC should be in the same manner, and so it is, except the test B0W34, which has the SC reduced from its precedent.

Singular variations campaign

The second test campaign consisted of singular variations from the nominal point. In this case, sink variation has been substituted by another test seeing the importance of the refrigerant dissolved inside the oil. This new test tries to heat the compressor oil sump by incrementing the superheat but maintaining the evaporation pressure, increasing the source's temperature.

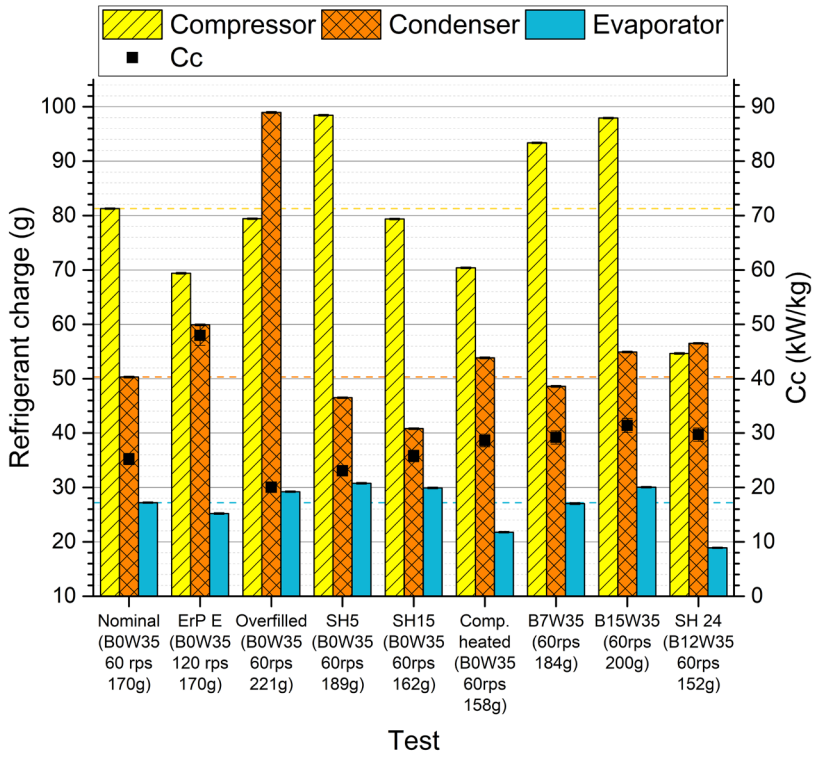

Figure 63: Refrigerant distribution in singular variations campaign of the second prototype.

Figure 63 shows the refrigerant distribution results in all of this campaign's tests. Horizontal dashed lines have been added to help the comparison to the reference test condition.

As seen in the previous campaign, increasing the compressor speed decreases the compressor's and evaporator's refrigerant charge due to the impact on the evaporation pressure, affecting the pressure ratio and the discharge and oil temperature. Condenser refrigerant mass increase is only a result of the previous statement because the total refrigerant mass is invariant from the nominal point.

Seeing the overfilled test, in this case, all the extra refrigerant went to the condenser, making this component carry most of the refrigerant. This refrigerant charge increased the SC to 7 K, forcing the condensing temperature to rise.

Continuing, the SH control changes affect this prototype differently. In this case, the increment to 15 K is negligible since it doesn't affect the evaporation pressure. However, there is a drop in the condenser refrigerant charge, even though the SC increased. In contrast, SH reduction dramatically increases the compressor's refrigerant charge (17 g) by decreasing discharge and oil temperatures.

Next, in the test of the compressor heated with the heating wire, this application reduced 10 g in the compressor's refrigerant charge by decreasing the oil's solubility. The evaporator's refrigerant charge decreased by 5 g, which is not straightforward. The maldistribution observed in the evaporator due to the condenser subcooling could explain the difference.

In the source variations, as in the previous prototype, increasing the source temperature raises evaporation pressure, reducing the pressure ratio and decreasing oil and discharge temperature. Increasing the brine temperature to 7 ^{o}C meant an increase of 12 g, and increasing the source to 12 ^{o}C increased this to 16.5 g. Within these tests, the other components maintained the refrigerant charge amount.

Lastly, with the test of the SH increase to 24 K but the source increase to 12 ^{o}C, a vast refrigerant charge reduction is observed in the compressor (16 g) due to the solubility reduction. Also, there is a decrement in the refrigerant charge in the evaporator of 10 g, provoked by the increase of SH.

3.3.3. Prototype comparison

After seeing the results, a few differences between the tests have been observed in the refrigerant charge amount.

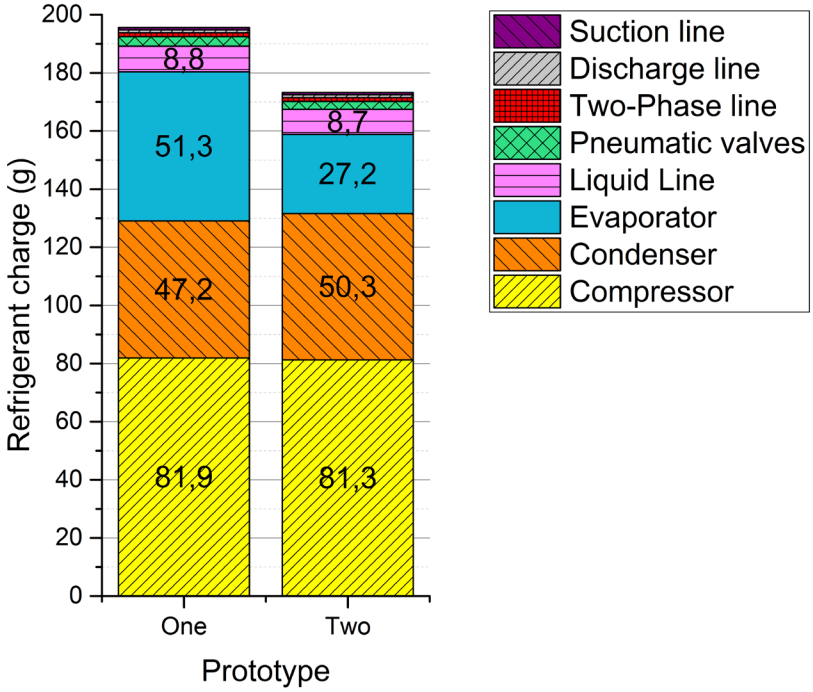

Figure 64: Comparison between prototypes in refrigerant charge distribution at the nominal point

In Figure 64, it can be observed that in the nominal point, the only differences appear in the evaporator. At this point, reducing the internal volume of the heat exchanger to almost a third part of the volume did not impact the rest of the components. The reduction of HE volume reduced the refrigerant charge of the evaporator itself by 24.1 g (47 % of the initial mass in the element).

Also, as seen in the previous sections, even though the change of the evaporator only affected the refrigerant charge in the evaporator itself at the nominal point, having it undersized instead of oversized changed the differences in the SCOP campaign. With the component oversized, no correlation could be observed in this campaign, as shown in Figure 59. In contrast, with the evaporator undersized, the linear trend is marked in Figure 62.

This different behaviour could be observed in the second test campaign too. The singular variations affected differently to the refrigerant charge not only in the amount of the variation but also in the sign.

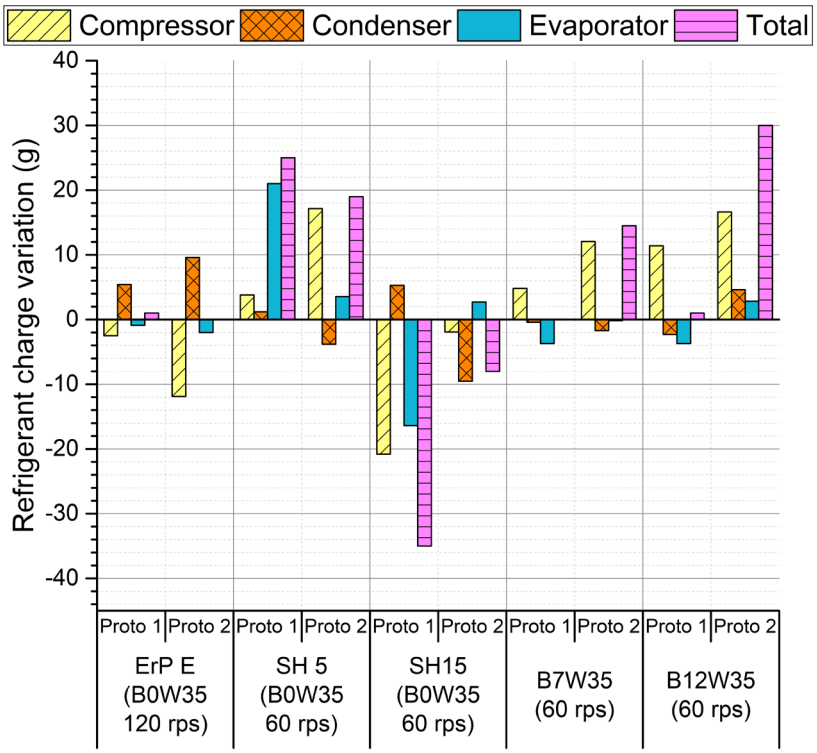

Figure 65: Refrigerant charge differences from the nominal point.

Figure 65 shows the differences from each test in the second campaign with their corresponding nominal point. As can be observed, increasing compressor speed affects considerably more in the second prototype due to its impact on the evaporation pressure. Also, the evaporator's effect gets doubled but is negligible compared to the compressor's.

Also, this evaporator volume/area reduction alters the effect of changing the superheat. In the first prototype, when the SH was reduced to 5 K, there was a low impact on the compressor's refrigerant charge but a high effect on the evaporator due to its soft affection in the suction temperature but high affection in evaporation pressure. In the second prototype, the change is the opposite, the increment is done primarily on the compressor,

and the effect in the evaporator is low. Nevertheless, the total mass increased in the same amount in both cases.

On the other hand, increasing the SH to 15 K greatly benefited the first prototype in the refrigerant mass reduction, decreasing the compressor and evaporator. However, in the second prototype, a little reduction is observed in the compressor, compensated by a little increment in the evaporator.

Heating the compressor with a heating wire reduced the compressor in the first prototype more than in the second. However, in the second, there is also a reduction in the evaporator that doesn't appear in the first.

Lastly, in the source variations, the refrigerant charge increment in the compressor is more affected in the second prototype and the rest of the components, where in some cases, even there is a change between refrigerant charge reduction or refrigerant charge increment.

3.3.4. Refrigerant charge prediction model

The results of refrigerant charge distribution had two primary purposes. Firstly, to identify refrigerant charge reduction techniques, analyse the refrigerant charge inside each component and their variations due to modifications on the external conditions or control variables. And secondly, to compare the current refrigerant prediction model of the software IMST-ART v4.0 and explain the differences in each heat pump component.

The performance results obtained with the software IMST-ART have been validated many times, making the software trustworthy to help design vapour compression cycles and understand these machines' behaviour. However, the results obtained were always underpredicted in refrigerant charge, as with all these types of software [6].

This part of the document is related to the second objective. The three main components will be analysed using the previous sections' data. Firstly, results from section 3.2 were used to match the performance between the test and the simulation. Then, results from section 1.3 were used to compare the refrigerant charge prediction of the components and the refrigerant charge amount inside the component.

Compressor initial

In this section, the compressor refrigerant charge amount from section 3.3 will be compared with the results of the current state of refrigerant amount prediction in the software after matching the results from section 3.2. This

refrigerant prediction consists of the refrigerant inside the lubricant, given a standard refrigerant-lubricant mixture curve of R290 and mineral oil.

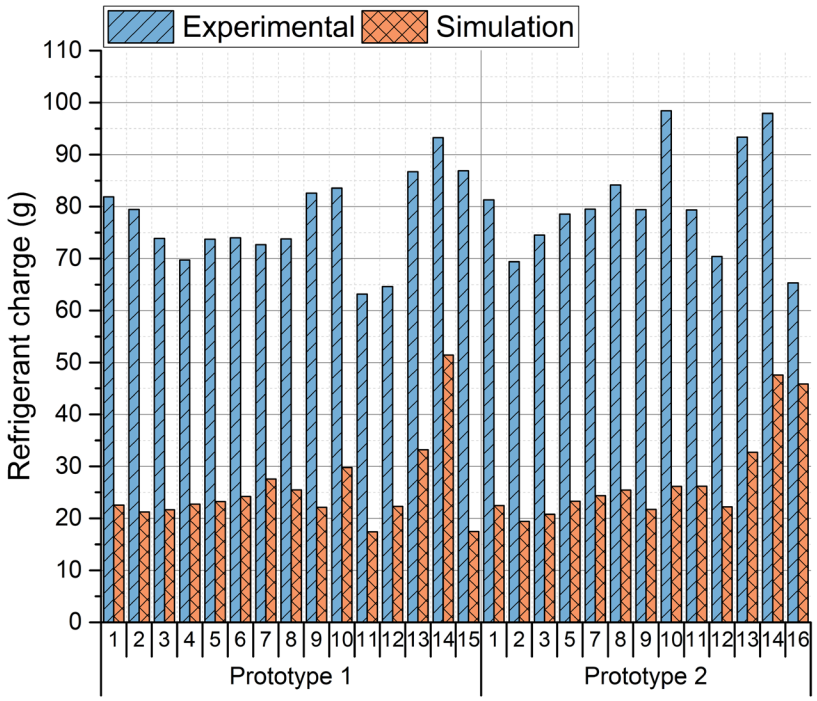

Figure 66: Refrigerant charge prediction in the compressor.

Figure 66 shows the refrigerant charge in the compressor of every test performed. It is divided into two zones marking the different prototypes. In the figure, the number of the test corresponds with the test definition from Table 12.

As mentioned in the previous section, the compressor is the component with the most refrigerant charge in this prototype, having almost half of the total refrigerant charge. As can be seen, the current prediction with standardised curves and without considering the gas volumes of the compressor has discrepancies with the values observed experimentally. The minimum difference observed is the last test, where the difference is 19.5 g, but this is not representative because the next less difference is test 14 from the first prototype, with a difference of 41.8 g. The average difference is 52.7 g considering the last test and 54 g without considering it. So, the

difference is more or less stable along the tests, and 50 g is missing from the prediction.

Also, no difference can be appreciated between both prototypes.

Compressor improved

A more accurate model was performed after seeing the difference between both results. In this model, three sources of refrigerant charge were considered: (i) oil solubility, (ii) gas at discharge pressure and (iii) gas at suction pressure, assuming the compression chamber was considered negligible.

For the oil solubility, the real solubility curve was obtained from the manufacturer, and it was transformed into the equation (16), acquiring the correct parameters of this mixture (discharge pressure and oil temperature were measured in every test). Then, to know the volumes of the different compressor parts, the suction side is easily calculated as a cylinder, and the discharge side from the volumes obtained with isothermal gas Table 6, Table 9, subtracting the suction side and the pipes.

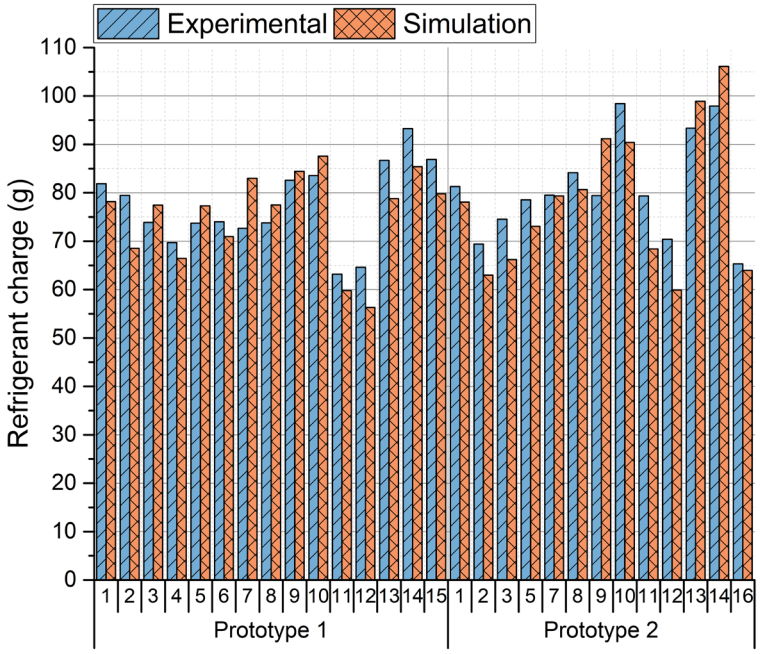

Figure 67: Refrigerant charge prediction in the compressor with the improved model.

Figure 67 shows the result of refrigerant charge prediction in the compressor using the improved model. As can be seen, the precision has improved, and now the maximum positive deviation is 13.7 g (underprediction), and the maximum negative deviation is 11.8 g (overprediction). The average of the differences is 1.7 g considering its sign, and in absolute values, 6.1 g, which is a considerable improvement.

Condenser initial

In the condenser model, the initial prediction is the value obtained with the software without any change. The software calculates the refrigerant charge using the finite volumes method in the heat exchanger area.

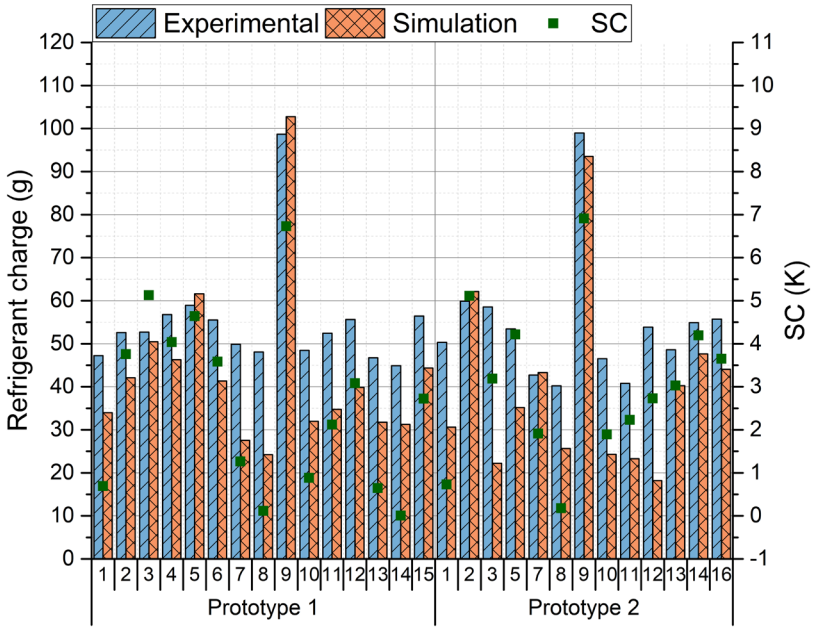

Figure 68: Refrigerant charge prediction in the condenser.

Figure 68 shows the result of this first comparison between the tests' results and the software's prediction. It can be seen in the figure that fewer discrepancies than the compressor are observed in this component. Also, these discrepancies are reduced when the SC value is higher than 5 K. However, when the SC is lower than this value, no linear relationship can be observed, and even in other points with low subcooling, such as test 7 of prototype 2, a reasonable prediction can be observed.

The maximum deviation is 36.3 g, and the average is 14 g.

Condenser improved

The simulation only considers the refrigerant charge in the heat transfer area. However, it was observed, and confirmed by heat exchanger manufacturers, that a reservoir of liquid refrigerant is accumulated at the bottom part of the heat exchanger, below the port. Therefore, this amount has been calculated and added to the previous simulation.

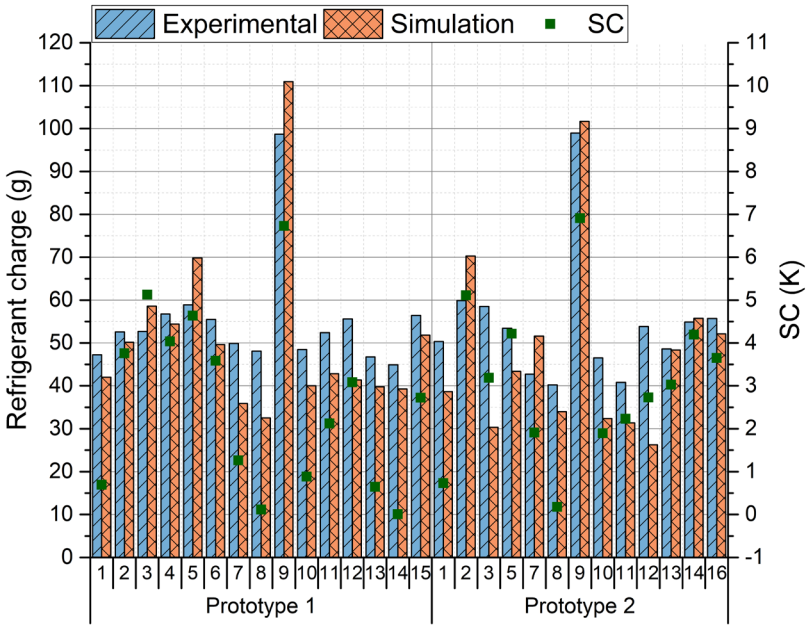

Figure 69: Refrigerant charge prediction of the condenser with the bottom part.

As seen in Figure 69, adding the bottom part of the refrigerant to the simulation improves the prediction; however, it is not the case with high SC values currently overpredicted.

Now the maximum deviation is 28.2 g, and the average difference has been reduced up to 7.3 g.

It can be said that the addition of the liquid bottom part positively impacts the refrigerant charge prediction. However, work is still pending to understand the cases when high SC is present in the test condition.

Evaporator initial

As a brazed plates heat exchanger, the evaporator uses the same model as the condenser. The first attempt is with the software, which only considers charge calculations in the channels.

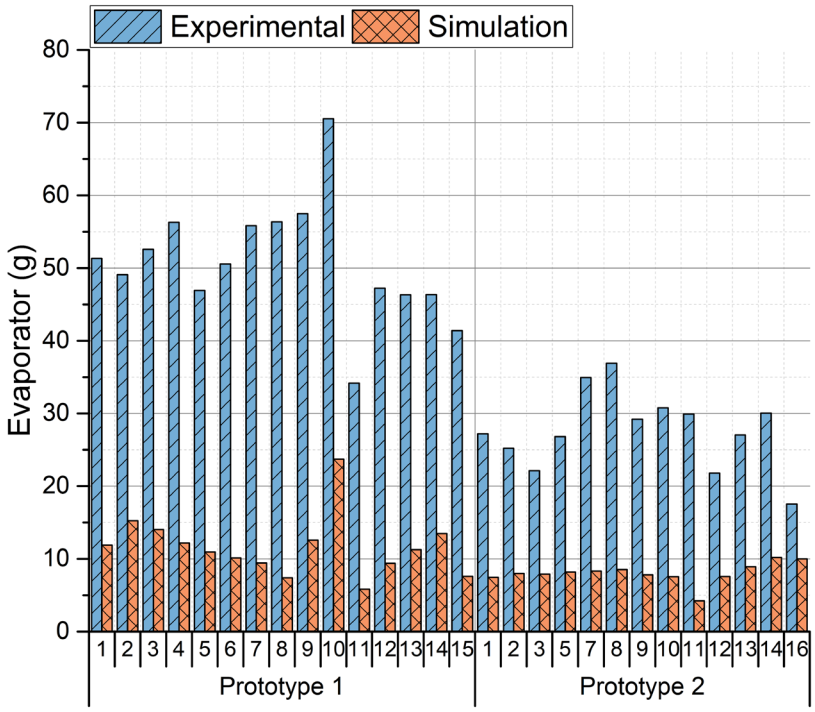

Figure 70: Initial refrigerant charge prediction in the evaporator.

As shown in Figure 70, the differences in this heat exchanger are higher than in the condenser. In this case, it can be observed that there is a difference in behaviour between both prototypes. Logically, only differences appear in this component because it is the only component changed between prototypes.

Firstly, as commented in 3.3.3, there is a big difference in the refrigerant charge of the evaporator between both prototypes due to the reduction of the internal volume and the degree of oversurfacing, changing the performance results. However, the prediction has not been reduced to the same or relative amount.

As mentioned, there is a big difference between the predictions and the experimental results in the first prototype. This difference varies from 28.3 g to 48.9 g, averaging 39 g. This average corresponded to approximately 80 % of the evaporator itself, proving that this prediction is insufficient.

On the other hand, in the second prototype, the difference varies between 7.5 g and 28.4 g, with an average of 19.6 g. The error corresponds to 70% of the actual value in this case.

The main differences between both components are (i) their size, having the first one more than twice the volume of the second one, varying from the oversized heat exchanger to the undersized one; (ii) the asymmetry, the first prototype has symmetric plate pitch and the second one is asymmetric; and (iii) the first evaporator has a distributor in the port and the second one does not have it.

One of these three differences should explain why the prediction is better in the second prototype. The distributor's absence may provoke less refrigerant amount in the bottom part of the heat exchanger.

Evaporator improved

In this heat exchanger, the same improvement that in the condenser was added. The volume of the liquid part is calculated geometrically, and the density is the density of the saturated liquid.

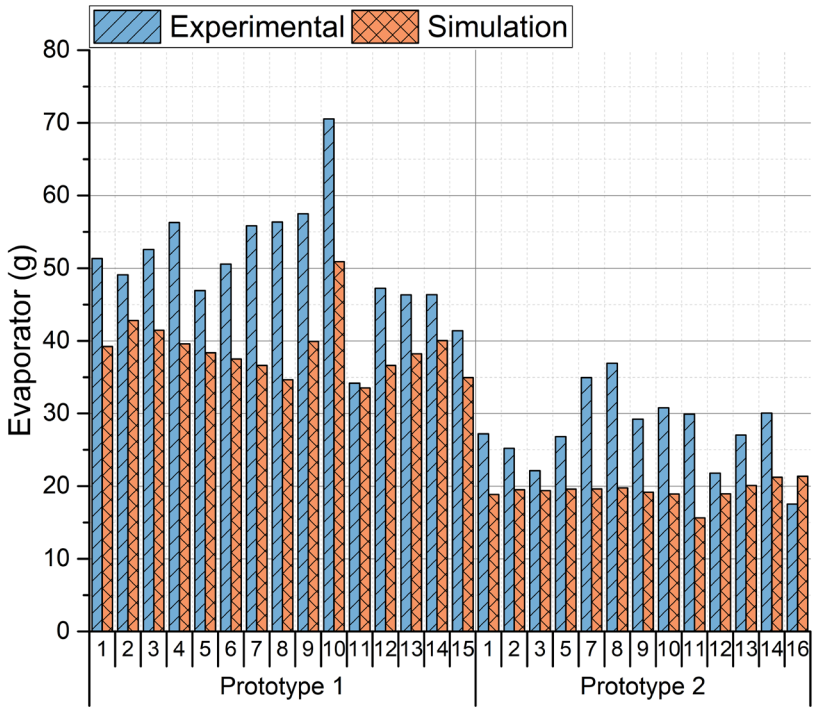

Figure 71: Refrigerant prediction in the evaporator after the improvement.

Figure 71 shows the refrigerant charge in the evaporator from the experimental results and from the prediction made by the addition of the software and the bottom part of the liquid refrigerant.

Comparing Figure 70 and Figure 71, it can be seen that with the addition of the bottom part, the difference between the prediction and the results has been significantly and consistently reduced in both prototypes.

The maximum difference observed in the first prototype is 21.7 g, and the minimum is less than 1g. The average is 11.9 g which is a reduction of 27 g in the difference.

On the other hand, the second prototype now has a difference that goes from 3.8 g of overprediction to 17 g of underprediction, with an average difference of 8.8 g. The overprediction only appears in one test.

In general, the improvement of the addition of the bottom part in the evaporator has a vast positive impact because it has reduced the difference

from 80 % of the refrigerant charge to 22 % in the first prototype and from 70 % to 30 % in the second prototype.

The study of which of the differences between the evaporators has more impact and made the former prediction work well is still pending. Additionally, some differences could be explained by studying the maldistribution in this component or by refrigerant trapped inside the component.

3.4. Discussion

After seeing all the results, some topics are highlighted and studied more deeply.

Firstly, the heating capacity obtained with 190g (9.5kW) makes the charge specific capacity get a value of 48.75kW/kg which is very near of the value of 50kW/kg which would mean a heating capacity of 7.5kW with 150g. In this prototype some additional features were added increasing slightly the refrigerant charge. If they were subtracted and the components scaled, the heating capacity and the refrigerant charge would be inside the limits previously said.

In the past only three examples could be found with similar results. First Primal Fernando obtained around 5kW with approximately 200g of propane at similar conditions [7], then Klas Anderson obtained 5.4kW with 100g of propane at higher brine temperatures[8] and lastly there is a commercial unit which claims obtaining 6kW of heating capacity with 150g of propane.

Then, in refrigerant distribution, the compressor has been detected as the component carrying the most considerable refrigerant charge in low-charge brine-to-water heat pumps. The oil solubility makes the refrigerant dissolved in oil useless because it is trapped inside the oil, changing its main properties such as density, viscosity, etc.

With the results of the refrigerant distribution of the singular variations campaign, it has been observed that reducing the oil solubility is crucial to reducing the refrigerant charge in the heat pump. In this test campaign, the solubility reduction was mainly made by increasing the crankcase temperature using an external device (heating wire) or controlling the SH. Both measurements imply efficiency reduction; the first is directly by

increasing the electric consumption by adding the load of the heating wire, and the second by increasing the pressure ratio and reducing efficiency in the compressor. In prototype 1, the refrigerant reduction provoked by the heating wire was 15 g, the COP reduction was 16.9 % (from 3.87 to 3.21), and the effect of increasing the superheat from 10 K to 15 K was a reduction of 35 g with a COP loss of 12.4 % (from 3.83 to 3.35). On the other hand, in the second prototype, the heating wire made the refrigerant charge reduce by 12 g with a COP reduction of 13 % (from 3.53 to 3.03) and lastly, the SH increase meant a refrigerant charge reduction of 8 g and a COP reduction of 2 % (from 3.53 to 3.46).

Both ways to reduce the refrigerant charge in the compressor show that increasing the superheat has more beneficial effects since the refrigerant reduction is more significant. The performance loss is similar or more minor. In both cases, the refrigerant charge reduction by performance loss ratio is much more meaningful when the SH is increased to 15 K.

There must be ways to reduce the solubility of the oil in the compressor without affecting that much the performance of the heat pump. Also, if the solubility is reduced, it may be tempting the possibility of reducing the amount of oil in the compressor, reducing even more the total amount of refrigerant inside the oil in the crankcase.

However, not all refrigerant in the compressor is stuck in the oil, and the gas refrigerant in the crankcase and the suction deposit is not negligible. Figure 72 shows the refrigerant in the different parts of the compressor. As can be seen, the refrigerant in the gas phase accounts for between 26 and 45 per cent of the total mass of the compressor. However, its variation along the different conditions is low, affected mainly by suction pressure (in the suction accumulator) and discharge pressure (in the crankcase).

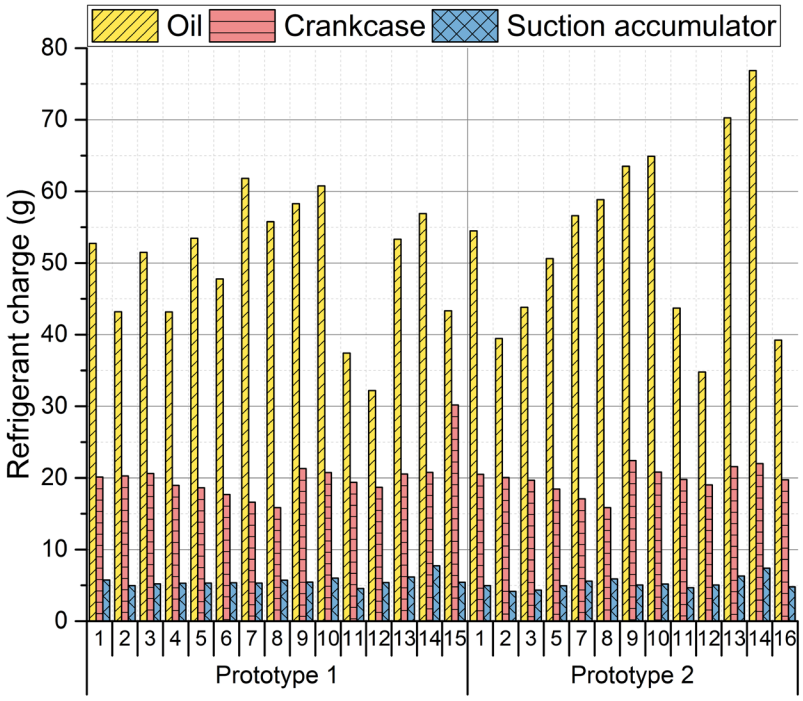

Figure 72: Refrigerant charge in the different parts of the compressor.

Also, it has been observed that the knowledge of the refrigerant oil mixture composition due to thermophysical properties and the internal volumes is essential to predict the refrigerant charge in the compressor.

The refrigerant charge in the condenser has been observed to be linked with the characteristics of the condenser and the SC measured. However, the relationship with the SC was expected to be stronger than the results.

Figure 73 shows the relationship between SC and refrigerant charge from experimental data. Also, in the figure, this relationship has been plotted from a simulation of the nominal point with the improvements added. It can be observed that when the SC is lower than 4 K, a little increment of refrigerant charge means an important increment in SC. For the region when SC is higher than 5 K, a considerable increment of refrigerant charge is needed to increase the SC. This means that in the case of low SC, the uncertainty of the refrigerant charge measured in the component plays a

significant role in this relationship. The SC measure's uncertainty is more important in the high SC region.

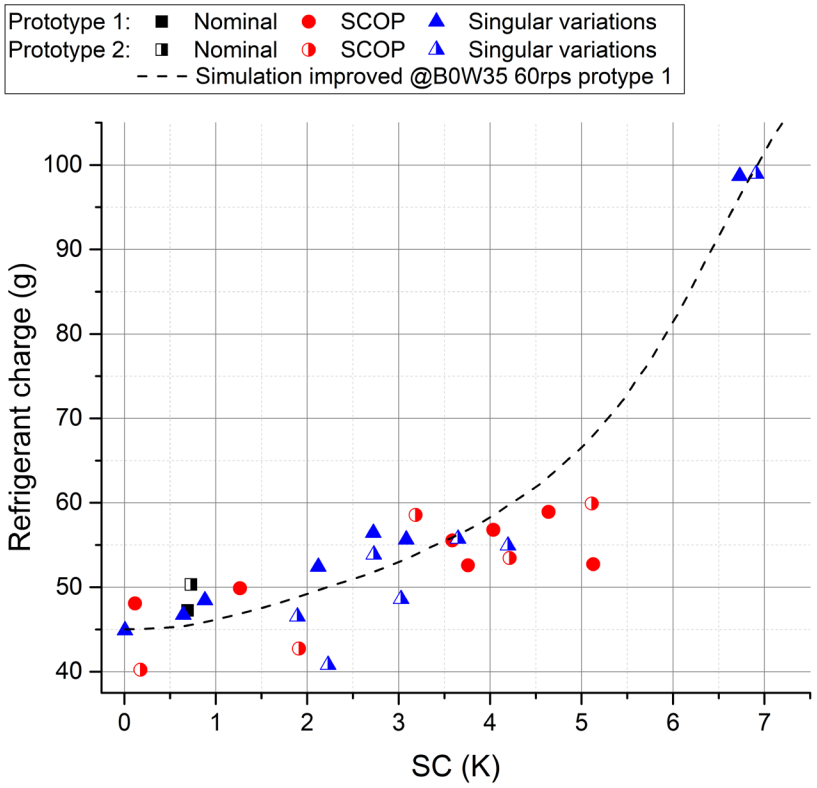

Figure 73: Relationship between SC and refrigerant charge in the condenser.

On the other hand, the evaporator was the only component tested with two different models: one oversized with a distributor and one undersized without a distributor. Both behave differently to the changes imposed by the control system.

The first difference is observed in the SH control variations in these components. As the first evaporator accounted for a bigger volume and heat transfer area, the SH control affected it in two ways: (i) it determined the evaporation temperature (with 5 K of SH, the evaporation temperature is near -5 ºC and with 15 near -15 ºC), and (ii) the volume repartition, with a low temperature difference between the refrigerant and secondary fluid it is needed more heat transfer area and more volume is used for the

refrigerant evaporation. However, as the second evaporator was a little undersized, the first effect of the SH control was negligible.

Another difference observed is the effect of the source variation. In the first prototype, as it accounted with a distributor, the increase in source temperature meant a decrease in refrigerant charge due to the rise in inlet velocity in the port of the evaporator. However, the increase in quality and pressure affect the second prototype more by increasing the refrigerant charge in this component with the source variation.

The maldistribution also highly influences this component, which adds uncertainties to the study. Regardless of this maldistribution, changing the evaporator has supposed to decrease 20 g of charge in the nominal point, compromising 1.34 kW of heating capacity and 0.16 points in SCOP. If the same process had been done to the condenser as well, the total refrigerant charge would probably have decreased below the limit of 150 g without losing that much heating capacity and COP.

Regarding the refrigerant charge in the heat exchangers, liquid refrigerant in the bottom of them has been identified, revealing the importance of the geometry of the heat exchangers and the possibility of reducing the refrigerant charge of them by decreasing the dead volumes or preventing them from being full of liquid refrigerant.

With the acknowledgement of the dead volumes, the refrigerant charge prediction of the brazed plates heat exchanger, more concretely, the ones working as evaporators, can greatly improve and be reliable as a first approximation.

With all the changes in refrigerant charge prediction, the improvements in the total refrigerant charge in the circuit can be seen in Figure 74 and Figure 75. Only the refrigerant charge of the three main components has been considered in these figures. The main differences in both prototypes have been corrected, but some tests still have a little underprediction. In conclusion, the final prediction of the refrigerant charge of every component is fair and reliable, and it can serve the purpose of knowing the order of magnitude of the total refrigerant charge amount.

Besides, there are still a few strange behaviours that should be studied deeper.

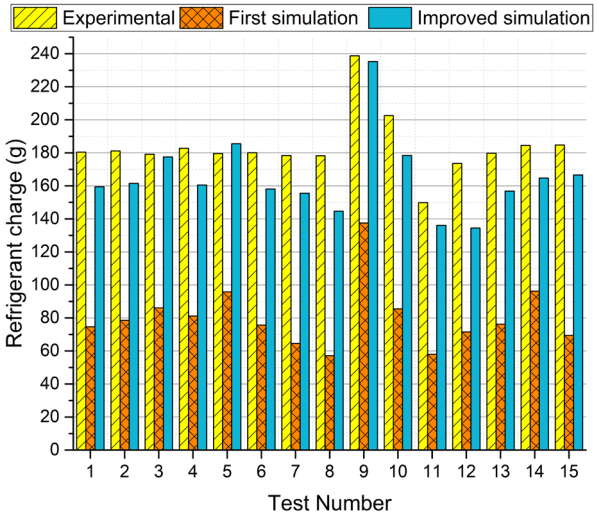

Figure 74: Refrigerant prediction in the first prototype.

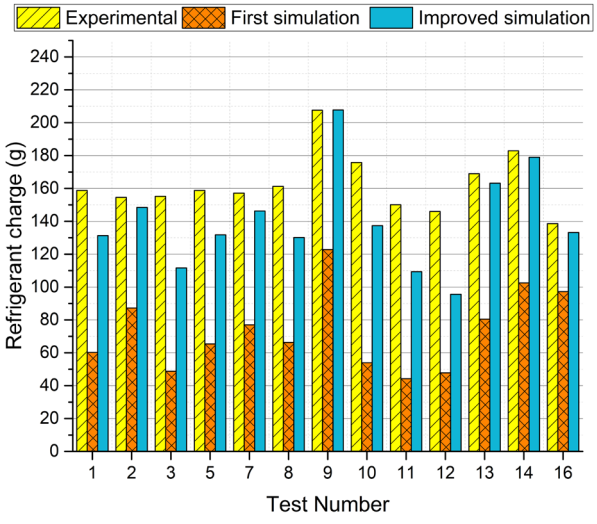

Figure 75: Refrigerant prediction in the second prototype

References

[1] J. M. Corberán, I. O. Martínez, and J. Gonzálvez, "Charge optimisation study of a reversible water-to-water propane heat pump," *International Journal of Refrigeration*, vol. 31, no. 4, pp. 716–726, Jun. 2008, doi: 10.1016/J.IJREFRIG.2007.12.011.

[2] European Committee for Standardization, "EN 14825 - Air conditioners, liquid chilling packages and heat pumps, with electrically driven compressors, for space heating and cooling - Testing and rating at part load conditions and calculation of seasonal performance.," 2019, Accessed: Sep. 22, 2021. [Online]. Available: https://www.en-standard.eu/din-en-14825-air-conditioners-liquid-chilling-packages-and-heat-pumps-with-electrically-driven-compressors-for-space-heating-and-cooling-testing-and-rating-at-part-load-conditions-and-calculation-of-seasonal-performance/

[3] T. Itami, K. Okoma, and K. Misawa, "An Experimental Study of Frequency-Controlled Compressors", Accessed: Jun. 17, 2023. [Online]. Available: https://docs.lib.purdue.edu/icec

[4] T. Li *et al.*, "Measurement of refrigerant mass distribution within a R290 split air conditioner," *International Journal of Refrigeration*, vol. 57, pp. 163–172, Sep. 2015, doi: 10.1016/J.IJREFRIG.2015.05.012.

[5] W. Tang, G. He, D. Cai, Y. Zhu, A. Zhang, and Q. Tian, "The experimental investigation of refrigerant distribution and leaking characteristics of R290 in split type household air conditioner," *Appl Therm Eng*, vol. 115, pp. 72–80, Mar. 2017, doi: 10.1016/j.applthermaleng.2016.12.083.

[6] T. M. Harms, E. A. Groll, and J. E. Braun, "Accurate Charge Inventory Modeling for Unitary Air Conditioners," 2011, doi: 10.1080/10789669.2003.10391056.

[7] Primal Fernando, "Experimental Investigation of Refrigerant Charge Minimisation of a Small Capacity Heat Pump Doctoral Thesis," 2007.

[8] K. Andersson, E. Granryd, and B. Palm, "Water to water heat pump with minimum charge of propane," in *Refrigeration Science and Technology*, International Institute of Refrigeration, 2018, pp. 725–732. doi: 10.18462/iir.gl.2018.1264.

Chapter 4: General conclusions and future work

4.1. Conclusions

Refrigerant charge amount has become a fundamental matter in domestic heating, cooling and DHW production due to environmental and safety concerns. The refrigerant charge amount (or the releasable charge amount) of flammable refrigerants (A3) without adding extra safety measures and without restrictions regarding specific floor area is 150 g.

There is a push from components manufacturers and heat pump producers toward refrigerant charge reduction. However, the number of units in the market using an environmentally friendly refrigerant with a safety-limited charge to be installed in any space is limited and insufficient.

For this reason, the objectives set for this doctoral thesis were (also described in section 1.4:

1. To prove that it is possible to have a ground-source heat pump to provide enough domestic space heating capacity.
2. To obtain resourceful experimental data about refrigerant charge distribution and performance of ground source heat pumps.
3. To analyse the performance data and refrigerant distribution and to extract conclusions about their relationship.
4. To develop strategies for refrigerant charge reduction.

The objectives have been fulfilled, and the results are the next:

1. It has been built and tested a brine-to-water with 195 g of propane, which would get a declared heating capacity of 7.31 kW with 150 g of refrigerant charge
2. Experimental data on performance and refrigerant charge distribution has been obtained with two prototypes.
3. Since the source temperature does not vary in brine-to-water heat pumps, the exact refrigerant charge amount can be used without high deterioration in performance due to overcharge/undercharge for all the ambient conditions during a year. Therefore, there is no need for a refrigerant accumulator.
4. Some strategies to reduce the refrigerant charge have been proposed, such as reducing oil's solubility. The refrigerant dissolved in the oil presents the best opportunity to reduce the refrigerant charge in the heat pump, and the brazed plates heat exchangers

also offer a great option if the designs are improved since dead volumes account for a non-negligible amount.

Additionally, discrepancies have been observed between the refrigerant charge measured in each component and the refrigerant charge prediction of the IMST-ART software. Consequently, potential improvements in refrigerant charge prediction have been presented.

Here below, the main conclusions are commented on with more detail.

4.1.1. Heating capacity

The heating capacity obtained in the prototypes was almost sufficient for heating a family household without adding any safety measures.

According to Lund, the reference was set at 7.5 kW for European households[1]. In the first prototype, the heating capacity obtained was 9.49 kW with 195 g of propane, which means including the fact that there are elements that increase the refrigerant amount slightly, with the limit charge of 150 g of propane, the heating capacity would be 7.31 kW. In the second prototype, the heating capacity dropped to 8.15 kW, but the refrigerant charge amount was reduced to 170 g. Knowing that there are still elements that helped the measurements but increased the refrigerant charge slightly, the heating capacity obtained with 150 g would be 7.19 kW.

Both prototypes are very near the objective, and knowing that the condenser is oversized and there is the possibility of reducing the refrigerant charge, it can be said that the prototypes are sufficient for the heating capacity objective for a regular household in Europe.

4.1.2. Refrigerant charge distribution

The refrigerant charge distribution has been studied experimentally for every test condition. To achieve that, a theoretical and experimental study of the different refrigerant extraction techniques has been performed first.

At the nominal point of the first prototype, 41.5 % of the refrigerant charge was located in the compressor, mainly dissolved in the oil. Almost the rest of the refrigerant charge was evenly distributed in the brazed plates heat exchangers, 23.9 % in the condenser and 27.8 % in the evaporator. The rest, 6.8 %, is stored in the pipes and accessories primarily located in the liquid line, 4.5 %.

This refrigerant distribution changed in every test condition. However, in almost all of them (except for the overfilled test), the compressor is still the component that gathers the most amount of refrigerant charge.

The evaporator was changed to a smaller BPHE in the second prototype, which meant a reduction of refrigerant charge. At the nominal point, the compressor and condenser had almost the same refrigerant charge as in the first prototype. Still, as the total amount was reduced, their percentage increased. The compressor gathered 47 % of the refrigerant charge amount in the second prototype. In this case, the condenser rose to 29.1 %, and the evaporator decreased to 15.7 %. The rest of the refrigerant charge was in the lines and accessories.

The total refrigerant charge amount varied similarly in both prototypes by changing external conditions. However, refrigerant distribution changed differently.

When the conditions were changed from the nominal point, if this variation meant a total refrigerant charge reduction, it was observed that there was a refrigerant charge reduction in both prototypes. Still, this refrigerant charge reduction's magnitude differed for each prototype. However, at the component level, it was not the case. Some variations made a certain component have a refrigerant charge reduction in prototype one but a refrigerant charge increase in prototype two or vice versa.

4.1.3. Refrigerant charge reduction strategies

After the experimental results, refrigerant charge reduction strategies have been identified.

Due to the importance of the refrigerant amount in the compressor's oil, the best method to reduce the refrigerant charge is to reduce the refrigerant amount that stays in the compressor inside the oil. There are two ways to do it: by reducing the amount of oil or its solubility. If the compressor's manufacturer already gives the oil type and quantity and there is no possible negotiation, reducing solubility is the only way to act. The means to reduce solubility is decreasing its pressure and increasing its temperature.

In this doctoral thesis, the oil temperature has been increased using two procedures: using a heating wire or increasing the superheat and, consequently, the pressure ratio and discharge temperature.

Both systems decreased the performance, but the SH increase obtained a better result than the heating wire. However, there can be thought possibilities that reduce oil solubility without affecting the COP that much.

It was also identified that the brazed plates heat exchangers store liquid refrigerant inside their dead volumes. Decreasing them would lower the refrigerant charge these heat exchangers need and the whole heat pump.

4.1.4. Refrigerant charge prediction

The refrigerant charge prediction has significantly been improved throughout this work.

The initial step was the software IMST-ART v.4.0.

From this reference, the compressor model was changed to a more specific model for this application adding the gas refrigerant to the volumes and the oil solubility curve. After the results, a good agreement between experimental data and simulation was observed.

The software only considered the heat transfer area in the heat exchanger, and the dead volumes of the bottom of the heat exchanger have been added. With it, a good agreement has been obtained in the condenser and evaporator of the first prototype, but a different behaviour is observed for the second prototype. Discrepancies between experimental data and refrigerant charge prediction have been reduced, but they are still non-negligible for the evaporator. Additional analysis, like maldistribution's effect, must be added to clarify the existing discrepancies.

4.2. Future work

The results obtained in the thesis encouraged further studies.

The next natural step would be to study the refrigerant charge distribution in air-to-water heat pumps, adding to this study the effect of ambient temperature and finned tube heat exchangers.

This study used the compressor model for a specific refrigerant and oil mixture. More data about more mixtures may be helpful to get a relationship between solubility curves and oil information (oil type, viscosity number, etc.). This can either enlarge the database of the refrigerant and oil mixtures used in the models or improve the generic solubility curve based on the characteristics of refrigerant and lubricant.

Also, in this work, the refrigerant amount dissolved in the oil has been calculated by knowing the pressure and temperature conditions at the crankcase. However, oil temperature should not be an input since it is not generally measured during the tests. Instead, this variable should be calculated using measured values of the thermodynamic cycle, such as suction and discharge pressures, suction and discharge temperature, SH, etc. A correlation to obtain the oil temperature would greatly help the compressor's refrigerant charge prediction.

Continuing in the compressor, when the energy balance was studied to understand the oil temperature, the heat losses to the ambient in this component were non-negligible. It should be studied more profoundly, and maybe with its understanding, it can be increased the oil temperature and therefore reduce the oil solubility and refrigerant charge in the component.

Moving to the heat exchangers, the importance of dead volumes was observed, more precisely, in the bottom part of the brazed plates heat exchanger. This volume must be added to the simulation software to be more precise when predicting the refrigerant charge amount. Besides, it should be studied with the manufacturers to reduce their impact, for example, by provoking that no liquid refrigerant is stored in these volumes.

Moreover, with the infrared pictures, there was observed that maldistribution was present in the experimental campaign in the evaporator. Still, these data need a more profound analysis that is out of the scope of this work. However, it may provide more precision in the refrigerant charge analysis of the evaporator.

Lastly, it is necessary to understand the difference between both evaporators used in the experimental tests. The lack of a distributor at the inlet port seems to help the absence of liquid in this dead volume. Still, confirmation is needed by studying the difference, using evaporators with a sight glass at the bottom or similar. Also, it would be interesting to explore the other differences between the evaporators selected in this work separately, studying only the effect of the asymmetry and the impact of undersizing/oversizing. Furthermore, studying the effect on refrigerant charge by adding a double wall in BPHE could also be interesting.

References

[1] J. Lund, "Geothermal heat pumps - An overview," *Geo-Heat Center Quarterly Bulletin*, vol. 22, no. 1, pp. 1–2, 2001, Accessed: Dec. 29, 2021. [Online]. Available: https://www.researchgate.net/publication/242159982

Appendix

Appendix A: Results from refrigerant extraction study:

This appendix presents the test campaign results of the different refrigerant extraction methods. From these results, it was decided to use liquid nitrogen as a cooling method for refrigerant extraction.

It shows the precision of the tests employing liquid nitrogen, PCM with a phase change temperature of -18 ^{o}C and ice. With the PCMs, the sample cylinder was submersed in a mixture of ethylene glycol-water

These results were presented at the 2021 International Refrigeration and Air Conditioning Conference at Purdue University [1].

For the uncertainty analysis, the variables not measured are calculated using the Taylor Series Method for the propagation of uncertainties.

The uncertainty of the sensors employed can be seen in Table 16.

Variable	Sensor	Uncertainty 2σ
Temperature	Type T ThermoCouple class 2	±2 ^{o}C
Mass	Scale Kern	±0.5 g
Pressure	Yokogawa EJA510E	±0.008 bar

Table 16: Sensors used in refrigerant extraction pre-study.

Test	Initial ref charge, (g)	Refrigerant extracted + calculated (g)	Time (h)	Final T secondary (°C)	Final P (bar)	Ref Amount remaining, (g)	Theoretical amount, (g)
LN2 1	305 ± 0.71	304.4 ± 0.71	0:30	-196 ± 2	0.006 ± 0.01	0.6 ± 1	~0
LN2 2	280 ± 0.71	279.82 ± 0.71	0:30	-196 ± 2	0.004 ± 0.01	0.18 ± 1	~0
LN2 3	296.9 ± 0.71	297.3 ± 0.71	0:30	-196 ± 2	0.003 ± 0.01	-0.4 ± 1	~0
LN2 4	306.1 ± 0.71	306.9 ± 0.71	0:30	-196 ± 2	0.002 ± 0.01	-0.8 ± 1	~0
LN2 5	296.6 ± 0.71	296.44 ± 0.71	0:30	-196 ± 2	0.003 ± 0.01	0.16 ± 1	~0
LN2 6	290 ± 0.71	288.96 ± 0.71	0:30	-196 ± 2	0.002 ± 0.01	1.04 ± 1	~0
LN2 7	288 ± 0.71	287.4 ± 0.71	0:30	-196 ± 2	0.002 ± 0.01	0.6 ± 1	~0
LN2 8	306.2 ± 0.71	304.5 ± 0.71	0:30	-196 ± 2	0.003 ± 0.01	1.7 ± 1	~0
LN2 9	299.4 ± 0.71	298.78 ± 0.71	0:35	-196 ± 2	0.002 ± 0.01	0.62 ± 1	~0
LN2 10	285 ± 0.71	285.2 ± 0.71	0:35	-196 ± 2	0.002 ± 0.01	-0.2 ± 1	~0
PCM(-18) 1	291.4 ± 0.71	292.38 ± 1.65	5:00	-17 ± 2	1.5 ± 0.01	3.4 ± 1	4.38 ± 4.38
PCM(-18) 2	299.7 ± 0.71	299.13 ± 1.66	1:00	-17.8 ± 2	1.55 ± 0.01	5 ± 1	4.43 ± 4.43
PCM(-18) 3	292.2 ± 0.71	292.72 ± 1.64	1:00	-17.24 ± 2	1.486 ± 0.01	3.8 ± 1	4.32 ± 4.32

Test	Initial ref charge (g)	Refrigerant extracted +calculated (g)	Time (h)	Final T secondary (ºC)	Final P (bar)	Ref Amount remaining (g)	Theoretical amount (g)
PCM(-18) 4	303.4	304.53 ± 1.67	1:00	-16.74 ± 2	1.566 ± 0.01	3.2 ± 1	4.33 ± 1.52
PCM(-18) 5	300.5	300.74 ± 1.64	1:00	-16.85 ± 2	1.495 ± 0.01	4.1 ± 1	4.34 ± 1.49
PCM(-18) 6	292.2	293.17 ± 1.68	1:00	-18.4 ± 2	1.426 ± 0.01	3.1 ± 1	4.07 ± 1.53
PCM(-18) 7	292.6	290.12 ± 1.67	1:00	-16 ± 2	1.63 ± 0.01	7.3 ± 1	4.82 ± 1.52
PCM(-18) 8	302.8	301.75 ± 1.69	1:00	-16.8 ± 2	1.56 ± 0.01	5.6 ± 1	4.55 ± 1.54
PCM(-18) 9	301.6	302.17 ± 1.6	1:00	-15.2 ± 2	1.68 ± 0.01	3.8 ± 1	4.37 ± 1.45
PCM(-18) 10	308.9	308.39 ± 1.63	1:00	-16.2 ± 2	1.57 ± 0.01	5 ± 1	4.49 ± 1.48
PCM(-18) 11	302.6	302.4 ± 1.58	1:00	-14.5 ± 2	1.69 ± 0.01	4.7 ± 1	4.5 ± 1.43
PCM(-18) 12	301.5	302.66 ± 1.6	0:20	-20.26 ± 2	1.343 ± 0.01	2.6 ± 1	3.76 ± 1.45

Test	Initial ref charge, (g)	Refrigerant extracted + calculated (g)	Time (h)	Final T secondary (°C)	Final P (bar)	Ref Amount remaining, (g)	Theoretical amount, (g)
PCM(-18) 13	304.2	303.94 ± 1.71	1:00	-16.5 ± 2	1.57 ± 0.01	4.9 ± 1	4.64 ± 1.56
Ice 1	309.8	308.86 ± 2.19	1:00	-3 ± 2	2.68 ± 0.01	8.7 ± 1	7.76 ± 2.04
Ice 2	304.2	302.42 ± 2.17	1:00	-3.8 ± 2	2.64 ± 0.01	9.3 ± 1	7.52 ± 2.02
Ice3	301.4	300.69 ± 2.33	1:00	-0.7 ± 2	2.98 ± 0.01	9.2 ± 1	8.49 ± 2.18

Table 17: Refrigerant extraction test results.

Appendix B: EES model

The compressor model was developed using the EES software [2], an equation solver.

Given the pressure and temperatures known from the experiment, the model is primarily used to calculate the refrigerant charge amount in the compressor. It is also prepared to calculate the heat losses inside the compressor for further analysis.

Geometrical dimensions

The compressor must be defined as much as possible. In this case, it is necessary to know the volume occupied by the refrigerant and the oil. The manufacturer does not provide the internal volume so that external dimensions can approximate it.

After the data of the internal free volume was measured, it was approximately 28 % of the total volume of the compressor. Then the total volume is calculated as the volume of a cylinder, knowing the height and the diameter (25).

$$V_c = h_c * \pi * \frac{\phi_c^2}{4} * 0.28 \tag{25}$$

$$V_r = h_r * \pi * \frac{\phi_r^2}{4} \tag{26}$$

The refrigerant receiver of the compressor can also be estimated as a cylinder using equation (26) and knowing the height and the diameter.

Then the total oil amount is given by the compressor's manufacturer, and it is considered to be inside the crankcase or the deposit at the inlet of the compressor because of the small length of pipes and compact system. The amount at the compressor can be seen with a sight-glass

Refrigerant charge

The refrigerant charge in the compressor can be divided into the different states in which it is present.

Firstly, there is a gas amount inside the compression chamber. Due to the size of this compression chamber and the refrigerant being in the gas phase, this amount can be neglected from the total amount in the compressor.

Secondly, a certain amount of refrigerant is stored in the crankcase in the gas phase. This amount in extensive systems can also be neglected, but it is not the case and must be considered. The refrigerant amount can be calculated as in equations (27) and (28), where the volumes are calculated with equations (25) and (26) and subtracting from them the volume occupied by the oil.

$$m_{gas} = \rho_{gas} * V_{c,ref} \tag{27}$$

$$\rho_{gas} = f(P, T, ref) \tag{28}$$

Lastly, there is the amount of refrigerant inside the oil in the liquid phase. In the compressor, there is a mixture of oil refrigerant in equilibrium due to the mutual solubility of both components. The solubility curve can be approximated to the equation (29) also seen in chapter 2.7.2.

$$\log_{10}(P) = a_1 + \frac{a_2}{T} + \frac{a_3}{T^2} + \log_{10}(\omega)\left(a_4 + \frac{a_5}{T} + \frac{a_6}{T^2}\right) + \log_{10}^2(\omega)\left(a_7 + \frac{a_8}{T} + \frac{a_9}{T^2}\right) \tag{29}$$

Calculating the mass fraction of refrigerant (ω) and knowing the amount of oil, the refrigerant amount in the oil can be calculated according to equation (30). Since the definition of (ω) can be seen in equation (17).

$$m_{ref} = \frac{w}{1 - w} * m_{oil} \tag{30}$$

Future work

Regarding this model, there is still open work to be done shortly. The first thing should be a correlation to calculate the oil temperature using the refrigerant cycle data, such as suction pressure, discharge pressure and suction temperature.

Another open discussion that can be performed using the model developed is the calculation of the heating losses of the compressor and, with it, a proper estimation of the discharge temperature.

Appendix C: Empirical results in SCOP campaign of different refrigerant charge amount.

During the realisation of the Thesis, there was also the possibility of supervising the work of a bachelor's student during his bachelor thesis preparation. This work [3] was based on the mass variation in the SCOP campaign in a water-to-water heat pump doing the mass variation tests on every test condition defined in the standard EN 14825 [4].

Figure 76 and Figure 77 show the results of heating capacity and COP from this testing campaign. It has added all the different steps of refrigerant charge on each test. Figure 77 also calculated the SCOP for average climate conditions at each refrigerant charge step.

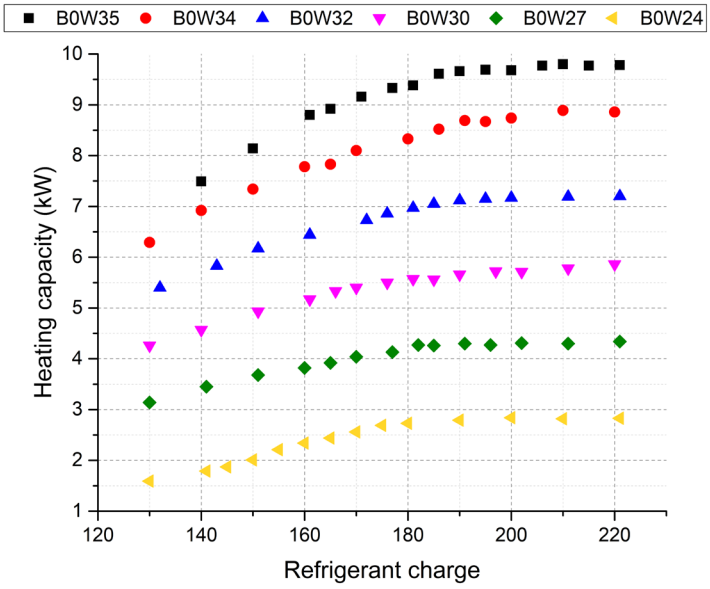

Figure 76: Results of heating capacity from [3].

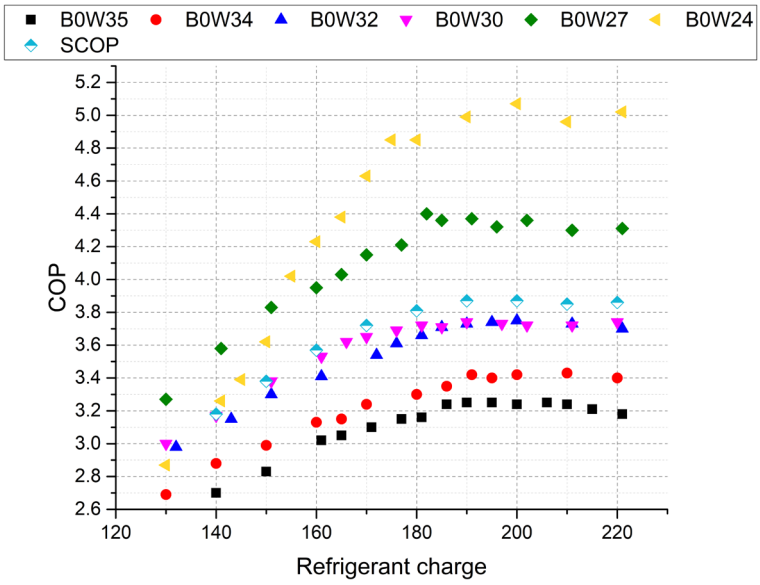

Figure 77: Results of COP from [3] about the refrigerant mass variation in the SCOP campaign.

It can be seen that in all tests with a refrigerant charge lower than 180 g, the heat pump is working with not enough refrigerant charge. After this limit, conditions with lower partial loads start to be optimal, and after 195 g, all tests are considered optimum. Seeing the value of the SCOP, it increases quasilinear until the already mentioned 180 g. Then the increment is reduced until the optimum is observed at 195 g. After this value, the SCOP remains almost constant, with slight decrements.

Appendix D: Performance results

This appendix presents the results of the tests while the heat pump is running. As explained in 2.5, the test stability is ensured following the restrictions defined by the standard EN 14511-3 [5]. Once the system is steady, the variables are measured for at least 35 minutes.

During the test, the principal variables are measured every second, and then COP and heating capacity are calculated, among others.

In this case, the correction of the pumps was not performed, and therefore the heating capacity and COP calculated are purely the ones measured in the heat pump. However, the pumps were external; consequently, there was no heat injection between the measured temperatures.

The heating capacity ($\dot{Q}_h$) and COP calculations are done using the equations (31) and (32):

$$\dot{Q}_h = \dot{m}_w c_p \left(T_{w,out} - T_{w,in}\right) \tag{31}$$

$$COP = \frac{\dot{Q}_h}{\dot{E}} \tag{32}$$

Where all the variables are measured except the c_p which is extracted from Tables knowing the pressure and temperature of the water.

The uncertainty analysis performed for each variable is also explained in 2.4 and depends on the type of variable: measured or calculated.

For measured variables, their uncertainty is calculated as (33).

$$U_{95} = 2u = 2\sqrt{s^2 + b^2} \tag{33}$$

For calculated variables, their uncertainty is calculated from the measured ones is calculated using the Taylor Series Method for the propagation of uncertainties (34).

$$U_{95} = \sqrt{\sum_{i=1}^{N} \left(\frac{\partial f}{\partial x_i}\right) U_i^2} \tag{34}$$

The variables presented in the appendix are the ones used to know COP and $\dot{Q}_h$, and also the variables considered important to know the behaviour of the refrigerant circuit.

Test	Ref [g]	$T_{w,in}$ [°C]	$T_{w,out}$ [°C]	$T_{b,in}$ [°C]	$T_{b,out}$ [°C]	$\dot{m}_w$ [kg/ s]	Q_h [kW]	$\dot{E}$ [kW]	COP	P_{cond} [bar]	P_{evap} [bar]	T_{cond} [°C]	T_{evap} [°C]	SC [K]	SH [K]	T_{dis} [°C]	T_{oil} [°C]
1	120 ± 0.75	30.52 ± 0.14	35.21 ± 0.15	0 ± 0.14	-2.86 ± 0.14	0.16 ± 0.002	3.21 ± 0.14	1.21 ± 0.06	2.64 ± 0.17	12.3 ± 0.02	3.1 ± 0.02	35.46 ± 0.06	-12.97 ± 0.16	-0.54 ± 0.8	15.31 ± 0.81	71.75 ± 0.8	60.58 ± 0.8
1	130 ± 0.75	30 ± 0.14	35.2 ± 0.15	-0.1 ± 0.14	-3.43 ± 0.14	0.16 ± 0.002	3.56 ± 0.14	1.22 ± 0.06	2.9 ± 0.18	12.36 ± 0.017	3.31 ± 0.017	35.61 ± 0.06	-11.28 ± 0.15	-0.39 ± 0.8	13.42 ± 0.81	68.45 ± 0.8	57.95 ± 0.8
1	140 ± 0.75	30.38 ± 0.14	35.35 ± 0.15	-0.18 ± 0.14	-3.99 ± 0.14	0.18 ± 0.002	3.82 ± 0.16	1.24 ± 0.06	3.07 ± 0.19	12.52 ± 0.017	3.52 ± 0.017	36.15 ± 0.06	-9.45 ± 0.14	0.15 ± 0.8	11.25 ± 0.81	65.64 ± 0.8	55.69 ± 0.8
1	150 ± 0.75	30.01 ± 0.14	35.08 ± 0.15	0.19 ± 0.14	-3.95 ± 0.14	0.2 ± 0.002	4.16 ± 0.17	1.24 ± 0.06	3.34 ± 0.21	12.47 ± 0.017	3.68 ± 0.017	36 ± 0.06	-8.07 ± 0.14	0 ± 0.8	10.09 ± 0.81	64.07 ± 0.8	54.52 ± 0.8
1	160 ± 0.75	29.74 ± 0.14	34.78 ± 0.15	0.24 ± 0.14	-4.28 ± 0.14	0.21 ± 0.002	4.37 ± 0.18	1.24 ± 0.06	3.52 ± 0.22	12.46 ± 0.017	3.68 ± 0.017	35.96 ± 0.06	-8.03 ± 0.14	-0.04 ± 0.8	9.87 ± 0.81	63.84 ± 0.8	54.49 ± 0.8
1	170 ± 0.75	30.08 ± 0.14	35.09 ± 0.15	-0.02 ± 0.14	-4.61 ± 0.14	0.21 ± 0.002	4.5 ± 0.18	1.23 ± 0.06	3.66 ± 0.23	12.33 ± 0.017	3.63 ± 0.017	35.53 ± 0.06	-8.51 ± 0.14	0.03 ± 0.8	10.02 ± 0.81	65.35 ± 0.8	53.84 ± 0.8
1	180 ± 0.75	30.01 ± 0.14	35.01 ± 0.15	0.01 ± 0.14	-4.87 ± 0.14	0.22 ± 0.002	4.68 ± 0.19	1.23 ± 0.06	3.8 ± 0.24	12.35 ± 0.017	3.62 ± 0.017	35.6 ± 0.06	-8.55 ± 0.14	0.4 ± 0.8	9.99 ± 0.81	65.51 ± 0.8	54.01 ± 0.8
1	185 ± 0.75	29.89 ± 0.14	34.88 ± 0.15	-0.22 ± 0.14	-5.01 ± 0.14	0.22 ± 0.002	4.74 ± 0.19	1.21 ± 0.06	3.83 ± 0.25	12.2 ± 0.017	3.57 ± 0.017	35.09 ± 0.06	-8.97 ± 0.14	0.09 ± 0.8	10.17 ± 0.81	62.69 ± 0.8	57.94 ± 0.8
1	190 ± 0.75	30.11 ± 0.14	35.16 ± 0.15	-0.14 ± 0.14	-5.09 ± 0.14	0.23 ± 0.002	4.79 ± 0.19	1.24 ± 0.06	3.88 ± 0.24	12.44 ± 0.017	3.6 ± 0.017	35.88 ± 0.06	-8.73 ± 0.14	1.38 ± 0.8	10.02 ± 0.81	65.85 ± 0.8	54.44 ± 0.8

Test	Ref [g]	$T_{w,in}$ [°C]	$T_{w,out}$ [°C]	$T_{b,in}$ [°C]	$T_{b,out}$ [°C]	$\dot{m}_w$ [kg/ s]	Q_h [kW]	$\dot{E}$ [kW]	COP	P_{cond} [bar]	P_{evap} [bar]	T_{cond} [°C]	T_{evap} [°C]	SC [K]	SH [K]	T_{dis} [°C]	T_{oil} [°C]
1	195.5 ± 0.75	30.09 ± 0.14	35.1 ± 0.15	0.19 ± 0.14	-4.73 ± 0.14	0.23 ± 0.002	4.83 ± 0.19	1.22 ± 0.06	3.92 ± 0.25	12.27 ± 0.017	3.54 ± 0.017	35.3 ± 0.06	-9.2 ± 0.14	2.3 ± 0.8	9.96 ± 0.81	62.68 ± 0.8	56.79 ± 0.8
1	200 ± 0.75	30.02 ± 0.14	35.04 ± 0.15	0.12 ± 0.14	-5 ± 0.14	0.23 ± 0.002	4.84 ± 0.2	1.24 ± 0.06	3.91 ± 0.25	12.27 ± 0.017	3.6 ± 0.017	35.32 ± 0.06	-8.69 ± 0.14	2.82 ± 0.8	9.98 ± 0.81	66.06 ± 0.8	54.68 ± 0.8
1	207.5 ± 0.75	29.9 ± 0.14	34.84 ± 0.15	-0.02 ± 0.14	-4.97 ± 0.14	0.23 ± 0.002	4.8 ± 0.19	1.22 ± 0.06	3.87 ± 0.25	12.28 ± 0.017	3.44 ± 0.017	35.34 ± 0.06	-10.13 ± 0.14	3.34 ± 0.8	10.1 ± 0.81	63.18 ± 0.8	56.96 ± 0.8
1	210 ± 0.75	30.04 ± 0.14	35.05 ± 0.15	0.08 ± 0.14	-5.03 ± 0.14	0.23 ± 0.002	4.78 ± 0.2	1.24 ± 0.06	3.84 ± 0.24	12.56 ± 0.017	3.59 ± 0.017	36.3 ± 0.06	-8.84 ± 0.14	5.3 ± 0.8	10.04 ± 0.81	66.7 ± 0.8	55.01 ± 0.8
1	220 ± 0.75	30.09 ± 0.14	35.08 ± 0.15	-0.41 ± 0.14	-5.43 ± 0.14	0.23 ± 0.002	4.77 ± 0.2	1.25 ± 0.06	3.81 ± 0.24	12.65 ± 0.017	3.56 ± 0.017	36.59 ± 0.06	-9.1 ± 0.14	6.59 ± 0.8	10.07 ± 0.81	66.96 ± 0.8	55.13 ± 0.8
10	190 ± 0.75	30.03 ± 0.14	35.03 ± 0.15	0.01 ± 0.14	-2.98 ± 0.14	0.22 ± 0.002	4.6 ± 0.2	1.24 ± 0.06	3.71 ± 0.23	12.03 ± 0.017	3.83 ± 0.017	34.49 ± 0.06	-6.79 ± 0.13	-0.05 ± 0.8	5.07 ± 0.81	56.82 ± 0.8	47.43 ± 0.8
10	200 ± 0.75	30.01 ± 0.14	35.01 ± 0.15	0 ± 0.14	-3 ± 0.14	0.23 ± 0.002	4.74 ± 0.9	1.24 ± 0.06	3.82 ± 0.24	12.05 ± 0.017	3.88 ± 0.017	34.55 ± 0.06	-6.44 ± 0.13	0.12 ± 0.8	5.05 ± 0.81	56.38 ± 0.8	47.71 ± 0.8
10	209.5 ± 0.75	29.97 ± 0.14	34.97 ± 0.15	0.01 ± 0.14	-3.03 ± 0.14	0.23 ± 0.002	4.89 ± 0.19	1.24 ± 0.06	3.94 ± 0.25	12.07 ± 0.017	3.85 ± 0.017	34.62 ± 0.06	-6.69 ± 0.13	0.84 ± 0.8	4.89 ± 0.81	56.18 ± 0.8	47.57 ± 0.8
10	214.5 ± 0.75	30 ± 0.14	35 ± 0.15	-0.01 ± 0.14	-3.01 ± 0.14	0.24 ± 0.002	4.95 ± 0.2	1.24 ± 0.06	3.98 ± 0.25	12.09 ± 0.017	3.85 ± 0.017	34.68 ± 0.06	-6.68 ± 0.13	1.07 ± 0.8	5.03 ± 0.81	56.55 ± 0.8	47.82 ± 0.8

Test	Ref [g]	$T_{w,in}$ [°C]	$T_{w,out}$ [°C]	$T_{b,in}$ [°C]	$T_{b,out}$ [°C]	$\dot{m}_w$ [kg/ s]	Q_h [kW]	$\dot{E}$ [kW]	COP	P_{cond} [bar]	P_{evap} [bar]	T_{cond} [°C]	T_{evap} [°C]	SC [K]	SH [K]	T_{dis} [°C]	T_{oil} [°C]
10	220 ± 0.75	30.01 ± 0.14	35.01 ± 0.15	0 ± 0.14	-3 ± 0.14	0.24 ± 0.002	4.96 ± 0.2	1.25 ± 0.06	3.98 ± 0.25	12.13 ± 0.017	3.81 ± 0.017	34.83 ± 0.06	-6.96 ± 0.13	2.79 ± 0.8	4.99 ± 0.81	56.74 ± 0.8	47.91 ± 0.8
10	225 ± 0.75	30.02 ± 0.14	35.03 ± 0.15	0.01 ± 0.14	-3.02 ± 0.14	0.24 ± 0.002	4.95 ± 0.2	1.25 ± 0.06	3.96 ± 0.25	12.18 ± 0.017	3.8 ± 0.017	35.02 ± 0.06	-7.07 ± 0.13	3.36 ± 0.8	4.96 ± 0.81	56.96 ± 0.8	48.22 ± 0.8
10	230 ± 0.75	30.02 ± 0.14	35 ± 0.15	0.01 ± 0.14	-2.96 ± 0.14	0.23 ± 0.002	4.84 ± 0.2	1.25 ± 0.06	3.85 ± 0.24	12.27 ± 0.017	3.71 ± 0.017	35.32 ± 0.06	-7.79 ± 0.14	4.28 ± 0.8	5.07 ± 0.81	57.49 ± 0.8	48.52 ± 0.8
10	235 ± 0.75	29.95 ± 0.14	34.98 ± 0.15	0 ± 0.14	-2.99 ± 0.14	0.23 ± 0.002	4.88 ± 0.2	1.26 ± 0.06	3.88 ± 0.24	12.29 ± 0.017	3.74 ± 0.017	35.37 ± 0.06	-7.6 ± 0.14	4.52 ± 0.8	5.04 ± 0.81	57.98 ± 0.8	49.15 ± 0.8
10	240 ± 0.75	29.94 ± 0.14	34.95 ± 0.15	0.01 ± 0.14	-2.99 ± 0.14	0.23 ± 0.002	4.84 ± 0.2	1.26 ± 0.06	3.84 ± 0.24	12.37 ± 0.017	3.74 ± 0.017	35.65 ± 0.06	-7.55 ± 0.14	5.16 ± 0.8	5.39 ± 0.81	58.51 ± 0.8	49.65 ± 0.8
10	250 ± 0.75	30.27 ± 0.14	35.34 ± 0.15	0.01 ± 0.14	-3.02 ± 0.14	0.23 ± 0.002	4.95 ± 0.2	1.28 ± 0.06	3.82 ± 0.24	12.57 ± 0.017	3.76 ± 0.017	36.32 ± 0.06	-7.36 ± 0.14	5.72 ± 0.8	4.41 ± 0.81	58.65 ± 0.8	50.02 ± 0.8
11	111 ± 0.75	29.98 ± 0.14	35.02 ± 0.15	-0.25 ± 0.14	-3.27 ± 0.14	0.14 ± 0.001	2.87 ± 0.12	1.18 ± 0.06	2.44 ± 0.16	11.68 ± 0.017	2.9 ± 0.017	33.26 ± 0.06	-15.15 ± 0.16	-0.61 ± 0.8	15.68 ± 0.81	71.38 ± 0.8	58.95 ± 0.8
11	120 ± 0.75	30.1 ± 0.14	32.6 ± 0.15	-0.06 ± 0.14	-3.08 ± 0.14	0.15 ± 0.002	3.19 ± 0.13	1.19 ± 0.06	2.68 ± 0.13	11.79 ± 0.017	2.99 ± 0.017	33.64 ± 0.06	-14.29 ± 0.16	-0.52 ± 0.8	14.91 ± 0.81	70 ± 0.8	57.81 ± 0.8
11	125 ± 0.75	30.07 ± 0.14	32.57 ± 0.15	-0.04 ± 0.14	-3.04 ± 0.14	0.16 ± 0.002	3.43 ± 0.14	1.2 ± 0.06	2.87 ± 0.14	11.82 ± 0.017	2.98 ± 0.017	33.75 ± 0.06	-14.34 ± 0.16	-0.45 ± 0.8	14.97 ± 0.81	70.33 ± 0.8	58.16 ± 0.8

Test	Ref [g]	$T_{w,in}$ [°C]	$T_{w,out}$ [°C]	$T_{b,in}$ [°C]	$T_{b,out}$ [°C]	$\dot{m}_w$ [kg/ s]	Q_h [kW]	$\dot{E}$ [kW]	COP	P_{cond} [bar]	P_{evap} [bar]	T_{cond} [°C]	T_{evap} [°C]	SC [K]	SH [K]	T_{dis} [°C]	T_{oil} [°C]
11	130 ± 0.75	29.98 ± 0.14	32.48 ± 0.15	-0.01 ± 0.14	-3.01 ± 0.14	0.17 ± 0.002	3.61 ± 0.15	1.2 ± 0.06	3.01 ± 0.15	11.83 ± 0.017	2.99 ± 0.017	33.77 ± 0.06	-14.29 ± 0.16	-0.36 ± 0.8	14.94 ± 0.81	70.49 ± 0.8	58.33 ± 0.8
11	135 ± 0.75	30 ± 0.14	32.5 ± 0.15	-0.01 ± 0.14	-3.02 ± 0.14	0.18 ± 0.002	3.75 ± 0.15	1.2 ± 0.06	3.12 ± 0.15	11.86 ± 0.017	2.98 ± 0.017	33.9 ± 0.06	-14.33 ± 0.16	-0.15 ± 0.8	14.99 ± 0.81	70.48 ± 0.8	58.28 ± 0.8
11	140 ± 0.75	30.02 ± 0.14	32.53 ± 0.15	-0.04 ± 0.14	-3.04 ± 0.14	0.18 ± 0.002	3.86 ± 0.16	1.2 ± 0.06	3.21 ± 0.15	11.89 ± 0.017	2.99 ± 0.017	34 ± 0.06	-14.31 ± 0.16	0.23 ± 0.8	14.95 ± 0.81	70.95 ± 0.8	58.78 ± 0.8
11	146 ± 0.75	30.04 ± 0.14	32.53 ± 0.15	-0.01 ± 0.14	-3.01 ± 0.14	0.19 ± 0.002	3.96 ± 0.16	1.2 ± 0.06	3.29 ± 0.16	11.91 ± 0.017	2.98 ± 0.017	34.07 ± 0.06	-14.37 ± 0.16	0.43 ± 0.8	15 ± 0.81	71.09 ± 0.8	58.96 ± 0.8
11	150.5 ± 0.75	30 ± 0.14	32.5 ± 0.15	-0.03 ± 0.14	-3.02 ± 0.14	0.19 ± 0.002	4.02 ± 0.17	1.2 ± 0.06	3.34 ± 0.16	11.91 ± 0.017	2.98 ± 0.017	34.08 ± 0.06	-14.36 ± 0.16	1.29 ± 0.8	15 ± 0.81	71.11 ± 0.8	58.99 ± 0.8
11	155.5 ± 0.75	29.99 ± 0.14	32.49 ± 0.15	-0.02 ± 0.14	-3.02 ± 0.14	0.19 ± 0.002	4.02 ± 0.17	1.21 ± 0.06	3.33 ± 0.16	11.94 ± 0.017	2.98 ± 0.017	34.15 ± 0.06	-14.36 ± 0.16	2.85 ± 0.8	15.01 ± 0.81	71.23 ± 0.8	59.12 ± 0.8
11	160.5 ± 0.75	29.91 ± 0.14	32.41 ± 0.15	-0.03 ± 0.14	-3.02 ± 0.14	0.19 ± 0.002	4.04 ± 0.17	1.21 ± 0.06	3.35 ± 0.16	11.94 ± 0.017	2.98 ± 0.017	34.16 ± 0.06	-14.36 ± 0.16	3.65 ± 0.8	15.02 ± 0.81	71.34 ± 0.8	59.27 ± 0.8
11	165 ± 0.75	30.1 ± 0.14	32.59 ± 0.15	0.02 ± 0.14	-2.98 ± 0.14	0.19 ± 0.002	4.02 ± 0.17	1.21 ± 0.06	3.32 ± 0.16	12 ± 0.017	2.98 ± 0.017	34.39 ± 0.06	-14.33 ± 0.16	3.92 ± 0.8	14.99 ± 0.81	71.48 ± 0.8	59.4 ± 0.8
11	169.5 ± 0.75	29.8 ± 0.14	32.29 ± 0.15	-0.03 ± 0.14	-3.03 ± 0.14	0.19 ± 0.002	4.05 ± 0.17	1.21 ± 0.06	3.35 ± 0.16	11.96 ± 0.017	2.99 ± 0.017	34.23 ± 0.06	-14.28 ± 0.16	4.1 ± 0.8	14.93 ± 0.81	71.2 ± 0.8	59.17 ± 0.8

Test	Ref [g]	$T_{w,in}$ [°C]	$T_{w,out}$ [°C]	$T_{b,in}$ [°C]	$T_{b,out}$ [°C]	$\dot{m}_w$ [kg/ s]	Q_h [kW]	$\dot{E}$ [kW]	COP	P_{cond} [bar]	P_{evap} [bar]	T_{cond} [°C]	T_{evap} [°C]	SC [K]	SH [K]	T_{dis} [°C]	T_{oil} [°C]
11	180 ± 0.75	30.05 ± 0.14	32.55 ± 0.15	-0.01 ± 0.14	-3 ± 0.14	0.19 ± 0.002	4.02 ± 0.17	1.22 ± 0.06	3.3 ± 0.16	12.11 ± 0.017	2.99 ± 0.017	34.76 ± 0.06	-14.32 ± 0.16	4.42 ± 0.8	14.99 ± 0.81	71.96 ± 0.8	59.92 ± 0.8
11	190 ± 0.75	29.96 ± 0.14	32.46 ± 0.15	-0.02 ± 0.14	-3.02 ± 0.14	0.19 ± 0.002	4 ± 0.17	1.23 ± 0.06	3.26 ± 0.16	12.21 ± 0.017	2.98 ± 0.017	35.11 ± 0.06	-14.32 ± 0.16	4.85 ± 0.8	15.01 ± 0.81	72.3 ± 0.8	60.24 ± 0.8
12	130 ± 0.75	29.97 ± 0.14	35.01 ± 0.15	0.24 ± 0.14	-2.78 ± 0.14	0.16 ± 0.002	3.41 ± 0.14	1.19 ± 0.06	2.86 ± 0.19	11.73 ± 0.017	3.18 ± 0.017	33.44 ± 0.06	-12.45 ± 0.15	-0.67 ± 0.8	13.58 ± 0.81	72.24 ± 0.8	68.9 ± 0.8
12	141 ± 0.75	30.01 ± 0.14	35 ± 0.15	0.09 ± 0.14	-2.91 ± 0.14	0.18 ± 0.002	3.7 ± 0.16	1.21 ± 0.06	3.06 ± 0.2	11.8 ± 0.017	3.36 ± 0.017	33.67 ± 0.06	-10.82 ± 0.15	-0.63 ± 0.8	11.65 ± 0.81	68.99 ± 0.8	65.88 ± 0.8
12	150.5 ± 0.75	30.01 ± 0.14	35.01 ± 0.15	0.02 ± 0.14	-2.97 ± 0.14	0.19 ± 0.002	3.9 ± 0.16	1.21 ± 0.06	3.21 ± 0.21	11.84 ± 0.017	3.52 ± 0.017	33.83 ± 0.06	-9.44 ± 0.15	-0.61 ± 0.8	10.12 ± 0.81	67.06 ± 0.8	65.37 ± 0.8
12	161.5 ± 0.75	30.01 ± 0.14	35.01 ± 0.15	0.02 ± 0.14	-2.99 ± 0.14	0.2 ± 0.002	4.15 ± 0.17	1.22 ± 0.06	3.4 ± 0.22	11.87 ± 0.017	3.62 ± 0.017	33.94 ± 0.06	-8.55 ± 0.14	-0.56 ± 0.8	9.92 ± 0.81	65.03 ± 0.8	64.25 ± 0.8
12	170 ± 0.75	29.98 ± 0.14	34.98 ± 0.15	0 ± 0.14	-3.01 ± 0.14	0.21 ± 0.002	4.41 ± 0.19	1.22 ± 0.06	3.61 ± 0.23	11.9 ± 0.017	3.62 ± 0.017	34.01 ± 0.06	-8.6 ± 0.14	-0.42 ± 0.8	9.96 ± 0.81	65.26 ± 0.8	64.5 ± 0.8
12	175 ± 0.75	30.02 ± 0.14	35.02 ± 0.15	0 ± 0.14	-3 ± 0.14	0.22 ± 0.002	4.53 ± 0.19	1.23 ± 0.06	3.7 ± 0.24	11.93 ± 0.017	3.61 ± 0.017	34.14 ± 0.06	-8.61 ± 0.14	-0.18 ± 0.8	9.93 ± 0.81	65.49 ± 0.8	64.81 ± 0.8
12	180.5 ± 0.75	29.99 ± 0.14	34.98 ± 0.15	0 ± 0.14	-3.01 ± 0.14	0.22 ± 0.002	4.63 ± 0.19	1.23 ± 0.06	3.78 ± 0.24	11.94 ± 0.017	3.61 ± 0.017	34.17 ± 0.06	-8.64 ± 0.14	0.17 ± 0.8	9.98 ± 0.81	65.61 ± 0.8	64.98 ± 0.8

Test	Ref [g]	$T_{w,in}$ [°C]	$T_{w,out}$ [°C]	$T_{b,in}$ [°C]	$T_{b,out}$ [°C]	$\dot{m}_w$ [kg/ s]	Q_h [kW]	$\dot{E}$ [kW]	COP	P_{cond} [bar]	P_{evap} [bar]	T_{cond} [°C]	T_{evap} [°C]	SC [K]	SH [K]	T_{dis} [°C]	T_{oil} [°C]
12	185 ± 0.75	29.88 ± 0.14	34.88 ± 0.15	-0.02 ± 0.14	-3.02 ± 0.14	0.22 ± 0.002	4.71 ± 0.2	1.22 ± 0.06	3.85 ± 0.25	11.93 ± 0.017	3.61 ± 0.017	34.12 ± 0.06	-8.62 ± 0.14	0.57 ± 0.8	9.96 ± 0.81	65.57 ± 0.8	64.91 ± 0.8
12	190.5 ± 0.75	30.01 ± 0.14	35.01 ± 0.15	0.01 ± 0.14	-2.99 ± 0.14	0.23 ± 0.002	4.73 ± 0.2	1.23 ± 0.06	3.85 ± 0.25	11.97 ± 0.017	3.61 ± 0.017	34.29 ± 0.06	-8.62 ± 0.14	0.78 ± 0.8	10.01 ± 0.81	65.8 ± 0.8	65.14 ± 0.8
12	195.5 ± 0.75	30.01 ± 0.14	35.01 ± 0.15	0.01 ± 0.14	-3 ± 0.14	0.23 ± 0.002	4.74 ± 0.2	1.23 ± 0.06	3.86 ± 0.25	11.99 ± 0.017	3.61 ± 0.017	34.33 ± 0.06	-8.64 ± 0.14	2.14 ± 0.8	9.99 ± 0.81	65.85 ± 0.8	65.21 ± 0.8
12	200.5 ± 0.75	30 ± 0.14	35.01 ± 0.15	-0.01 ± 0.14	-3.01 ± 0.14	0.23 ± 0.002	4.75 ± 0.2	1.23 ± 0.06	3.85 ± 0.25	12.02 ± 0.017	3.62 ± 0.017	34.45 ± 0.06	-8.58 ± 0.14	3.31 ± 0.8	9.99 ± 0.81	65.91 ± 0.8	65.27 ± 0.8
12	211 ± 0.75	30.02 ± 0.14	35.02 ± 0.15	-0.01 ± 0.14	-3.01 ± 0.14	0.23 ± 0.002	4.75 ± 0.2	1.24 ± 0.06	3.82 ± 0.25	12.07 ± 0.017	3.62 ± 0.017	34.63 ± 0.06	-8.59 ± 0.14	4.24 ± 0.8	10 ± 0.81	66.13 ± 0.8	65.48 ± 0.8
13	130 ± 0.75	30 ± 0.14	35 ± 0.15	7.1 ± 0.14	4.1 ± 0.14	0.17 ± 0.002	3.53 ± 0.15	1.2 ± 0.06	2.95 ± 0.19	11.74 ± 0.017	3.3 ± 0.017	33.48 ± 0.06	-11.34 ± 0.15	-0.7 ± 0.8	18.29 ± 0.81	70.54 ± 0.8	60.03 ± 0.8
13	141 ± 0.75	30.05 ± 0.14	35.05 ± 0.15	7.01 ± 0.14	4.01 ± 0.14	0.19 ± 0.002	3.94 ± 0.17	1.21 ± 0.06	3.25 ± 0.21	11.83 ± 0.017	3.59 ± 0.017	33.77 ± 0.06	-8.84 ± 0.14	-0.67 ± 0.8	15.62 ± 0.81	66.86 ± 0.8	56.92 ± 0.8
13	151 ± 0.75	29.97 ± 0.14	34.97 ± 0.15	7.03 ± 0.14	4 ± 0.14	0.2 ± 0.002	4.29 ± 0.18	1.22 ± 0.06	3.52 ± 0.23	11.86 ± 0.017	3.83 ± 0.017	33.89 ± 0.06	-6.82 ± 0.13	-0.63 ± 0.8	13.53 ± 0.81	64.01 ± 0.8	54.55 ± 0.8
13	160.5 ± 0.75	30.03 ± 0.14	35.02 ± 0.15	7 ± 0.14	4 ± 0.14	0.22 ± 0.002	4.54 ± 0.19	1.22 ± 0.06	3.71 ± 0.24	11.91 ± 0.017	4.01 ± 0.017	34.06 ± 0.06	-5.37 ± 0.13	-0.6 ± 0.8	11.97 ± 0.81	61.58 ± 0.8	52.3 ± 0.8

Test	Ref [g]	$T_{w,in}$ [°C]	$T_{w,out}$ [°C]	$T_{b,in}$ [°C]	$T_{b,out}$ [°C]	$\dot{m}_w$ [kg/ s]	Q_h [kW]	$\dot{E}$ [kW]	COP	P_{cond} [bar]	P_{evap} [bar]	T_{cond} [°C]	T_{evap} [°C]	SC [K]	SH [K]	T_{dis} [°C]	T_{oil} [°C]
13	170.5 ± 0.75	30.01 ± 0.14	35.01 ± 0.15	7 ± 0.14	4.01 ± 0.14	0.23 ± 0.002	4.82 ± 0.2	1.23 ± 0.06	3.92 ± 0.25	11.94 ± 0.017	4.2 ± 0.017	34.17 ± 0.06	-3.94 ± 0.12	-0.56 ± 0.8	10.49 ± 0.81	59.47 ± 0.8	50.66 ± 0.8
13	175 ± 0.75	30.01 ± 0.14	35.01 ± 0.15	7 ± 0.14	4.01 ± 0.14	0.23 ± 0.002	5.07 ± 0.2	1.23 ± 0.06	3.92 ± 0.25	11.94 ± 0.017	4.2 ± 0.017	34.17 ± 0.06	-3.94 ± 0.12	-0.56 ± 0.8	10.49 ± 0.81	59.47 ± 0.8	50.66 ± 0.8
13	180 ± 0.75	30.01 ± 0.14	35.01 ± 0.15	7 ± 0.14	4 ± 0.14	0.24 ± 0.002	5.21 ± 0.21	1.23 ± 0.06	4.12 ± 0.26	11.98 ± 0.017	4.28 ± 0.017	34.32 ± 0.06	-3.29 ± 0.12	-0.42 ± 0.8	9.83 ± 0.81	58.53 ± 0.8	49.84 ± 0.8
13	185 ± 0.75	30 ± 0.14	35.01 ± 0.15	7 ± 0.14	3.99 ± 0.14	0.25 ± 0.002	5.35 ± 0.22	1.23 ± 0.06	4.22 ± 0.27	12.01 ± 0.017	4.28 ± 0.017	34.42 ± 0.06	-3.37 ± 0.12	-0.16 ± 0.8	9.92 ± 0.81	58.8 ± 0.8	50.05 ± 0.8
13	190.5 ± 0.75	30.01 ± 0.14	35.01 ± 0.15	7.01 ± 0.14	4 ± 0.14	0.25 ± 0.003	5.43 ± 0.22	1.24 ± 0.06	4.33 ± 0.28	12.04 ± 0.017	4.28 ± 0.017	34.51 ± 0.06	-3.31 ± 0.12	0.32 ± 0.8	9.88 ± 0.81	58.91 ± 0.8	50.16 ± 0.8
13	195 ± 0.75	30 ± 0.14	35 ± 0.15	7 ± 0.14	3.99 ± 0.14	0.26 ± 0.003	5.44 ± 0.23	1.24 ± 0.06	4.4 ± 0.28	12.05 ± 0.017	4.28 ± 0.017	34.55 ± 0.06	-3.35 ± 0.12	0.7 ± 0.8	9.91 ± 0.81	59.02 ± 0.8	50.25 ± 0.8
13	200.5 ± 0.75	29.98 ± 0.14	34.98 ± 0.15	7 ± 0.14	4 ± 0.14	0.26 ± 0.003	5.45 ± 0.23	1.24 ± 0.06	4.45 ± 0.29	12.06 ± 0.017	4.28 ± 0.017	34.59 ± 0.06	-3.33 ± 0.12	1.16 ± 0.8	9.88 ± 0.81	59 ± 0.8	50.27 ± 0.8
13	170.5 ± 0.75	30.01 ± 0.14	35.01 ± 0.15	7 ± 0.14	4.01 ± 0.14	0.23 ± 0.002	4.82 ± 0.2	1.23 ± 0.06	3.92 ± 0.25	11.94 ± 0.017	4.2 ± 0.017	34.17 ± 0.06	-3.94 ± 0.12	-0.56 ± 0.8	10.49 ± 0.81	59.47 ± 0.8	50.66 ± 0.8
13	209.5 ± 0.75	29.98 ± 0.14	34.98 ± 0.15	7 ± 0.14	4 ± 0.14	0.26 ± 0.003	5.47 ± 0.23	1.24 ± 0.06	4.45 ± 0.28	12.11 ± 0.017	4.27 ± 0.017	34.75 ± 0.06	-3.44 ± 0.12	3.86 ± 0.8	9.99 ± 0.81	59.48 ± 0.8	50.75 ± 0.8

Test	Ref [g]	$T_{w,in}$ [°C]	$T_{w,out}$ [°C]	$T_{b,in}$ [°C]	$T_{b,out}$ [°C]	$\dot{m}_w$ [kg/ s]	Q_h [kW]	$\dot{E}$ [kW]	COP	P_{cond} [bar]	P_{evap} [bar]	T_{cond} [°C]	T_{evap} [°C]	SC [K]	SH [K]	T_{dis} [°C]	T_{oil} [°C]
13	214.5 ± 0.75	29.98 ± 0.14	34.99 ± 0.15	7 ± 0.14	4 ± 0.14	0.26 ± 0.003	5.47 ± 0.23	1.25 ± 0.06	4.44 ± 0.28	12.14 ± 0.017	4.26 ± 0.017	34.88 ± 0.06	-3.46 ± 0.12	4.43 ± 0.8	10.01 ± 0.81	59.62 ± 0.8	50.95 ± 0.8
14	130 ± 0.75	30.02 ± 0.14	35.02 ± 0.15	13.8 ± 0.14	10.8 ± 0.14	0.2 ± 0.002	4.17 ± 0.18	1.21 ± 0.06	3.24 ± 0.22	11.85 ± 0.017	3.76 ± 0.017	33.84 ± 0.06	-7.38 ± 0.14	-0.44 ± 0.8	20.68 ± 0.81	71.6 ± 0.8	60.07 ± 0.8
14	140.5 ± 0.75	30.11 ± 0.14	35.11 ± 0.15	13.81 ± 0.14	10.81 ± 0.14	0.22 ± 0.002	4.61 ± 0.19	1.23 ± 0.06	3.56 ± 0.24	11.94 ± 0.017	4.09 ± 0.017	34.18 ± 0.06	-4.78 ± 0.13	-0.31 ± 0.8	18.02 ± 0.81	68.21 ± 0.8	57.58 ± 0.8
14	150 ± 0.75	30.03 ± 0.14	35.05 ± 0.15	13.65 ± 0.14	10.64 ± 0.14	0.24 ± 0.002	5.02 ± 0.21	1.23 ± 0.06	3.88 ± 0.26	11.99 ± 0.017	4.37 ± 0.017	34.33 ± 0.06	-2.67 ± 0.12	-0.17 ± 0.8	15.72 ± 0.81	65.2 ± 0.8	55.33 ± 0.8
14	159 ± 0.75	30.03 ± 0.14	35.02 ± 0.15	13.51 ± 0.14	10.51 ± 0.14	0.25 ± 0.003	5.32 ± 0.22	1.23 ± 0.06	4.13 ± 0.28	12.05 ± 0.017	4.62 ± 0.017	34.54 ± 0.06	-0.87 ± 0.12	-0.03 ± 0.8	13.71 ± 0.81	62.25 ± 0.8	52.99 ± 0.8
14	165 ± 0.75	30.02 ± 0.14	35.03 ± 0.15	13.49 ± 0.14	10.49 ± 0.14	0.27 ± 0.003	5.62 ± 0.24	1.23 ± 0.06	4.38 ± 0.29	12.08 ± 0.017	4.84 ± 0.017	34.67 ± 0.06	0.64 ± 0.11	0.1 ± 0.8	12.12 ± 0.81	60.27 ± 0.8	51.36 ± 0.8
14	170.5 ± 0.75	30 ± 0.14	35 ± 0.15	13.43 ± 0.14	10.43 ± 0.14	0.28 ± 0.003	5.85 ± 0.25	1.22 ± 0.06	4.58 ± 0.31	12.1 ± 0.017	5.02 ± 0.017	34.74 ± 0.06	1.87 ± 0.11	0.21 ± 0.8	10.75 ± 0.81	58.13 ± 0.8	50.01 ± 0.8
14	175.5 ± 0.75	29.99 ± 0.14	34.99 ± 0.15	13.3 ± 0.14	10.3 ± 0.14	0.29 ± 0.003	6.06 ± 0.25	1.22 ± 0.06	4.76 ± 0.32	12.15 ± 0.017	5.16 ± 0.017	34.89 ± 0.06	2.8 ± 0.11	0.41 ± 0.8	9.69 ± 0.81	56.73 ± 0.8	48.95 ± 0.8
14	180.5 ± 0.75	30 ± 0.14	35 ± 0.15	13.31 ± 0.14	10.3 ± 0.14	0.3 ± 0.003	6.2 ± 0.26	1.23 ± 0.06	4.85 ± 0.33	12.18 ± 0.017	5.13 ± 0.017	35.01 ± 0.06	2.56 ± 0.11	1.04 ± 0.8	9.94 ± 0.81	57.23 ± 0.8	49.32 ± 0.8

Test	Ref [g]	$T_{w,in}$ [°C]	$T_{w,out}$ [°C]	$T_{b,in}$ [°C]	$T_{b,out}$ [°C]	$\dot{m}_w$ [kg/ s]	Q_h [kW]	$\dot{E}$ [kW]	COP	P_{cond} [bar]	P_{evap} [bar]	T_{cond} [°C]	T_{evap} [°C]	SC [K]	SH [K]	T_{dis} [°C]	T_{oil} [°C]
14	185.5 ± 0.75	29.97 ± 0.14	34.98 ± 0.15	13.25 ± 0.14	10.24 ± 0.14	0.3 ± 0.003	6.3 ± 0.26	1.23 ± 0.06	4.92 ± 0.33	12.2 ± 0.017	5.12 ± 0.017	35.07 ± 0.06	2.54 ± 0.11	1.58 ± 0.8	9.92 ± 0.81	57.27 ± 0.8	49.38 ± 0.8
14	190.5 ± 0.75	30.01 ± 0.14	35.01 ± 0.15	13.24 ± 0.14	10.22 ± 0.14	0.3 ± 0.003	6.38 ± 0.27	1.23 ± 0.06	4.98 ± 0.33	12.24 ± 0.017	5.12 ± 0.017	35.2 ± 0.06	2.53 ± 0.11	2.34 ± 0.8	9.88 ± 0.81	57.37 ± 0.8	49.47 ± 0.8
14	195.5 ± 0.75	29.99 ± 0.14	34.99 ± 0.15	13.29 ± 0.14	10.27 ± 0.14	0.31 ± 0.003	6.45 ± 0.27	1.23 ± 0.06	5.02 ± 0.33	12.26 ± 0.017	5.12 ± 0.017	35.27 ± 0.06	2.54 ± 0.11	3.15 ± 0.8	9.92 ± 0.81	57.48 ± 0.8	49.57 ± 0.8
14	200 ± 0.75	30 ± 0.14	35 ± 0.15	13.23 ± 0.14	10.17 ± 0.14	0.31 ± 0.003	6.46 ± 0.27	1.24 ± 0.06	5.03 ± 0.33	12.28 ± 0.017	5.11 ± 0.017	35.36 ± 0.06	2.44 ± 0.11	3.97 ± 0.8	9.94 ± 0.81	57.6 ± 0.8	49.69 ± 0.8
14	205 ± 0.75	29.99 ± 0.14	35 ± 0.15	13.25 ± 0.14	10.19 ± 0.14	0.31 ± 0.003	6.49 ± 0.27	1.24 ± 0.06	5.02 ± 0.33	12.33 ± 0.017	5.1 ± 0.017	35.5 ± 0.06	2.41 ± 0.11	4.76 ± 0.8	9.99 ± 0.81	57.92 ± 0.8	49.97 ± 0.8
14	210 ± 0.75	30 ± 0.14	35 ± 0.15	13.26 ± 0.14	10.19 ± 0.14	0.31 ± 0.003	6.5 ± 0.27	1.25 ± 0.06	4.99 ± 0.33	12.45 ± 0.017	5.1 ± 0.017	35.91 ± 0.06	2.41 ± 0.11	5.55 ± 0.8	10 ± 0.81	58.32 ± 0.8	50.29 ± 0.8
15	140.5 ± 0.75	51.49 ± 0.14	55.01 ± 0.15	-0.04 ± 0.14	-1.58 ± 0.14	0.14 ± 0.001	2.07 ± 0.12	1.66 ± 0.06	1.25 ± 0.09	18.15 ± 0.017	3.49 ± 0.017	52.68 ± 0.04	-9.7 ± 0.14	-1.09 ± 0.8	10.14 ± 0.81	89.66 ± 0.8	77.21 ± 0.8
15	145.5 ± 0.75	51.14 ± 0.14	54.99 ± 0.15	0.2 ± 0.14	-1.65 ± 0.14	0.14 ± 0.001	2.27 ± 0.12	1.67 ± 0.06	1.36 ± 0.09	18.16 ± 0.017	3.53 ± 0.017	52.7 ± 0.04	-9.3 ± 0.14	-1.08 ± 0.8	9.99 ± 0.81	89.07 ± 0.8	76.81 ± 0.8
15	150.5 ± 0.75	50.67 ± 0.14	54.99 ± 0.15	0.05 ± 0.14	-2.28 ± 0.14	0.14 ± 0.001	2.53 ± 0.12	1.67 ± 0.06	1.51 ± 0.09	18.17 ± 0.017	3.52 ± 0.017	52.73 ± 0.04	-9.43 ± 0.14	-1.06 ± 0.8	9.98 ± 0.81	89.3 ± 0.8	77.28 ± 0.8

Test	Ref [g]	$T_{w,in}$ [°C]	$T_{w,out}$ [°C]	$T_{b,in}$ [°C]	$T_{b,out}$ [°C]	$\dot{m}_w$ [kg/ s]	Q_h [kW]	$\dot{E}$ [kW]	COP	P_{cond} [bar]	P_{evap} [bar]	T_{cond} [°C]	T_{evap} [°C]	SC [K]	SH [K]	T_{dis} [°C]	T_{oil} [°C]
15	155 ± 0.75	50.26 ± 0.14	54.98 ± 0.15	0 ± 0.14	-2.71 ± 0.14	0.14 ± 0.001	2.76 ± 0.12	1.67 ± 0.06	1.65 ± 0.09	18.18 ± 0.017	3.52 ± 0.017	52.75 ± 0.04	-9.39 ± 0.14	-1.04 ± 0.8	9.92 ± 0.81	89.23 ± 0.8	77.39 ± 0.8
15	160 ± 0.75	49.8 ± 0.14	54.97 ± 0.15	0.01 ± 0.14	-3.15 ± 0.14	0.14 ± 0.001	3.02 ± 0.12	1.67 ± 0.06	1.8 ± 0.1	18.19 ± 0.017	3.52 ± 0.017	52.78 ± 0.04	-9.37 ± 0.14	-1.01 ± 0.8	9.92 ± 0.81	89.23 ± 0.8	77.41 ± 0.8
15	165 ± 0.75	49.99 ± 0.14	54.99 ± 0.15	0.01 ± 0.14	-3.02 ± 0.14	0.16 ± 0.002	3.28 ± 0.14	1.68 ± 0.06	1.95 ± 0.11	18.3 ± 0.017	3.53 ± 0.017	53.07 ± 0.04	-9.37 ± 0.14	-0.95 ± 0.8	9.94 ± 0.81	89.65 ± 0.8	77.7 ± 0.8
15	170 ± 0.75	49.89 ± 0.14	54.89 ± 0.15	0.01 ± 0.14	-3.02 ± 0.14	0.17 ± 0.002	3.48 ± 0.15	1.68 ± 0.06	2.07 ± 0.11	18.33 ± 0.017	3.53 ± 0.017	53.13 ± 0.04	-9.33 ± 0.14	-0.89 ± 0.8	9.87 ± 0.81	89.63 ± 0.8	77.72 ± 0.8
15	174.5 ± 0.75	49.88 ± 0.14	54.89 ± 0.15	0.5 ± 0.14	-2.51 ± 0.14	0.18 ± 0.002	3.73 ± 0.16	1.69 ± 0.06	2.22 ± 0.12	18.4 ± 0.017	3.57 ± 0.017	53.32 ± 0.04	-9.02 ± 0.14	-0.8 ± 0.8	10 ± 0.81	89.99 ± 0.8	77.74 ± 0.8
15	180 ± 0.75	49.79 ± 0.14	54.81 ± 0.15	0.21 ± 0.14	-2.83 ± 0.14	0.18 ± 0.002	3.89 ± 0.16	1.69 ± 0.06	2.31 ± 0.13	18.39 ± 0.017	3.55 ± 0.017	53.28 ± 0.04	-9.14 ± 0.14	-0.59 ± 0.8	9.87 ± 0.81	90.11 ± 0.8	77.64 ± 0.8
15	185.5 ± 0.75	49.88 ± 0.14	54.92 ± 0.15	0.02 ± 0.14	-2.99 ± 0.14	0.19 ± 0.002	4.03 ± 0.17	1.69 ± 0.06	2.4 ± 0.13	18.47 ± 0.017	3.53 ± 0.017	53.5 ± 0.04	-9.36 ± 0.14	-0.27 ± 0.8	9.94 ± 0.81	90.91 ± 0.8	78.6 ± 0.8
15	190 ± 0.75	49.9 ± 0.14	54.9 ± 0.15	0 ± 0.14	-3 ± 0.14	0.19 ± 0.002	4.05 ± 0.17	1.69 ± 0.06	2.4 ± 0.13	18.47 ± 0.017	3.52 ± 0.017	53.5 ± 0.04	-9.41 ± 0.14	-0.08 ± 0.8	9.98 ± 0.81	90.5 ± 0.8	78.54 ± 0.8
15	195 ± 0.75	49.98 ± 0.14	54.98 ± 0.15	-0.02 ± 0.14	-3.02 ± 0.14	0.2 ± 0.002	4.11 ± 0.17	1.69 ± 0.06	2.43 ± 0.13	18.54 ± 0.017	3.53 ± 0.017	53.66 ± 0.04	-9.33 ± 0.14	0.75 ± 0.8	9.92 ± 0.81	90.28 ± 0.8	78.44 ± 0.8

Test	Ref [g]	$T_{w,in}$ [°C]	$T_{w,out}$ [°C]	$T_{b,in}$ [°C]	$T_{b,out}$ [°C]	$\dot{m}_w$ [kg/s]	Q_h [kW]	$\dot{E}$ [kW]	COP	P_{cond} [bar]	P_{evap} [bar]	T_{cond} [°C]	T_{evap} [°C]	SC [K]	SH [K]	T_{dis} [°C]	T_{oil} [°C]
15	201 ± 0.75	50.13 ± 0.14	55.12 ± 0.15	-0.01 ± 0.14	-3 ± 0.14	0.2 ± 0.002	4.14 ± 0.17	1.7 ± 0.06	2.43 ± 0.13	18.63 ± 0.017	3.53 ± 0.017	53.9 ± 0.04	-9.36 ± 0.14	2.53 ± 0.8	9.98 ± 0.81	90.63 ± 0.8	78.72 ± 0.8
15	205.5 ± 0.75	50.01 ± 0.14	55.01 ± 0.15	-0.01 ± 0.14	-3.01 ± 0.14	0.2 ± 0.002	4.17 ± 0.17	1.7 ± 0.06	2.45 ± 0.13	18.62 ± 0.017	3.53 ± 0.017	53.88 ± 0.04	-9.36 ± 0.14	3.28 ± 0.8	9.99 ± 0.81	90.83 ± 0.8	78.94 ± 0.8
15	210 ± 0.75	49.96 ± 0.14	54.97 ± 0.15	0 ± 0.14	-3 ± 0.14	0.2 ± 0.002	4.17 ± 0.17	1.71 ± 0.06	2.45 ± 0.13	18.7 ± 0.017	3.53 ± 0.017	54.06 ± 0.04	-9.36 ± 0.14	3.79 ± 0.8	10.02 ± 0.81	91.19 ± 0.8	79.21 ± 0.8

Table 18: Performance result of refrigerant charge determination of prototype 1.

Test	Ref [g]	$T_{w,in}$ [°C]	$T_{w,out}$ [°C]	$T_{b,in}$ [°C]	$T_{b,out}$ [°C]	$\dot{m}_w$ [kg/s]	Q_h [kW]	$\dot{E}$ [kW]	COP	P_{cond} [bar]	P_{evap} [bar]	T_{cond} [°C]	T_{evap} [°C]	SC [K]	SH [K]	T_{dis} [°C]	T_{oil} [°C]
1	110 ± 0.75	23.39 ± 0.14	24.01 ± 0.15	24.47 ± 0.14	23.94 ± 0.14	0.14 ± 0.001	0.37 ± 0.12	0.6 ± 0.06	2.82 ± 0.21	9.01 ± 0.017	4.24 ± 0.017	22.85 ± 0.07	-3.66 ± 0.12	-1.15 ± 0.8	26.54 ± 0.81	33.62 ± 0.8	23.89 ± 0.8
1	115 ± 0.75	30.31 ± 0.14	35.02 ± 0.15	-0.11 ± 0.14	-2.66 ± 0.14	0.13 ± 0.001	2.57 ± 0.11	1.16 ± 0.06	2.2 ± 0.15	11.61 ± 0.017	2.78 ± 0.017	33.01 ± 0.06	-16.42 ± 0.17	-0.75 ± 0.8	18.44 ± 0.81	73.7 ± 0.8	54.8 ± 0.8
1	124.5 ± 0.75	29.8 ± 0.14	34.91 ± 0.15	-0.02 ± 0.14	-3.13 ± 0.14	0.14 ± 0.001	3.02 ± 0.12	1.18 ± 0.06	2.56 ± 0.17	11.63 ± 0.017	3 ± 0.017	33.07 ± 0.06	-14.17 ± 0.16	-0.69 ± 0.8	16.11 ± 0.81	70.39 ± 0.8	52.98 ± 0.8

Test	Ref [g]	$T_{w,in}$ [°C]	$T_{w,out}$ [°C]	$T_{b,in}$ [°C]	$T_{b,out}$ [°C]	$\dot{m}_w$ [kg/ s]	Q_h [kW]	$\dot{E}$ [kW]	COP	P_{cond} [bar]	P_{evap} [bar]	T_{cond} [°C]	T_{evap} [°C]	SC [K]	SH [K]	T_{dis} [°C]	T_{oil} [°C]
1	135 ± 0.75	29.98 ± 0.14	34.99 ± 0.15	0 ± 0.14	-3 ± 0.14	0.16 ± 0.002	3.33 ± 0.14	1.2 ± 0.06	2.78 ± 0.18	11.72 ± 0.017	3.2 ± 0.017	33.41 ± 0.06	-12.28 ± 0.15	-0.68 ± 0.8	13.75 ± 0.81	66.6 ± 0.8	50.27 ± 0.8
1	144.5 ± 0.75	29.97 ± 0.14	34.98 ± 0.15	0.01 ± 0.14	-2.99 ± 0.14	0.17 ± 0.002	3.54 ± 0.15	1.21 ± 0.06	2.93 ± 0.19	11.77 ± 0.017	3.33 ± 0.017	33.58 ± 0.06	-11.07 ± 0.15	-0.65 ± 0.8	10.36 ± 0.81	63.93 ± 0.8	48.06 ± 0.8
1	156 ± 0.75	29.97 ± 0.14	35 ± 0.15	0 ± 0.14	-3.06 ± 0.14	0.19 ± 0.002	3.92 ± 0.16	1.21 ± 0.06	3.23 ± 0.21	11.84 ± 0.017	3.33 ± 0.017	33.81 ± 0.06	-11.11 ± 0.15	-0.52 ± 0.8	9.04 ± 0.81	62.75 ± 0.8	47.36 ± 0.8
1	160.5 ± 0.75	30 ± 0.14	35.01 ± 0.15	-0.01 ± 0.14	-3.02 ± 0.14	0.2 ± 0.002	4.12 ± 0.17	1.21 ± 0.06	3.39 ± 0.22	11.86 ± 0.017	3.28 ± 0.017	33.91 ± 0.06	-11.52 ± 0.15	-0.18 ± 0.8	9.92 ± 0.81	64.12 ± 0.8	48.27 ± 0.8
1	166 ± 0.75	29.98 ± 0.14	34.98 ± 0.15	0.01 ± 0.14	-3.01 ± 0.14	0.2 ± 0.002	4.24 ± 0.18	1.22 ± 0.06	3.48 ± 0.23	11.88 ± 0.017	3.28 ± 0.017	33.97 ± 0.06	-11.5 ± 0.15	0.22 ± 0.8	9.87 ± 0.81	64.32 ± 0.8	48.5 ± 0.8
1	173 ± 0.75	30.03 ± 0.14	35.02 ± 0.15	0 ± 0.14	-3 ± 0.14	0.2 ± 0.002	4.25 ± 0.18	1.22 ± 0.06	3.5 ± 0.23	11.92 ± 0.017	3.22 ± 0.017	34.09 ± 0.06	-12.12 ± 0.15	1.67 ± 0.8	10.12 ± 0.81	64.91 ± 0.8	48.96 ± 0.8
1	180 ± 0.75	29.99 ± 0.14	34.99 ± 0.15	0.14 ± 0.14	-2.86 ± 0.14	0.21 ± 0.002	4.32 ± 0.18	1.22 ± 0.06	3.55 ± 0.23	11.93 ± 0.017	3.25 ± 0.017	34.13 ± 0.06	-11.78 ± 0.15	3.05 ± 0.8	9.99 ± 0.81	64.73 ± 0.8	49.08 ± 0.8
1	190.5 ± 0.75	30.01 ± 0.14	35 ± 0.15	0.04 ± 0.14	-2.96 ± 0.14	0.2 ± 0.002	4.27 ± 0.18	1.22 ± 0.06	3.5 ± 0.23	11.99 ± 0.017	3.21 ± 0.017	34.35 ± 0.06	-12.22 ± 0.15	4.16 ± 0.8	10.04 ± 0.81	65.32 ± 0.8	49.51 ± 0.8

Test	Ref [g]	$T_{w,in}$ [°C]	$T_{w,out}$ [°C]	$T_{b,in}$ [°C]	$T_{b,out}$ [°C]	$\dot{m}_w$ [kg/ s]	Q_h [kW]	$\dot{E}$ [kW]	COP	P_{cond} [bar]	P_{evap} [bar]	T_{cond} [°C]	T_{evap} [°C]	SC [K]	SH [K]	T_{dis} [°C]	T_{oil} [°C]
10	130 ± 0.75	30.23 ± 0.14	35.2 ± 0.15	2.06 ± 0.14	-0.92 ± 0.14	0.16 ± 0.002	3.36 ± 0.14	1.21 ± 0.06	2.79 ± 0.18	11.92 ± 0.017	3.27 ± 0.017	34.1 ± 0.06	-11.66 ± 0.15	0.14 ± 0.8	14.87 ± 0.81	66.56 ± 0.8	48.9 ± 0.8
10	140 ± 0.75	29.98 ± 0.14	34.98 ± 0.15	-0.09 ± 0.14	-3.1 ± 0.14	0.17 ± 0.002	3.63 ± 0.15	1.22 ± 0.06	2.97 ± 0.19	11.91 ± 0.017	3.37 ± 0.017	34.08 ± 0.06	-10.7 ± 0.15	0.23 ± 0.8	8.69 ± 0.81	63.09 ± 0.8	48.14 ± 0.8
10	150 ± 0.75	29.92 ± 0.14	34.93 ± 0.15	0.12 ± 0.14	-2.89 ± 0.14	0.18 ± 0.002	3.74 ± 0.16	1.23 ± 0.06	3.05 ± 0.2	11.95 ± 0.017	3.45 ± 0.017	34.21 ± 0.06	-10.06 ± 0.14	0.3 ± 0.8	5.64 ± 0.81	58.69 ± 0.8	45.69 ± 0.8
10	160 ± 0.75	29.89 ± 0.14	34.89 ± 0.15	0.04 ± 0.14	-2.95 ± 0.14	0.21 ± 0.002	4.31 ± 0.18	1.23 ± 0.06	3.5 ± 0.22	12.05 ± 0.017	3.37 ± 0.017	34.56 ± 0.06	-10.77 ± 0.15	1.7 ± 0.8	4.98 ± 0.81	58.71 ± 0.8	45.69 ± 0.8
10	170 ± 0.75	28.69 ± 0.14	33.94 ± 0.15	0.17 ± 0.14	-3.05 ± 0.14	0.2 ± 0.002	4.42 ± 0.18	1.21 ± 0.06	3.66 ± 0.23	11.75 ± 0.017	3.34 ± 0.017	33.51 ± 0.06	-11.04 ± 0.15	1.95 ± 0.8	4.89 ± 0.81	60 ± 0.8	46.56 ± 0.8
10	175 ± 0.75	29.45 ± 0.14	34.45 ± 0.15	0.18 ± 0.14	-2.87 ± 0.14	0.21 ± 0.002	4.42 ± 0.19	1.23 ± 0.06	3.61 ± 0.23	11.95 ± 0.017	3.37 ± 0.017	34.22 ± 0.06	-10.73 ± 0.15	2.35 ± 0.8	5.19 ± 0.81	60 ± 0.8	46.44 ± 0.8
10	181 ± 0.75	30.11 ± 0.14	35.1 ± 0.15	0.24 ± 0.14	-2.78 ± 0.14	0.21 ± 0.002	4.39 ± 0.18	1.24 ± 0.06	3.54 ± 0.23	12.15 ± 0.017	3.36 ± 0.017	34.89 ± 0.06	-10.84 ± 0.15	2.97 ± 0.8	5.06 ± 0.81	59.55 ± 0.8	46.14 ± 0.8
10	186 ± 0.75	29.91 ± 0.14	34.91 ± 0.15	0.15 ± 0.14	-2.85 ± 0.14	0.21 ± 0.002	4.4 ± 0.19	1.23 ± 0.06	3.57 ± 0.23	12.1 ± 0.017	3.33 ± 0.017	34.72 ± 0.06	-11.07 ± 0.15	3.64 ± 0.8	5.07 ± 0.81	60.01 ± 0.8	46.35 ± 0.8

Test	Ref [g]	$T_{w,in}$ [°C]	$T_{w,out}$ [°C]	$T_{b,in}$ [°C]	$T_{b,out}$ [°C]	$\dot{m}_w$ [kg/ s]	Q_h [kW]	$\dot{E}$ [kW]	COP	P_{cond} [bar]	P_{evap} [bar]	T_{cond} [°C]	T_{evap} [°C]	SC [K]	SH [K]	T_{dis} [°C]	T_{oil} [°C]
10	191 ± 0.75	29.95 ± 0.14	34.96 ± 0.15	0.07 ± 0.14	-2.92 ± 0.14	0.21 ± 0.002	4.41 ± 0.19	1.24 ± 0.06	3.56 ± 0.23	12.13 ± 0.017	3.33 ± 0.017	34.82 ± 0.06	-11.09 ± 0.15	3.9 ± 0.8	4.35 ± 0.81	59.72 ± 0.8	46.33 ± 0.8
11	125.5 ± 0.75	30.12 ± 0.14	35.14 ± 0.15	-0.04 ± 0.14	-3.03 ± 0.14	0.14 ± 0.001	2.94 ± 0.12	1.19 ± 0.06	2.48 ± 0.16	11.71 ± 0.017	3 ± 0.017	33.37 ± 0.06	-14.16 ± 0.16	-0.73 ± 0.8	15.87 ± 0.81	70.34 ± 0.8	52.87 ± 0.8
11	134.5 ± 0.75	29.94 ± 0.14	34.94 ± 0.15	0 ± 0.14	-3.02 ± 0.14	0.16 ± 0.002	3.38 ± 0.14	1.2 ± 0.06	2.83 ± 0.18	11.74 ± 0.017	3.12 ± 0.017	33.49 ± 0.06	-13.02 ± 0.16	-0.64 ± 0.8	14.49 ± 0.81	68.15 ± 0.8	51.6 ± 0.8
11	139.5 ± 0.75	29.94 ± 0.14	34.97 ± 0.15	-0.02 ± 0.14	-3.05 ± 0.14	0.17 ± 0.002	3.66 ± 0.15	1.2 ± 0.06	3.06 ± 0.2	11.78 ± 0.017	3.1 ± 0.017	33.61 ± 0.06	-13.21 ± 0.16	-0.55 ± 0.8	14.81 ± 0.81	68.67 ± 0.8	51.77 ± 0.8
11	145 ± 0.75	29.89 ± 0.14	34.9 ± 0.15	0 ± 0.14	-3.02 ± 0.14	0.18 ± 0.002	3.87 ± 0.16	1.2 ± 0.06	3.23 ± 0.21	11.8 ± 0.017	3.07 ± 0.017	33.67 ± 0.06	-13.47 ± 0.16	-0.22 ± 0.8	14.86 ± 0.81	69.08 ± 0.8	52.14 ± 0.8
11	150 ± 0.75	29.99 ± 0.14	34.99 ± 0.15	-0.01 ± 0.14	-3.02 ± 0.14	0.19 ± 0.002	4.01 ± 0.17	1.2 ± 0.06	3.34 ± 0.22	11.83 ± 0.017	3.09 ± 0.017	33.8 ± 0.06	-13.35 ± 0.16	0.14 ± 0.8	14.94 ± 0.81	69.32 ± 0.8	52.38 ± 0.8
11	155 ± 0.75	30.13 ± 0.14	35.14 ± 0.15	0 ± 0.14	-3 ± 0.14	0.2 ± 0.002	4.1 ± 0.17	1.21 ± 0.06	3.4 ± 0.22	11.89 ± 0.017	3.09 ± 0.017	33.98 ± 0.06	-13.28 ± 0.16	0.24 ± 0.8	14.89 ± 0.81	69.3 ± 0.8	52.34 ± 0.8
11	160 ± 0.75	30 ± 0.14	35 ± 0.15	0 ± 0.14	-3 ± 0.14	0.2 ± 0.002	4.13 ± 0.17	1.21 ± 0.06	3.43 ± 0.22	11.88 ± 0.017	3.08 ± 0.017	33.94 ± 0.06	-13.36 ± 0.16	2.52 ± 0.8	15 ± 0.81	69.61 ± 0.8	52.53 ± 0.8

Test	Ref [g]	$T_{w,in}$ [°C]	$T_{w,out}$ [°C]	$T_{b,in}$ [°C]	$T_{b,out}$ [°C]	$\dot{m}_w$ [kg/ s]	Q_h [kW]	$\dot{E}$ [kW]	COP	P_{cond} [bar]	P_{evap} [bar]	T_{cond} [°C]	T_{evap} [°C]	SC [K]	SH [K]	T_{dis} [°C]	T_{oil} [°C]
11	165 ± 0.75	30 ± 0.14	35 ± 0.15	0 ± 0.14	-3 ± 0.14	0.2 ± 0.002	4.15 ± 0.17	1.21 ± 0.06	3.44 ± 0.22	11.9 ± 0.017	3.09 ± 0.017	34.02 ± 0.06	-13.32 ± 0.16	3.18 ± 0.8	14.99 ± 0.81	69.68 ± 0.8	52.42 ± 0.8
12	115 ± 0.75	30.11 ± 0.14	35.09 ± 0.15	3.24 ± 0.14	0.52 ± 0.14	0.15 ± 0.001	3.08 ± 0.13	1.18 ± 0.06	2.64 ± 0.17	11.63 ± 0.017	3.06 ± 0.017	33.09 ± 0.06	-13.61 ± 0.16	-0.83 ± 0.8	19.91 ± 0.81	77.06 ± 0.8	62.85 ± 0.8
12	120 ± 0.75	29.85 ± 0.14	34.86 ± 0.15	-0.22 ± 0.14	-3.31 ± 0.14	0.16 ± 0.002	3.32 ± 0.14	1.18 ± 0.06	2.84 ± 0.18	11.64 ± 0.017	3.12 ± 0.017	33.1 ± 0.06	-12.99 ± 0.16	-0.69 ± 0.8	13.88 ± 0.81	76.02 ± 0.8	66.59 ± 0.8
12	124.5 ± 0.75	29.75 ± 0.14	34.78 ± 0.15	-0.09 ± 0.14	-3.11 ± 0.14	0.17 ± 0.002	3.52 ± 0.15	1.19 ± 0.06	2.96 ± 0.19	11.63 ± 0.017	3.25 ± 0.017	33.06 ± 0.06	-11.83 ± 0.16	-0.76 ± 0.8	13.3 ± 0.81	73.74 ± 0.8	65.17 ± 0.8
12	135.5 ± 0.75	30.05 ± 0.14	35.08 ± 0.15	-0.04 ± 0.14	-3.07 ± 0.14	0.18 ± 0.002	3.89 ± 0.16	1.21 ± 0.06	3.22 ± 0.21	11.76 ± 0.017	3.38 ± 0.017	33.54 ± 0.06	-10.67 ± 0.15	-0.74 ± 0.8	9.27 ± 0.81	71.35 ± 0.8	64.05 ± 0.8
12	140.5 ± 0.75	29.91 ± 0.14	34.93 ± 0.15	-0.01 ± 0.14	-3.04 ± 0.14	0.2 ± 0.002	4.15 ± 0.17	1.2 ± 0.06	3.45 ± 0.22	11.76 ± 0.017	3.32 ± 0.017	33.54 ± 0.06	-11.18 ± 0.15	-0.61 ± 0.8	9.74 ± 0.81	72.35 ± 0.8	65.07 ± 0.8
12	145 ± 0.75	29.91 ± 0.14	34.95 ± 0.15	0.01 ± 0.14	-3.02 ± 0.14	0.2 ± 0.002	4.23 ± 0.18	1.21 ± 0.06	3.5 ± 0.23	11.8 ± 0.017	3.29 ± 0.017	33.67 ± 0.06	-11.48 ± 0.15	-0.29 ± 0.8	9.66 ± 0.81	69.86 ± 0.8	60.21 ± 0.8
12	156 ± 0.75	29.98 ± 0.14	34.98 ± 0.15	0.01 ± 0.14	-2.99 ± 0.14	0.21 ± 0.002	4.47 ± 0.19	1.21 ± 0.06	3.69 ± 0.24	11.83 ± 0.017	3.31 ± 0.017	33.8 ± 0.06	-11.31 ± 0.15	0.13 ± 0.8	9.98 ± 0.81	73.24 ± 0.8	66.11 ± 0.8

Test	Ref [g]	$T_{w,in}$ [°C]	$T_{w,out}$ [°C]	$T_{b,in}$ [°C]	$T_{b,out}$ [°C]	$\dot{m}_w$ [kg/ s]	Q_h [kW]	$\dot{E}$ [kW]	COP	P_{cond} [bar]	P_{evap} [bar]	T_{cond} [°C]	T_{evap} [°C]	SC [K]	SH [K]	T_{dis} [°C]	T_{oil} [°C]
12	161 ± 0.75	29.97 ± 0.14	34.97 ± 0.15	0 ± 0.14	-3 ± 0.14	0.21 ± 0.002	4.42 ± 0.19	1.21 ± 0.06	3.66 ± 0.24	11.84 ± 0.017	3.23 ± 0.017	33.81 ± 0.06	-12.03 ± 0.15	1.56 ± 0.8	9.93 ± 0.81	73.77 ± 0.8	66.41 ± 0.8
12	165 ± 0.75	30.03 ± 0.14	35.03 ± 0.15	-0.01 ± 0.14	-3 ± 0.14	0.21 ± 0.002	4.44 ± 0.19	1.21 ± 0.06	3.66 ± 0.24	11.86 ± 0.017	3.22 ± 0.017	33.9 ± 0.06	-12.06 ± 0.15	2.56 ± 0.8	10 ± 0.81	74.06 ± 0.8	66.49 ± 0.8
12	170 ± 0.75	30.05 ± 0.14	35.06 ± 0.15	0.01 ± 0.14	-2.99 ± 0.14	0.21 ± 0.002	4.45 ± 0.19	1.21 ± 0.06	3.66 ± 0.24	11.91 ± 0.017	3.22 ± 0.017	34.07 ± 0.06	-12.09 ± 0.15	3.5 ± 0.8	9.95 ± 0.81	74.07 ± 0.8	66.87 ± 0.8
13	122 ± 0.75	30.03 ± 0.14	34.89 ± 0.15	6.76 ± 0.14	3.88 ± 0.14	0.15 ± 0.002	3.13 ± 0.13	1.19 ± 0.06	2.65 ± 0.17	11.68 ± 0.017	3.12 ± 0.017	33.26 ± 0.06	-13.01 ± 0.16	-0.43 ± 0.8	21.44 ± 0.81	71.61 ± 0.8	52.12 ± 0.8
13	130 ± 0.75	29.9 ± 0.14	34.94 ± 0.15	7.11 ± 0.14	4.03 ± 0.14	0.19 ± 0.002	4.01 ± 0.17	1.21 ± 0.06	3.3 ± 0.21	11.8 ± 0.017	3.62 ± 0.017	33.67 ± 0.06	-8.57 ± 0.14	-0.3 ± 0.8	16.73 ± 0.81	69.36 ± 0.8	53.56 ± 0.8
13	140 ± 0.75	30.09 ± 0.14	35.08 ± 0.15	7.05 ± 0.14	4.04 ± 0.14	0.2 ± 0.002	4.29 ± 0.18	1.23 ± 0.06	3.5 ± 0.22	11.89 ± 0.017	3.84 ± 0.017	34 ± 0.06	-6.77 ± 0.13	-0.27 ± 0.8	14.65 ± 0.81	65.81 ± 0.8	50.68 ± 0.8
13	150 ± 0.75	30.03 ± 0.14	35.06 ± 0.15	7.02 ± 0.14	3.99 ± 0.14	0.22 ± 0.002	4.6 ± 19	1.23 ± 0.06	3.74 ± 0.24	11.94 ± 0.017	4.05 ± 0.017	34.19 ± 0.06	-5.08 ± 0.13	-0.18 ± 0.8	11.68 ± 0.81	62.65 ± 0.8	48.54 ± 0.8
13	159.5 ± 0.75	30 ± 0.14	35.01 ± 0.15	7 ± 0.14	3.99 ± 0.14	0.23 ± 0.002	4.75 ± 0.2	1.24 ± 0.06	3.84 ± 0.25	11.98 ± 0.017	4.12 ± 0.017	34.32 ± 0.06	-4.56 ± 0.13	-0.09 ± 0.8	9.72 ± 0.81	59.53 ± 0.8	46.51 ± 0.8

Test	Ref [g]	$T_{w,in}$ [°C]	$T_{w,out}$ [°C]	$T_{b,in}$ [°C]	$T_{b,out}$ [°C]	$\dot{m}_w$ [kg/ s]	Q_h [kW]	$\dot{E}$ [kW]	COP	P_{cond} [bar]	P_{evap} [bar]	T_{cond} [°C]	T_{evap} [°C]	SC [K]	SH [K]	T_{dis} [°C]	T_{oil} [°C]
13	165 ± 0.75	30.01 ± 0.14	35.01 ± 0.15	7.01 ± 0.14	4.01 ± 0.14	0.23 ± 0.002	4.89 ± 0.21	1.24 ± 0.06	3.96 ± 0.25	12 ± 0.017	4.06 ± 0.017	34.39 ± 0.06	-5.02 ± 0.13	0.13 ± 0.8	9.95 ± 0.81	60.44 ± 0.8	46.66 ± 0.8
13	170 ± 0.75	29.98 ± 0.14	34.99 ± 0.15	6.99 ± 0.14	3.98 ± 0.14	0.24 ± 0.002	5.07 ± 0.21	1.24 ± 0.06	4.09 ± 0.26	12.03 ± 0.017	4.08 ± 0.017	34.47 ± 0.06	-4.88 ± 0.13	0.51 ± 0.8	9.84 ± 0.81	60.35 ± 0.8	46.79 ± 0.8
13	175 ± 0.75	29.93 ± 0.14	34.94 ± 0.15	7 ± 0.14	3.99 ± 0.14	0.25 ± 0.002	5.16 ± 0.22	1.24 ± 0.06	4.16 ± 0.27	12.03 ± 0.017	4.09 ± 0.017	34.49 ± 0.06	-4.79 ± 0.13	0.86 ± 0.8	9.89 ± 0.81	60.28 ± 0.8	46.75 ± 0.8
13	180 ± 0.75	29.99 ± 0.14	34.99 ± 0.15	7 ± 0.14	3.99 ± 0.14	0.25 ± 0.003	5.28 ± 0.22	1.24 ± 0.06	4.24 ± 0.27	12.07 ± 0.017	4.1 ± 0.017	34.63 ± 0.06	-4.71 ± 0.13	1.46 ± 0.8	9.8 ± 0.81	60.56 ± 0.8	46.84 ± 0.8
13	185 ± 0.75	30 ± 0.14	35 ± 0.15	7 ± 0.14	4 ± 0.14	0.25 ± 0.003	5.28 ± 0.22	1.25 ± 0.06	4.24 ± 0.27	12.09 ± 0.017	4.08 ± 0.017	34.71 ± 0.06	-4.84 ± 0.13	3.36 ± 0.8	9.99 ± 0.81	60.96 ± 0.8	47.11 ± 0.8
13	190 ± 0.75	30 ± 0.14	35 ± 0.15	7 ± 0.14	4 ± 0.14	0.25 ± 0.003	5.31 ± 0.22	1.26 ± 0.06	4.22 ± 0.27	12.25 ± 0.017	4.09 ± 0.017	35.25 ± 0.06	-4.79 ± 0.13	5.08 ± 0.8	10 ± 0.81	61.63 ± 0.8	47.54 ± 0.8
14	170 ± 0.75	29.98 ± 0.14	34.99 ± 0.15	12.7 ± 0.14	9.67 ± 0.14	0.27 ± 0.003	5.71 ± 0.24	1.24 ± 0.06	4.61 ± 0.29	12.15 ± 0.017	4.88 ± 0.017	34.9 ± 0.06	0.95 ± 0.11	0.6 ± 0.8	9.97 ± 0.81	57.85 ± 0.8	45.87 ± 0.8
14	175 ± 0.75	29.97 ± 0.14	34.98 ± 0.15	12.76 ± 0.14	9.75 ± 0.14	0.28 ± 0.003	5.81 ± 0.24	1.24 ± 0.06	4.69 ± 0.3	12.17 ± 0.017	4.94 ± 0.017	34.97 ± 0.06	1.3 ± 0.11	0.72 ± 0.8	9.46 ± 0.81	57.04 ± 0.8	45.18 ± 0.8

Test	Ref [g]	$T_{w,in}$ [°C]	$T_{w,out}$ [°C]	$T_{b,in}$ [°C]	$T_{b,out}$ [°C]	$\dot{m}_w$ [kg/ s]	Q_h [kW]	$\dot{E}$ [kW]	COP	P_{cond} [bar]	P_{evap} [bar]	T_{cond} [°C]	T_{evap} [°C]	SC [K]	SH [K]	T_{dis} [°C]	T_{oil} [°C]
14	180.5 ± 0.75	29.99 ± 0.14	35 ± 0.15	12.65 ± 0.14	9.65 ± 0.14	0.28 ± 0.003	5.96 ± 0.25	1.24 ± 0.06	4.79 ± 0.31	12.21 ± 0.017	4.92 ± 0.017	35.12 ± 0.06	1.22 ± 0.11	1.1 ± 0.8	9.94 ± 0.81	57.11 ± 0.8	45.01 ± 0.8
14	185 ± 0.75	29.98 ± 0.14	35 ± 0.15	12.51 ± 0.14	9.49 ± 0.14	0.29 ± 0.003	6.07 ± 0.25	1.25 ± 0.06	4.87 ± 0.31	12.24 ± 0.017	4.9 ± 0.017	35.21 ± 0.06	1.08 ± 0.11	1.59 ± 0.8	9.83 ± 0.81	57.52 ± 0.8	45.2 ± 0.8
14	190 ± 0.75	29.98 ± 0.14	35 ± 0.15	12.55 ± 0.14	9.54 ± 0.14	0.29 ± 0.003	6.19 ± 0.26	1.25 ± 0.06	4.96 ± 0.32	12.27 ± 0.017	4.94 ± 0.017	35.32 ± 0.06	1.32 ± 0.11	2.09 ± 0.8	10.01 ± 0.81	57.25 ± 0.8	45.19 ± 0.8
14	195 ± 0.75	30 ± 0.14	35 ± 0.15	12.58 ± 0.14	9.58 ± 0.14	0.3 ± 0.003	6.28 ± 0.26	1.25 ± 0.06	5.01 ± 0.32	12.32 ± 0.017	4.91 ± 0.017	35.49 ± 0.06	1.11 ± 0.11	4.23 ± 0.8	9.99 ± 0.81	57.53 ± 0.8	45.42 ± 0.8
14	200 ± 0.75	29.99 ± 0.14	34.99 ± 0.15	12.59 ± 0.14	9.59 ± 0.14	0.3 ± 0.003	6.27 ± 0.26	1.25 ± 0.06	5.01 ± 0.32	12.32 ± 0.017	4.91 ± 0.017	35.48 ± 0.06	1.15 ± 0.11	4.23 ± 0.8	9.99 ± 0.81	57.57 ± 0.8	45.38 ± 0.8
16	115.5 ± 0.75	29.43 ± 0.14	34.43 ± 0.15	12.58 ± 0.14	9.58 ± 0.14	0.16 ± 0.002	3.36 ± 0.14	1.18 ± 0.06	2.86 ± 0.19	11.51 ± 0.017	3.24 ± 0.017	32.66 ± 0.06	-11.94 ± 0.15	-0.61 ± 0.8	25.16 ± 0.81	77.01 ± 0.8	58.88 ± 0.8
16	125 ± 0.75	30.06 ± 0.14	35.1 ± 0.15	11.73 ± 0.14	8.7 ± 0.14	0.18 ± 0.002	3.79 ± 0.16	1.2 ± 0.06	3.16 ± 0.21	11.75 ± 0.017	3.26 ± 0.017	33.52 ± 0.06	-11.68 ± 0.15	-0.57 ± 0.8	23.98 ± 0.81	76.27 ± 0.8	58.44 ± 0.8
16	129.5 ± 0.75	30.02 ± 0.14	35.03 ± 0.15	11.6 ± 0.14	8.59 ± 0.14	0.19 ± 0.002	4.05 ± 0.17	1.2 ± 0.06	3.38 ± 0.22	11.78 ± 0.017	3.29 ± 0.017	33.62 ± 0.06	-11.42 ± 0.15	-0.4 ± 0.8	23.75 ± 0.81	76.21 ± 0.8	58.47 ± 0.8

Test	Ref [g]	$T_{w,in}$ [°C]	$T_{w,out}$ [°C]	$T_{b,in}$ [°C]	$T_{b,out}$ [°C]	$\dot{m}_w$ [kg/s]	Q_h [kW]	$\dot{E}$ [kW]	COP	P_{cond} [bar]	P_{evap} [bar]	T_{cond} [°C]	T_{evap} [°C]	SC [K]	SH [K]	T_{dis} [°C]	T_{oil} [°C]
16	135 ± 0.75	29.98 ± 0.14	34.98 ± 0.15	11.22 ± 0.14	8.21 ± 0.14	0.2 ± 0.002	4.19 ± 0.18	1.2 ± 0.06	3.49 ± 0.23	11.8 ± 0.017	3.24 ± 0.017	33.69 ± 0.06	-11.92 ± 0.15	0.13 ± 0.8	23.87 ± 0.81	76.77 ± 0.8	58.75 ± 0.8
16	139.5 ± 0.75	29.97 ± 0.14	34.98 ± 0.15	11.28 ± 0.14	8.27 ± 0.14	0.2 ± 0.002	4.29 ± 0.18	1.2 ± 0.06	3.57 ± 0.23	11.81 ± 0.017	3.25 ± 0.017	33.71 ± 0.06	-11.84 ± 0.15	0.24 ± 0.8	23.9 ± 0.81	76.99 ± 0.8	58.89 ± 0.8
16	145.5 ± 0.75	30.02 ± 0.14	35.02 ± 0.15	11.29 ± 0.14	8.29 ± 0.14	0.21 ± 0.002	4.35 ± 0.18	1.2 ± 0.06	3.62 ± 0.24	11.83 ± 0.017	3.23 ± 0.017	33.79 ± 0.06	-11.96 ± 0.15	0.8 ± 0.8	24 ± 0.81	77.03 ± 0.8	58.95 ± 0.8
16	150.5 ± 0.75	30 ± 0.14	35 ± 0.15	11.14 ± 0.14	8.14 ± 0.14	0.21 ± 0.002	4.34 ± 0.18	1.2 ± 0.06	3.6 ± 0.23	11.84 ± 0.017	3.22 ± 0.017	33.82 ± 0.06	-12.08 ± 0.15	2.46 ± 0.8	23.99 ± 0.81	77.31 ± 0.8	59.13 ± 0.8
16	155.5 ± 0.75	30.01 ± 0.14	35.01 ± 0.15	11.17 ± 0.14	8.17 ± 0.14	0.21 ± 0.002	4.36 ± 0.18	1.21 ± 0.06	3.62 ± 0.24	11.87 ± 0.017	3.22 ± 0.017	33.92 ± 0.06	-12.05 ± 0.15	3.41 ± 0.8	23.99 ± 0.81	77.4 ± 0.8	59.18 ± 0.8
16	160 ± 0.75	30.02 ± 0.14	35.02 ± 0.15	11.21 ± 0.14	8.2 ± 0.14	0.21 ± 0.002	4.35 ± 0.18	1.21 ± 0.06	3.6 ± 0.23	11.91 ± 0.017	3.23 ± 0.017	34.08 ± 0.06	-12.01 ± 0.15	3.82 ± 0.8	23.99 ± 0.81	77.56 ± 0.8	59.26 ± 0.8

Table 19: Performance result of refrigerant charge determination of prototype 2.

Test	Ref [g]	$T_{w,in}$ [°C]	$T_{w,out}$ [°C]	$T_{b,in}$ [°C]	$T_{b,out}$ [°C]	$\dot{m}_w$ [kg/ s]	Q_h [kW]	$\dot{E}$ [kW]	COP	P_{cond} [bar]	P_{evap} [bar]	T_{cond} [°C]	T_{evap} [°C]	SC [K]	SH [K]	T_{dis} [°C]	T_{oil} [°C]
1	195.5 ± 0.75	29.85 ± 0.14	34.85 ± 0.15	0.26 ± 0.14	-2.74 ± 0.14	0.22 ± 0.002	4.51 ± 0.19	1.21 ± 0.06	3.73 ± 0.24	11.81 ± 0.02	3.57 ± 0.02	33.71 ± 0.06	-8.99 ± 0.14	0.69 ± 0.8	10.05 ± 0.81	62.53 ± 0.8	48.84 ± 0.8
1	200 ± 0.75	30 ± 0.14	35.01 ± 0.15	0.26 ± 0.14	-2.74 ± 0.14	0.22 ± 0.002	4.62 ± 0.19	1.21 ± 0.06	3.8 ± 0.25	11.87 ± 0.02	3.57 ± 0.02	33.93 ± 0.06	-9.01 ± 0.14	2.93 ± 0.8	10.09 ± 0.81	62.91 ± 0.8	48.3 ± 0.8
1	196 ± 0.75	30.22 ± 0.14	34.48 ± 0.15	0.3 ± 0.14	-2.83 ± 0.14	0.26 ± 0.003	4.64 ± 0.23	1.21 ± 0.06	3.84 ± 0.27	11.8 ± 0.02	3.59 ± 0.02	33.68 ± 0.06	-8.83 ± 0.14	0.01 ± 0.8	9.53 ± 0.81	63.46 ± 0.8	48.27 ± 0.8
1	196.5 ± 0.75	30.16 ± 0.14	35.17 ± 0.15	0.38 ± 0.14	-2.63 ± 0.14	0.21 ± 0.002	4.48 ± 0.19	1.22 ± 0.06	3.66 ± 0.24	11.98 ± 0.02	3.54 ± 0.02	34.32 ± 0.06	-9.27 ± 0.14	1.86 ± 0.8	9.98 ± 0.81	64.18 ± 0.8	47.16 ± 0.8
2	196 ± 0.75	28.54 ± 0.14	34.84 ± 0.15	-0.02 ± 0.14	-3.76 ± 0.14	0.36 ± 0.004	9.49 ± 0.32	2.96 ± 0.06	3.2 ± 0.13	12.31 ± 0.02	3.21 ± 0.02	35.44 ± 0.06	-12.22 ± 0.15	3.76 ± 0.8	9.96 ± 0.81	72.29 ± 0.8	55.86 ± 0.8
2	195 ± 0.75	28.61 ± 0.14	34.97 ± 0.15	-0.04 ± 0.14	-3.84 ± 0.14	0.36 ± 0.004	9.55 ± 0.32	2.93 ± 0.06	3.26 ± 0.13	12.37 ± 0.02	3.18 ± 0.02	35.67 ± 0.06	-12.5 ± 0.15	4.45 ± 0.8	10.02 ± 0.81	72.8 ± 0.8	61.7 ± 0.8
3	195 ± 0.75	28.25 ± 0.14	34.03 ± 0.15	0.01 ± 0.14	-3.47 ± 0.14	0.36 ± 0.004	8.69 ± 0.32	2.54 ± 0.06	3.42 ± 0.15	12.15 ± 0.02	3.39 ± 0.02	34.89 ± 0.06	-10.56 ± 0.15	5.13 ± 0.8	10.01 ± 0.81	69.98 ± 0.8	50.1 ± 0.8
3	195 ± 0.75	28.32 ± 0.14	34.01 ± 0.15	0.06 ± 0.14	-3.42 ± 0.14	0.36 ± 0.004	8.55 ± 0.32	2.52 ± 0.06	3.4 ± 0.15	11.99 ± 0.02	3.34 ± 0.02	34.33 ± 0.06	-10.99 ± 0.15	1.91 ± 0.8	10.02 ± 0.81	69.87 ± 0.8	50.66 ± 0.8

Test	Ref [g]	$T_{w,in}$ [°C]	$T_{w,out}$ [°C]	$T_{b,in}$ [°C]	$T_{b,out}$ [°C]	$\dot{m}_w$ [kg/ s]	Q_h [kW]	$\dot{E}$ [kW]	COP	P_{cond} [bar]	P_{evap} [bar]	T_{cond} [°C]	T_{evap} [°C]	SC [K]	SH [K]	T_{dis} [°C]	T_{oil} [°C]
4	198 ± 0.75	27.03 ± 0.14	32.02 ± 0.15	0.16 ± 0.14	-3 ± 0.14	0.35 ± 0.004	7.32 ± 0.31	1.93 ± 0.06	3.8 ± 0.2	11.49 ± 0.02	3.45 ± 0.02	32.58 ± 0.06	-10.05 ± 0.14	4.04 ± 0.8	10 ± 0.81	63.84 ± 0.8	52.62 ± 0.8
5	195.5 ± 0.75	26.27 ± 0.14	29.99 ± 0.15	-0.02 ± 0.14	-3.02 ± 0.14	0.37 ± 0.004	5.7 ± 0.32	1.45 ± 0.06	3.92 ± 0.27	10.89 ± 0.02	3.46 ± 0.02	30.37 ± 0.06	-9.9 ± 0.14	4.64 ± 0.8	9.99 ± 0.81	60.94 ± 0.8	44.77 ± 0.8
5	195.5 ± 0.75	26.25 ± 0.14	29.98 ± 0.15	0.07 ± 0.14	-2.91 ± 0.14	0.37 ± 0.004	5.71 ± 0.32	1.45 ± 0.06	3.93 ± 0.27	10.92 ± 0.02	3.48 ± 0.02	30.49 ± 0.06	-9.76 ± 0.14	4.38 ± 0.8	9.99 ± 0.81	61.17 ± 0.8	44.05 ± 0.8
5	195.5 ± 0.75	25.05 ± 0.14	30.04 ± 0.15	0.03 ± 0.14	-2.96 ± 0.14	0.28 ± 0.003	5.8 ± 0.25	1.44 ± 0.06	4.02 ± 0.24	10.79 ± 0.02	3.48 ± 0.02	29.99 ± 0.06	-9.79 ± 0.14	4.99 ± 0.8	9.99 ± 0.81	60.22 ± 0.8	44.62 ± 0.8
6	195.5 ± 0.75	23.99 ± 0.14	28.97 ± 0.15	0.17 ± 0.14	-2.82 ± 0.14	0.23 ± 0.002	4.75 ± 0.2	1.1 ± 0.06	4.32 ± 0.3	10.42 ± 0.02	3.5 ± 0.02	28.6 ± 0.06	-9.56 ± 0.14	3.59 ± 0.8	9.99 ± 0.81	55.23 ± 0.8	45.18 ± 0.8
7	195 ± 0.75	21.82 ± 0.14	26.85 ± 0.15	2.13 ± 0.14	-1 ± 0.14	0.16 ± 0.002	3.3 ± 0.14	0.69 ± 0.06	4.76 ± 0.46	9.8 ± 0.02	3.81 ± 0.02	26.15 ± 0.07	-6.99 ± 0.13	1.26 ± 0.8	10.23 ± 0.81	47.45 ± 0.8	37.31 ± 0.8
7	197.5 ± 0.75	21.79 ± 0.14	26.79 ± 0.15	0.43 ± 0.14	-2.57 ± 0.14	0.16 ± 0.002	3.27 ± 0.14	0.67 ± 0.06	4.88 ± 0.48	9.77 ± 0.02	3.67 ± 0.02	26.04 ± 0.07	-8.16 ± 0.14	2.09 ± 0.8	10 ± 0.81	49.39 ± 0.8	28.82 ± 0.8
8	195 ± 0.75	21.19 ± 0.14	24.12 ± 0.15	0.05 ± 0.14	-2.48 ± 0.14	0.13 ± 0.001	1.57 ± 0.11	0.32 ± 0.06	4.96 ± 1.01	9.19 ± 0.02	3.75 ± 0.02	23.63 ± 0.07	-7.5 ± 0.14	0.12 ± 0.8	10 ± 0.81	45.46 ± 0.8	36.32 ± 0.8

Test	Ref [g]	$T_{w,in}$ [°C]	$T_{w,out}$ [°C]	$T_{b,in}$ [°C]	$T_{b,out}$ [°C]	$\dot{m}_w$ [kg/ s]	Q_h [kW]	$\dot{E}$ [kW]	COP	P_{cond} [bar]	P_{evap} [bar]	T_{cond} [°C]	T_{evap} [°C]	SC [K]	SH [K]	T_{dis} [°C]	T_{oil} [°C]
9	254 ± 0.75	29.31 ± 0.14	34.31 ± 0.15	0.41 ± 0.14	-2.58 ± 0.14	0.22 ± 0.002	4.67 ± 0.2	1.25 ± 0.06	3.74 ± 0.24	12.35 ± 0.02	3.55 ± 0.02	35.58 ± 0.06	-9.13 ± 0.14	6.73 ± 0.8	10 ± 0.81	64.76 ± 0.8	48.37 ± 0.8
10	220 ± 0.75	29.99 ± 0.14	34.99 ± 0.15	0 ± 0.14	-2.99 ± 0.14	0.24 ± 0.002	4.91 ± 0.21	1.24 ± 0.06	3.97 ± 0.25	12.07 ± 0.02	3.84 ± 0.02	34.64 ± 0.06	-6.75 ± 0.13	0.88 ± 0.8	5 ± 0.81	56.41 ± 0.8	48.15 ± 0.8
11	160 ± 0.75	29.98 ± 0.14	34.98 ± 0.15	0.01 ± 0.14	-3 ± 0.14	0.19 ± 0.002	4.03 ± 0.17	1.21 ± 0.06	3.35 ± 0.22	11.92 ± 0.02	3.02 ± 0.02	34.09 ± 0.06	-14.03 ± 0.16	2.12 ± 0.8	15 ± 0.81	70.62 ± 0.8	58.24 ± 0.8
12	190 ± 0.75	29.98 ± 0.14	34.98 ± 0.15	0.02 ± 0.14	-2.98 ± 0.14	0.22 ± 0.002	4.69 ± 0.2	1.22 ± 0.06	3.83 ± 0.25	11.97 ± 0.02	3.49 ± 0.02	34.26 ± 0.06	-9.64 ± 0.14	3.08 ± 0.8	10 ± 0.81	66.87 ± 0.8	65.33 ± 0.8
12	185 ± 0.75	29.98 ± 0.14	34.98 ± 0.15	-0.02 ± 0.14	-3.03 ± 0.14	0.23 ± 0.002	4.77 ± 0.2	1.24 ± 0.06	3.85 ± 0.25	12.06 ± 0.02	3.5 ± 0.02	34.6 ± 0.06	-9.59 ± 0.14	3.36 ± 0.8	10 ± 0.81	71.36 ± 0.8	72.87 ± 0.8
12	180 ± 0.75	29.99 ± 0.14	34.99 ± 0.15	0.01 ± 0.14	-2.99 ± 0.14	0.23 ± 0.002	4.76 ± 0.2	1.23 ± 0.06	3.87 ± 0.25	12.01 ± 0.02	3.51 ± 0.02	34.41 ± 0.06	-9.51 ± 0.14	1.53 ± 0.8	10.01 ± 0.81	70.93 ± 0.8	73.28 ± 0.8
13	195 ± 0.75	29.99 ± 0.14	34.98 ± 0.15	7.11 ± 0.14	4.12 ± 0.14	0.26 ± 0.003	5.43 ± 0.23	1.23 ± 0.06	4.4 ± 0.29	12.06 ± 0.02	4.29 ± 0.02	34.58 ± 0.06	-3.23 ± 0.12	0.65 ± 0.8	10.01 ± 0.81	59.79 ± 0.8	50.63 ± 0.8
14	196 ± 0.75	30.01 ± 0.14	35 ± 0.15	13.47 ± 0.14	10.46 ± 0.14	0.29 ± 0.003	6.1 ± 0.26	1.21 ± 0.06	5.02 ± 0.33	12.08 ± 0.02	5.13 ± 0.02	34.65 ± 0.06	2.57 ± 0.11	0.01 ± 0.8	9.98 ± 0.81	56.81 ± 0.8	49.09 ± 0.8

Test	Ref [g]	$T_{w,in}$ [°C]	$T_{w,out}$ [°C]	$T_{b,in}$ [°C]	$T_{b,out}$ [°C]	$\dot{m}_w$ [kg/s]	Q_h [kW]	$\dot{E}$ [kW]	COP	P_{cond} [bar]	P_{evap} [bar]	T_{cond} [°C]	T_{evap} [°C]	SC [K]	SH [K]	T_{dis} [°C]	T_{oil} [°C]
15	196 ± 0.75	49.78 ± 0.14	54.78 ± 0.15	-0.04 ± 0.14	-3.05 ± 0.14	0.2 ± 0.002	4.17 ± 0.18	1.69 ± 0.06	2.47 ± 0.14	18.51 ± 0.02	3.53 ± 0.02	53.58 ± 0.04	-9.37 ± 0.14	2.72 ± 0.8	10 ± 0.81	90.84 ± 0.8	78.1 ± 0.8

Table 20: Performance result of tests of prototype 1.

Test	Ref [g]	$T_{w,in}$ [°C]	$T_{w,out}$ [°C]	$T_{b,in}$ [°C]	$T_{b,out}$ [°C]	$\dot{m}_w$ [kg/s]	Q_h [kW]	$\dot{E}$ [kW]	COP	P_{cond} [bar]	P_{evap} [bar]	T_{cond} [°C]	T_{evap} [°C]	SC [K]	SH [K]	T_{dis} [°C]	T_{oil} [°C]
1	170 ± 0.75	30.13 ± 0.14	35.13 ± 0.15	0.26 ± 0.14	-3.01 ± 0.14	0.21 ± 0.002	4.28 ± 0.18	1.22 ± 0.06	3.53 ± 0.23	11.94 ± 0.02	3.24 ± 0.02	34.18 ± 0.06	-11.93 ± 0.15	0.73 ± 0.8	11.92 ± 0.81	63.67 ± 0.8	48.94 ± 0.8
2	170 ± 0.75	29.53 ± 0.14	34.98 ± 0.15	-0.34 ± 0.14	-3.36 ± 0.14	0.36 ± 0.004	8.15 ± 0.32	2.84 ± 0.06	2.87 ± 0.13	12.35 ± 0.02	2.67 ± 0.02	35.58 ± 0.06	-17.49 ± 0.18	5.11 ± 0.8	10.04 ± 0.82	77.94 ± 0.8	59.1 ± 0.8
3	170 ± 0.75	28.92 ± 0.14	33.93 ± 0.15	0.04 ± 0.14	-2.97 ± 0.14	0.36 ± 0.004	7.44 ± 0.31	2.46 ± 0.06	3.03 ± 0.15	11.89 ± 0.02	2.79 ± 0.02	34.01 ± 0.06	-16.27 ± 0.17	3.19 ± 0.8	10.01 ± 0.82	72.32 ± 0.8	54.58 ± 0.8
5	169.5 ± 0.75	25 ± 0.14	30.02 ± 0.15	0 ± 0.14	-3 ± 0.14	0.26 ± 0.003	5.43 ± 0.23	1.45 ± 0.06	3.75 ± 0.22	10.87 ± 0.02	3.2 ± 0.02	30.31 ± 0.06	-12.24 ± 0.15	4.21 ± 0.8	9.81 ± 0.81	61.48 ± 0.8	46.11 ± 0.8
7	169.5 ± 0.75	22 ± 0.14	27 ± 0.15	-0.02 ± 0.14	-3.02 ± 0.14	0.15 ± 0.002	3.14 ± 0.13	0.68 ± 0.06	4.62 ± 0.45	9.89 ± 0.02	3.65 ± 0.02	26.48 ± 0.07	-8.31 ± 0.14	1.91 ± 0.8	10.01 ± 0.81	50.56 ± 0.8	39.1 ± 0.8

Test	Ref [g]	$T_{w,in}$ [°C]	$T_{w,out}$ [°C]	$T_{b,in}$ [°C]	$T_{b,out}$ [°C]	$\dot{m}_w$ [kg/s]	Q_h [kW]	$\dot{E}$ [kW]	COP	P_{cond} [bar]	P_{evap} [bar]	T_{cond} [°C]	T_{evap} [°C]	SC [K]	SH [K]	T_{dis} [°C]	T_{oil} [°C]
8	170 ± 0.75	21.18 ± 0.14	24.17 ± 0.15	0.03 ± 0.14	-2.17 ± 0.14	0.13 ± 0.001	1.57 ± 0.11	0.31 ± 0.06	5 ± 1.05	9.13 ± 0.02	3.86 ± 0.02	23.37 ± 0.07	-6.58 ± 0.13	0.18 ± 0.8	10.06 ± 0.81	44.07 ± 0.8	34.83 ± 0.8
9	221 ± 0.75	30.11 ± 0.14	35.1 ± 0.15	0 ± 0.14	-3 ± 0.14	0.21 ± 0.002	4.42 ± 0.19	1.28 ± 0.06	3.44 ± 0.22	12.84 ± 0.02	3.27 ± 0.02	37.23 ± 0.05	-11.6 ± 0.15	6.91 ± 0.8	10.04 ± 0.81	66.84 ± 0.8	51.04 ± 0.8
9	186.5 ± 0.75	30.01 ± 0.14	35.01 ± 0.15	0.02 ± 0.14	-2.97 ± 0.14	0.21 ± 0.002	4.34 ± 0.18	1.22 ± 0.06	3.55 ± 0.23	12.02 ± 0.02	3.23 ± 0.02	34.43 ± 0.06	-12.04 ± 0.15	4.25 ± 0.8	9.95 ± 0.81	65.22 ± 0.8	50.3 ± 0.8
9	196.5 ± 0.75	29.98 ± 0.14	34.98 ± 0.15	-0.01 ± 0.14	-3.01 ± 0.14	0.21 ± 0.002	4.37 ± 0.18	1.28 ± 0.06	3.41 ± 0.22	12.74 ± 0.02	3.34 ± 0.02	36.9 ± 0.06	-11.02 ± 0.15	6.74 ± 0.8	10 ± 0.81	67.86 ± 0.8	51.25 ± 0.8
10	189 ± 0.75	30.08 ± 0.14	35.08 ± 0.15	-0.03 ± 0.14	-3.03 ± 0.14	0.21 ± 0.002	4.36 ± 0.18	1.22 ± 0.06	3.56 ± 0.23	11.99 ± 0.02	3.28 ± 0.02	34.35 ± 0.06	-11.51 ± 0.15	1.89 ± 0.8	5.04 ± 0.81	59.91 ± 0.8	46.31 ± 0.8
11	162 ± 0.75	29.91 ± 0.14	34.91 ± 0.15	-0.09 ± 0.14	-3.1 ± 0.14	0.2 ± 0.002	4.18 ± 0.18	1.21 ± 0.06	3.46 ± 0.22	11.87 ± 0.02	3.1 ± 0.02	33.93 ± 0.06	-13.23 ± 0.16	2.23 ± 0.8	15 ± 0.82	70.17 ± 0.8	53.07 ± 0.8
12	158 ± 0.75	30.11 ± 0.14	35.11 ± 0.15	0.02 ± 0.14	-2.97 ± 0.14	0.22 ± 0.002	4.52 ± 0.19	1.22 ± 0.06	3.7 ± 0.24	12.01 ± 0.02	3.28 ± 0.02	34.41 ± 0.06	-11.51 ± 0.15	2.73 ± 0.8	10.42 ± 0.81	75.21 ± 0.8	67.79 ± 0.8
13	184.5 ± 0.75	30 ± 0.14	35 ± 0.15	4.03 ± 0.14	7.03 ± 0.14	0.26 ± 0.003	5.38 ± 0.23	1.26 ± 0.06	4.29 ± 0.27	12.2 ± 0.02	4.15 ± 0.02	35.06 ± 0.06	-4.32 ± 0.13	3.03 ± 0.8	10.02 ± 0.81	60.32 ± 0.8	46.63 ± 0.8

Test	Ref [g]	$T_{w,in}$ [°C]	$T_{w,out}$ [°C]	$T_{b,in}$ [°C]	$T_{b,out}$ [°C]	$\dot{m}_w$ [kg/s]	Q_h [kW]	$\dot{E}$ [kW]	COP	P_{cond} [bar]	P_{evap} [bar]	T_{cond} [°C]	T_{evap} [°C]	SC [K]	SH [K]	T_{dis} [°C]	T_{oil} [°C]
14	200 ± 0.75	30 ± 0.14	34.99 ± 0.15	12.53 ± 0.14	9.53 ± 0.14	0.3 ± 0.003	6.27 ± 0.27	1.25 ± 0.06	5.01 ± 0.32	12.32 ± 0.02	4.9 ± 0.02	35.48 ± 0.06	1.08 ± 0.11	4.2 ± 0.8	9.99 ± 0.81	57.48 ± 0.8	45.35 ± 0.8
16	152 ± 0.75	30 ± 0.14	35 ± 0.15	11.96 ± 0.14	8.96 ± 0.14	0.22 ± 0.002	4.51 ± 0.19	1.22 ± 0.06	3.71 ± 0.24	11.95 ± 0.02	3.32 ± 0.02	34.2 ± 0.06	-11.17 ± 0.15	3.65 ± 0.8	23.98 ± 0.81	77.02 ± 0.8	58.99 ± 0.8
16	150.5 ± 0.75	29.97 ± 0.14	34.97 ± 0.15	11.13 ± 0.14	8.14 ± 0.14	0.21 ± 0.002	4.35 ± 0.18	1.2 ± 0.06	3.62 ± 0.24	11.84 ± 0.02	3.21 ± 0.02	33.82 ± 0.06	-12.15 ± 0.15	3.17 ± 0.8	23.98 ± 0.81	77.12 ± 0.8	58.74 ± 0.8

Table 21: Performance result of tests of prototype 2.

Appendix E: Mass distribution results

This appendix presents the results of refrigerant distribution in the different sections during the tests. This refrigerant was extracted from each section after running steadily for at least 35 minutes. After the recording time, the quick closing valves were closed, isolating the sections from one another, and the refrigerant was extracted and weighed.

The tables present the data of the refrigerant inserted before starting the test, with a prior evacuation, the refrigerant extracted data from each section, and the total refrigerant extracted.

The refrigerant measured from each section also considers the remaining refrigerant in gas phase still present in the section.

The measured variables' uncertainty is calculated considering the systematic and random uncertainty of the measure. And for the calculated variables, the error propagation method was employed.

With the data of each section in each test, the refrigerant inside the component has been calculated by subtracting the refrigerant inside the pipes. This result is not present in this appendix, but it has been presented in the work in section 3.3. The refrigerant inside the pipe is calculated knowing the internal volume (35), as a cylinder using the inner diameter, and the density (36).

$$m = V \cdot \rho \tag{35}$$

$$V = \pi \cdot \frac{\phi^2}{4} \cdot L \tag{36}$$

For the two-phase flow, the density has been calculated using the void fraction σ, calculated using the Chisholm correlation

$$\sigma = \frac{1}{1 + \frac{1 - x_{in}}{x_{in}} \frac{\rho_{vap}}{\rho_{liq}} S} \tag{37}$$

$$S = \sqrt{1 - x_{in}\left(1 - \left(\frac{\rho_{liq}}{\rho_{vap}}\right)\right)} \tag{38}$$

$$dm = \left(\rho_{vap}\alpha + \rho_{liq}\,(1 - \alpha)\right) A\, dL \tag{39}$$

Test	Ref_{ins} [g]	Ref_{ext} [g]	Ref_{comp} [g]	Ref_{cond} [g]	Ref_{evap} [g]	Ref_{valves} [g]
1	195.5 ± 1.8	195 ± 0.3	83.65 ± 0.19	51.64 ± 0.17	56.89 ± 0.16	2.85 ± 0.16
1	200 ± 1.8	190.1 ± 0.47	72.25 ± 0.4	52.82 ± 0.17	62.22 ± 0.17	2.84 ± 0.17
1	196 ± 1.8	196.8 ± 0.31	81.67 ± 0.2	52.61 ± 0.18	61.18 ± 0.16	1.38 ± 0.17
1	196.5 ± 1.8	197.8 ± 0.31	87.59 ± 0.2	49.12 ± 0.17	58.46 ± 0.16	2.69 ± 0.16
2	196 ± 1.8	194.9 ± 0.33	81.12 ± 0.22	57.02 ± 0.17	54.72 ± 0.17	2.03 ± 0.17
2	195 ± 1.8	196.1 ± 0.37	75.64 ± 0.18	64.52 ± 0.27	55.95 ± 0.18	0 ± 0.26
3	195 ± 1.8	194.3 ± 0.28	75.64 ± 0.17	57.16 ± 0.16	58.28 ± 0.16	3.24 ± 0.15
3	195 ± 1.8	193.6 ± 0.29	79.32 ± 0.17	51.05 ± 0.16	60.89 ± 0.17	2.34 ± 0.16
4	198 ± 1.8	197.2 ± 0.32	71.43 ± 0.17	61.28 ± 0.21	61.98 ± 0.17	2.52 ± 0.2
5	195.5 ± 1.8	193 ± 0.31	75.19 ± 0.17	63.41 ± 0.18	52.6 ± 0.18	1.77 ± 0.18
5	195.5 ± 1.8	192.9 ± 0.29	73.4 ± 0.19	63.06 ± 0.16	52.76 ± 0.16	3.65 ± 0.15
5	195.5 ± 1.8	194.8 ± 0.32	77.05 ± 0.18	60.9 ± 0.21	55.12 ± 0.16	1.75 ± 0.19
6	195.5 ± 1.8	194.7 ± 0.3	75.64 ± 0.17	60.05 ± 0.16	56.31 ± 0.18	2.72 ± 0.17
7	195 ± 1.8	193.7 ± 0.29	74.34 ± 0.17	54.44 ± 0.17	61.68 ± 0.17	3.26 ± 0.16
7	197.5 ± 1.8	187.8 ± 0.38	75.82 ± 0.2	48.76 ± 0.23	62.84 ± 0.24	0.37 ± 0.26
8	195 ± 1.8	192.4 ± 0.31	75.35 ± 0.2	52.62 ± 0.18	62.08 ± 0.17	2.38 ± 0.17
9	254 ± 1.8	253.3 ± 0.31	84.4 ± 0.19	103.1 ± 0.18	63.09 ± 0.17	2.67 ± 0.17
10	220 ± 1.8	218.2 ± 0.28	85.42 ± 0.17	52.84 ± 0.17	76.17 ± 0.16	3.77 ± 0.16

11	160 ± 1.8	163.2 ± 0.3	64.87 ± 0.19	56.84 ± 0.17	39.74 ± 0.17	1.8 ± 0.17
Test	Ref_{ins} [g]	Ref_{ext} [g]	Ref_{comp} [g]	Ref_{cond} [g]	Ref_{evap} [g]	Ref_{valves} [g]
12	190 ± 1.8	187.45 ± 0.31	72.47 ± 0.17	60.1 ± 0.19	52.75 ± 0.18	2.13 ± 0.18
12	185 ± 1.8	183.6 ± 0.36	66.21 ± 0.18	61.2 ± 0.27	53.03 ± 0.16	3.15 ± 0.25
12	180 ± 1.8	180 ± 0.3	66.39 ± 0.19	56.26 ± 0.16	57.32 ± 0.16	2.59 ± 0.16
13	195 ± 1.8	193.8 ± 0.31	88.64 ± 0.18	51.11 ± 0.18	51.95 ± 0.18	2.11 ± 0.18
14	196 ± 1.8	197.8 ± 0.28	95.27 ± 0.17	49.17 ± 0.15	51.97 ± 0.16	1.43 ± 0.15
15	196 ± 1.8	196.3 ± 0.3	89.04 ± 0.19	60.53 ± 0.17	46.72 ± 0.16	2.73 ± 0.16

Table 22: Results of refrigerant distribution of test with prototype 1.

Test	Ref_{ins} [g]	Ref_{ext} [g]	Ref_{comp} [g]	Ref_{cond} [g]	Ref_{evap} [g]	Ref_{valves} [g]
1	170 ± 1.8	172.5 ± 0.3	83 ± 0.18	54.71 ± 0.18	32.76 ± 0.15	2.26 ± 0.17
2	170 ± 1.8	168.7 ± 0.29	70.97 ± 0.17	64.42 ± 0.17	30.83 ± 0.16	2.48 ± 0.16
3	170 ± 1.8	169 ± 0.33	76.07 ± 0.21	63.01 ± 0.18	27.78 ± 0.18	2.15 ± 0.18
5	169.5 ± 1.8	170.6 ± 0.34	80.16 ± 0.2	57.97 ± 0.21	32.49 ± 0.17	1.97 ± 0.2
7	169.5 ± 1.8	170.6 ± 0.29	81.13 ± 0.18	47.25 ± 0.16	40.71 ± 0.17	2.58 ± 0.16
8	170 ± 1.8	175 ± 0.53	85.75 ± 0.45	44.78 ± 0.2	42.66 ± 0.19	1.89 ± 0.2
9	221 ± 1.8	222.7 ± 0.3	82.04 ± 0.18	103.7 ± 0.19	34.55 ± 0.16	2.39 ± 0.17
9	186.5 ± 1.8	187.8 ± 0.37	80.96 ± 0.21	77.42 ± 0.25	29.37 ± 0.18	1.53 ± 0.24
9	196.5 ± 1.8	196 ± 0.33	61.21 ± 0.17	71.61 ± 0.23	61.33 ± 0.16	1.89 ± 0.22
10	189 ± 1.8	190 ± 0.29	100.2 ± 0.18	50.86 ± 0.16	36.33 ± 0.16	2.75 ± 0.15
11	162 ± 1.8	161.7 ± 0.3	80.99 ± 0.18	45.21 ± 0.18	35.54 ± 0.16	2.98 ± 0.17
12	158 ± 1.8	160 ± 0.3	72.05 ± 0.17	58.28 ± 0.2	27.44 ± 0.16	1.5 ± 0.18

13	184.5 ± 1.8	184.2 ± 0.31	96.02 ± 0.18	53.31 ± 0.18	32.67 ± 0.18	2.15 ± 0.18
Test	$\boldsymbol{Ref_{ins}}$ [g]	$\boldsymbol{Ref_{ext}}$ [g]	$\boldsymbol{Ref_{comp}}$ [g]	$\boldsymbol{Ref_{cond}}$ [g]	$\boldsymbol{Ref_{evap}}$ [g]	$\boldsymbol{Ref_{valves}}$ [g]
14	200 ± 1.8	198.3 ± 0.29	100.3 ± 0.17	59.37 ± 0.15	35.91 ± 0.17	2.75 ± 0.16
16	152 ± 1.8	154.1 ± 0.28	67.83 ± 0.18	60.17 ± 0.15	23.24 ± 0.16	2.92 ± 0.15
16	150.5 ± 1.8	148.8 ± 0.34	60.05 ± 0.21	61.59 ± 0.19	25.15 ± 0.19	1.99 ± 0.19

Table 23: Results of refrigerant distribution of test with prototype 2.

Appendix F: IIR pictures

This appendix shows the infrared pictures taken during each test's recording data phase. In several tests, IR pictures of the evaporator and condenser were taken.

Firstly it will be shown the pictures from the evaporator are the most important since they show the maldistribution existent in this component. In the images, the refrigerant inlet port is situated in the bottom right part, and the outlet is at the top right. The side shown is the one near the refrigerant ports, and it was painted with white chalk to avoid reflections. Then the condenser also shows the refrigerant side.

Test 1	Test 2	Test 3	Test 4	Test 5	Test 6
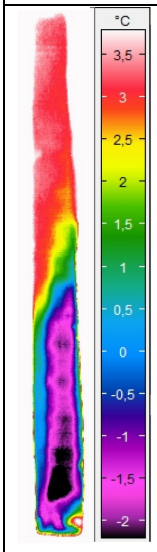	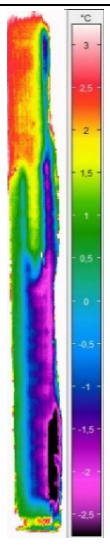	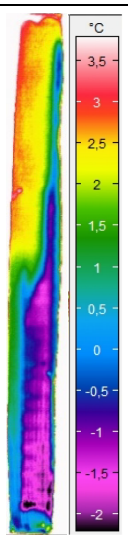	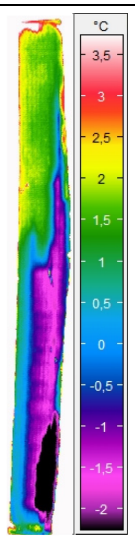	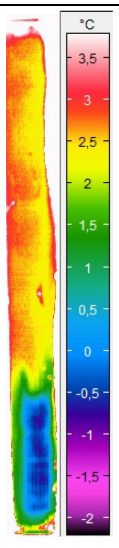	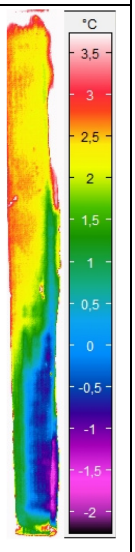

Test 10	Test 11	Test 12	Test 13	Test 14	Test 15
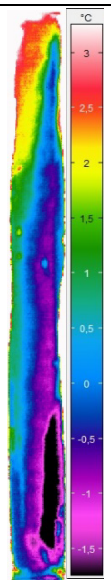	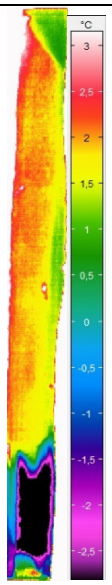	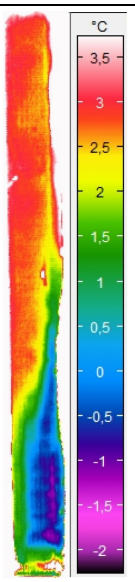	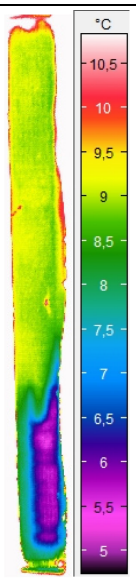	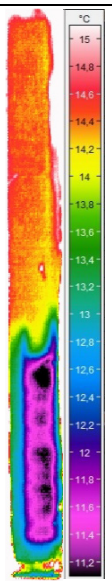	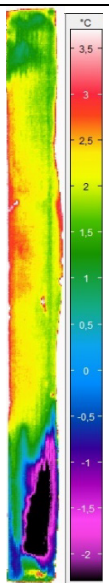

Table 24; Infrared pictures of the evaporator of prototype 1.

Test 1	Test 2	Test 3	Test 7	Test 9
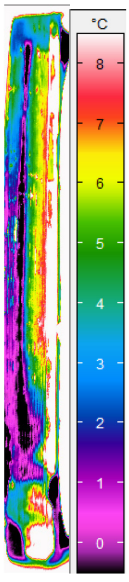	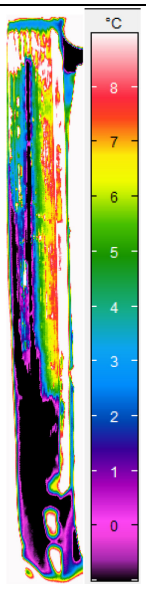	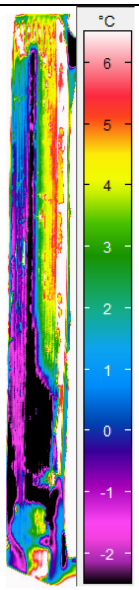	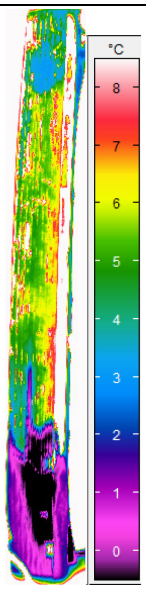	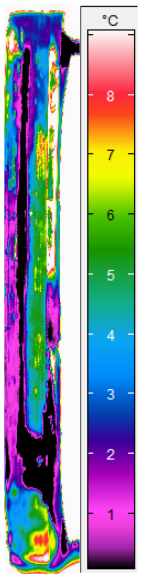

Test 10	Test 11	Test 16
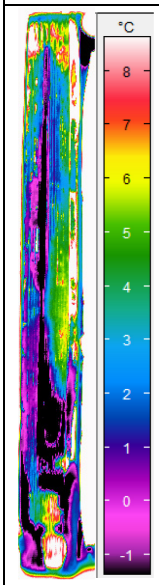	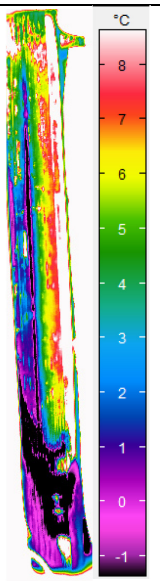	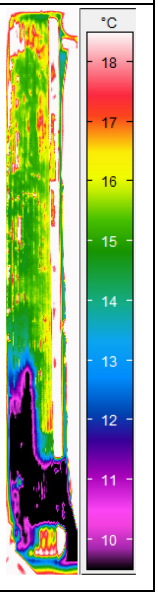

Table 25: Infrared pictures of the evaporator of prototype 2.

Test 1	Test 2	Test 3	Test 4	Test 5
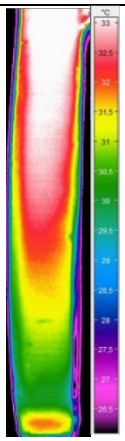	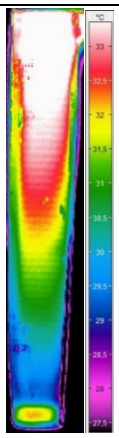	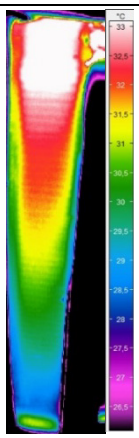	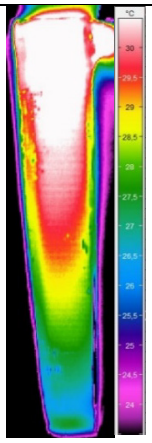	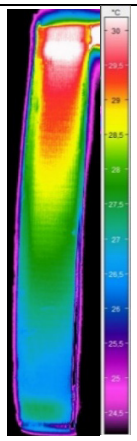

Test 6	Test 7	Test 8	Test 12	Test 13
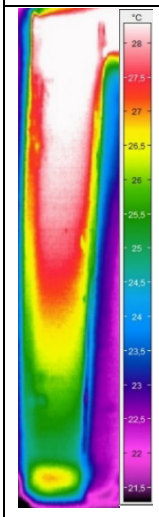	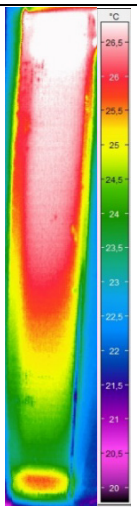	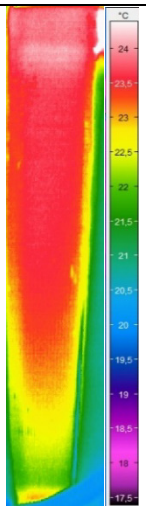	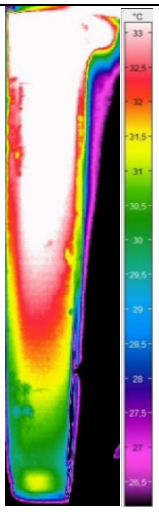	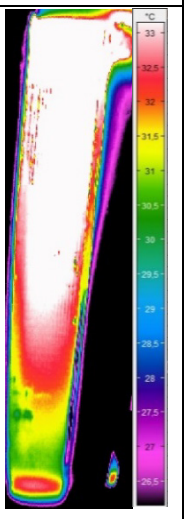

Test 14	Test 15
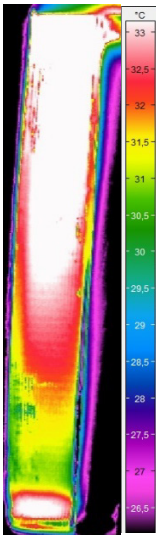	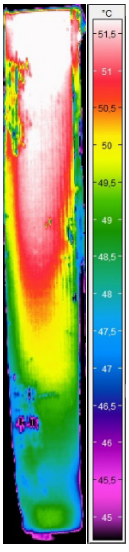

Table 26: Infrared pictures of the condenser of prototype 1.

Test 1	Test 3	Test 10	Test 11
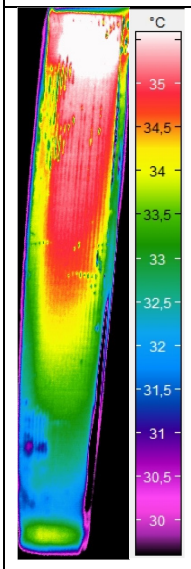	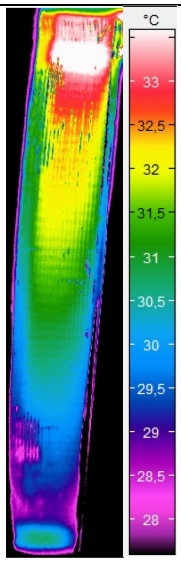	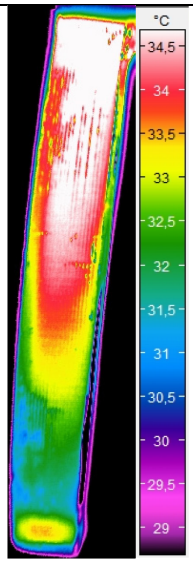	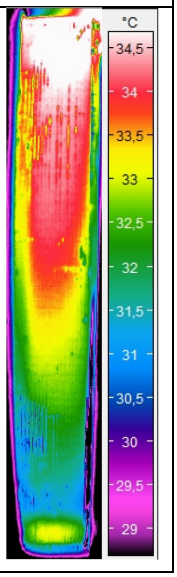

Table 27: Infrared pictures of the condenser of prototype 2.

References

[1] L. Sánchez-Moreno-Giner, F. Barceló-Ruescas, A. López-Navarro, and J. Gonzálvez-Maciá, "Experimental and Theoretical Analysis of Refrigerant Charge Extraction Methods," 2021. Accessed: Nov. 13, 2021. [Online]. Available: https://docs.lib.purdue.edu/iracc

[2] S. Klein, "EES, Engineering Equation Solver v10." 2020.

[3] "Bestimmung der minimalen Kältemittelfüllmenge einer Low-Charge Propan Sole-Wasser Wärmepumpe für einen maximalen SCOP im mittleren Klima," 2021.

[4] European Committee for Standardization, "EN 14825 - Air conditioners, liquid chilling packages and heat pumps, with electrically driven compressors, for space heating and cooling - Testing and rating at part load conditions and calculation of seasonal performance.," 2019, Accessed: Sep. 22, 2021. [Online]. Available: https://www.en-standard.eu/din-en-14825-air-conditioners-liquid-chilling-packages-and-heat-pumps-with-electrically-driven-compressors-for-space-heating-and-cooling-testing-and-rating-at-part-load-conditions-and-calculation-of-seasonal-performance/

[5] European Committee for Standardization, "EN 14511-3 Air conditioners, liquid chilling packages and heat pumps for space heating and cooling and process chillers, with electrically driven compressors - Part 3: Test methods," 2019, Accessed: Sep. 21, 2021. [Online]. Available: https://www.techstreet.com/standards/din-en-14511-3?product_id=2076455